Jürg Andreas Stückelberger

A Weighted-Graph Optimization Approach for Automatic Location of Forest Road Networks

v/d/f

Jürg Andreas Stückelberger

A Weighted-Graph Optimization Approach for Automatic Location of Forest Road Networks

vdf Hochschulverlag AG an der ETH Zürich

A dissertation submitted to the
ETH Zurich
for the degree of Doctor of Sciences

Diss. ETH No. 17366

accepted on the recommendation of
Prof. Dr. Hans Rudolf Heinimann, examiner
Prof. Dr. Woodam Chung, co-examiner
Prof. Dr. Angelika Steger, co-examiner

This book contains information obtained from authentic sources. Reprinted materials is quoted with permission, and sources are indicated. Chapter 1 is reprinted with kind permission of Springer Science+Business Media, Germany. Chapter 2 is reprinted with kind permission of National Research Council Press, Canada. Chapter 3 ist reprinted with kind permission of Council on Forest Engineering, USA.

Bibliographic information published by Die Deutsche Bibliothek
Die Deutsche Bibliothek lists this publication in the Deutsche Nationalbibliografie; detailed bibliographic data is available in the Internet. at http://dnb.ddb.de.

This work is available as printed version on www.vdf.ethz.ch

vdf Hochschulverlag AG an der ETH Zürich

ISBN 978-3-7281-3217-8
DOI 10.3218/3217-8 (open access)

www.vdf.ethz.ch
verlag@vdf.ethz.ch

Abstract

In a large majority of regions where forestry activities occur, roads are the backbone of their efficient management. Automatic planning of a road network is an ongoing, challenging task. Advances have been aided by the increased availability and accuracy of digital terrain models, greater computing power, and improvements in optimization techniques. Defining the objectives and deriving adequate objective functions are crucial steps in guiding the solution toward an ideal network, especially when individual goals may conflict. For example, whereas the conservationist might prefer that a layout minimizes any detrimental impacts on the environment, the forest landowner may favor cost-minimal roads while the forest operator would like to have a dense network in order to reduce transportation costs. This thesis introduces models for three objective functions: (1) forest road construction and maintenance costs, (2) negative ecological effects from such roads, and (3) the suitability, or attractiveness, of a network for cable-yarding. Case studies in mountainous project areas illustrate the trade-offs among these conflicting goals, and demonstrate how to optimize different objectives in order to make an optimal decision overall.

Contents

List of Figures

List of Tables

List of Symbols and Abbreviations

a	year (lat. annus)
ArcGIS	a → GIS software package of ESRI company, today's market leading desktop GIS
CHF	Swiss Franc (currency unit): 1 $CHF \approx 0.78 \rightarrow USD$
EUR	Euro (currency unit): 1 $EUR \approx 1.15 \rightarrow USD$
ft	foot: 1 $ft \approx 0.3048\ m$
GIS	Geographic Information System, a system for creating, storing, analyzing and managing spatial data and associated attributes
ha	hectares = 10'000 m^2
km	kilometer: 1 $km \approx 0.621\ miles$
m	meter: 1 $m \approx 3.281\ ft$
mNN	meters above zero; zero ≈ see level
MST	Minimum Spanning Tree: a subgraph within a weighted graph, which connects all vertices by a minimal weight. The MST is a → $\mathcal{P}$-problem.
$\mathcal{NP}$	Problems of the complexity class $\mathcal{NP}$ are solvable in polynomial time depending on the problem size on a non-deterministic Turing machine. Up to now, there is no non-deterministic Turing machine available.
$\mathcal{NP}$-hard	For problems of the complexity class $\mathcal{NP}$-hard there is no known algorithm which is able to solve the problem in polynomial time depending on the problem size with a deterministic Turing machine. To find the mathematical best solution for large problems is very often "hard" or even not feasible within a limited time span. Most probably $\mathcal{NP}$-hard $\notin \mathcal{N}$.
NPV	Net Present Value: a standard method for the financial appraisal of long-term projects
$\mathcal{P}$	Problems of the complexity class $\mathcal{P}$ are solvable in polynomial time depending on the problem size on a deterministic Turing machine. A deterministic Turing machine works with the same logic of any today's computer. In most case, such problems can be solved "quickly". $\mathcal{P} \subset \mathcal{NP}$. It is most likely that $\mathcal{P} \neq \mathcal{NP}$, however it is one of the unsolved problems in Mathematics.
$\mathbb{R}$	set of real numbers
$\mathbb{R}^n$	set of n-dimensional real vectors
SMT	Steiner Minimal Tree: a subgraph within a weighted graph, which connects a subset of vertices by a minimal weight. The SMT is a → $\mathcal{NP}$-problem.
SP	Shortest Path between two vertices in a graph. 'Short' refers to the weight of the edges and not to the Euclidian distance. The SP is a → $\mathcal{P}$-problem.
USD	US-Dollar (currency unit)
X	decision space = solution space
x^*	Pareto optimal solution
Y	objective space = criterion space
y^*	efficient point in the criterion space

Preface

In engineering sciences, the development of new tools for planning forest road networks is not considered a top subject. For example, in central Europe, most networks have already been designed and, in some regions, the existing system is extremely dense, thereby encumbering high maintenance costs. However, in rural areas, forest roads are still the backbone of effective management practices. Their existence is a main reason for our continued focus on this topic.

In the research described here, the root was expertise from the local forest agency for the Canton of Uri in Switzerland. Located in a very important transit valley, this Canton requires extremely well managed forests that can provide protection against such natural hazards as rock fall, landslides, and avalanches. The aim in that region was to build an initial forest road network in an otherwise roadless area. Due to the steepness of the terrain and the high rock ratio of the subsoil, construction costs are very high. Therefore, in collaboration with a forest engineer familiar with local conditions, ETH was asked to locate an economical and optimal road network. While evaluating the existing optimization tools, we noted that none could handle different geological types and steep terrain. Thus, these challenges led us to formulate a prototype of our first road optimization model.

While installing these roads in the Canton of Uri, we were able to enhance our prototype for general application. The goal was to develop a program for identifying an optimized network that automatically fulfills all mathematical criteria. The benchmark for this was a conventional approach involving an expert solution drawn on a map. Although the project described here did not beat that benchmark at every point, we learned that some components of these newer tools proved much better than an expert solution, while other features of the models were limited. Because we acknowledge that we are not the first research group to deal with road network optimization, here we have described a framework that entails different stand-alone tools and allows for flexible use of those models. For example, it is possible that one management group will choose to employ only our model for estimating road construction costs when devising their particular decision-support system while others may opt to follow the general framework but will also exchange or add some new components for their specific project area.

Because construction costs are a decisive factor in determining the general layout for forest roads, we have expended considerable effort in developing a model that precisely predicts those costs. Furthermore, I happen to have a strong affinity for basic forest engineering and soil mechanics, especially with regard to unstable subsoil. Thus, it is not surprising that such aspects are some of the best verified components in the entire framework of this model. However, the constraint of construction costs is not the only key to achieving good network design. Environmental factors are also becoming more important, such that ecological models are incorporated here in an attempt to find a multi-criteria optimization. In this particular research, two important ecological topics are of major relevance: Capercaillie (a mountain grouse) and marshlands. These tests were conducted primarily in the area of Wägital, Canton of Schwyz, which is located on the northern slopes of the Swiss Alps. I undertook my evaluation of this region because ETH has been utilizing it for research and teaching purposes since 2001. However, although the

abundance of available data and expertise might ordinarily simplify such an evaluation, the fact that this area has numerous contradictory goals, challenging geological subsoil, and different ecological constraints means that execution of our proposed road network will not be realized over its entire length.

This thesis comprises several components, a result of intensive, hard work based on experience, discussions, and field verification. One component represents the standard modeling of construction costs. Another two components, however, are products of innovation. One of those is the introduction of a new dimension for direction in the graph model. This new feature allows one to solve layout problems using well-known graph algorithms. I got this idea while making a ski tour in the Swiss Alps. Hiking with skis in a mountainous area is very similar to dealing with the problem of building forest roads in steep terrain. In both situations, one must find a constant gradient for the trail. Switchbacks on roads should be minimized because they necessitate high construction costs, and they require hikers to expend much energy when maneuvering turns.

Another innovative point is the introduction of a different scale to the graph. The inspiration for this came when my godchild and I were playing with a rubber ball. When a ball is bounced, it will seek the lowest local position. If the ball is allowed to go into a staircase, it will of course immediately begin to move downward; any surface unevenness is irrelevant then. However, when that ball reaches the ground floor, it will cease bouncing and, instead, begin to roll. Even though the ground may seem perfectly flat, just a bit of unevenness will determine whether that ball stops or continues to roll. Now, back to road design. When we are looking for a minimum network we can present the general road centerline in a resolution of about 10 $m \times 10$ m. However, for switchbacks, which are important contributors to the total costs of a project, we must adopt a more precise resolution. Another parallel to the bouncing rubber ball is the fragility of certain objects, such as vases and porcelain – these might correspond to weak subsoil or rare ecotypes within the road model. By their very nature, both porcelain and delicate habitats must, of course, be excluded from either the playground or the solution space.

These two innovations – turning constraints and applying a different scale to the graph – are the most interesting facets of my thesis. Neither must be restricted to road network problems only, and may, in fact, be appropriate when tackling other challenges as well. However, because they are novel, their proposed utility has often led to some differences with reviewers, such that we have not emphasized them too much in the ensuing publications. Nevertheless, we are very pleased to report that the paper included here as the third chapter was judged by the Council on Forest Engineering as the best presented paper in 2006.

The design tools that have become viable as a result of this thesis can find many applications. I briefly describe four possible scenarios: (1) In steep terrain and difficult geology, the model can be used to identify the minimum-cost road network, provided that spatial data and engineering parameters are available in a small-scale resolution. Whereas Switzerland has only a few roadless areas, regions in Eastern Europe, South and North America, or Asia provide much potential. Nonetheless, even when a road network seems to be optimal for a specific location, its installation is not always possible. For example, we employed the existing model while conducting a project in the Western Carpathians (Ukraine). However, that project will not be realized due to a lack of investment capital from forest and wood enterprises. (2) In a project area that has two or three objectives, such as minimizing construction costs and ecological penalties, the model provides Pareto-optimal solutions. The benefit of our new model is demonstrated when we evaluate expertly designed road networks. Taking an analytical approach, we can judge whether the solution is Pareto-optimal or else how far it is from the goal. (3) In central European countries, many road networks were designed in the 1960s, or even before. Since then, their transporta-

tion and harvesting systems have changed. In trying to meet current needs, the road density has become too high but the pavement structure is not strong enough, resulting in expensive maintenance. One possibility for decreasing such costs would be to reduce the existing network while improving the remaining roads. In such cases, our model could solve those problems as well. (4) Although these new tools have been developed for road network design, some ideas are portable, and can be adapted for use in addressing challenges within other engineering sciences, such as devising models for natural hazards. In fact, numerous debris-flow tools that are relied upon by experts are based on a simple grid-raster model. Moreover, their results are sometimes very startling. I am convinced that our enhanced neighborhood definitions and proposed graph model with additional dimensions will provide better solutions.

The end of this Ph.D. project should be the start for solving future real-world problems. I hope that engineers will be able to extract some ideas from this current report, and that they and other research groups will recognize the potential available for collaborations.

Jürg Stückelberger

Summary

In most regions that support forestry activities, roads are the backbone of efficient management. Planning of a road network is still a challenging task, whether the goal is to design new routes or to improve or reduce existing systems. Automatic road network planning is a very complex locational problem that involves elevation, the geotechnical subsoil, different types of harvesting systems, and ecological effects.

Most existing optimization tools for such planning do not work well in steep terrain due to various shortcomings: (1) the assumption that road construction costs are homogenous over the entire project area, (2) neglect of the turning constraints for a road centerline and limited road directions, and (3) optimization of a road network for one objective only. The goal of the thesis presented here was to remedy these shortcomings and provide a model framework so that planners could automatically locate an optimal forest road network in mountainous areas of up to 50 km^2, and at a resolution of 10 m.

This problem is mapped here on a mathematical weighted graph. A graph (G) consists of a set of vertices (V, i.e., nodes) and a set of edges (E, i.e., road links) between two vertices. The weight (w) of an edge represents road costs or the ecological impact of a link. If one supposes that the mandatory access points are known, the situation can be formulated as a Steiner Minimum Tree problem (SMT). For example, if the weight of the edges represents construction costs, the SMT produces a cost-minimal network between given mandatory access points. There is most probably no exact algorithm that can solve this within a polynomial time deterministically; thus, the problem is $\mathcal{NP}$-hard. My thesis, therefore, presents some intelligent heuristics for finding near-optimal solutions to this problem.

In the first step, we try to identify the cost-minimal network. Our focus is on road life-cycle costs, which comprise expenses for construction and maintenance over the life-cycle period. To solve this problem, we require good models that can give accurate cost estimates (cf., Chapter 1) as well as a useful model representation for forest road alignment (cf., Chapter 2). In our second step, we incorporate other objectives, including harvesting-attractiveness and penalties for negative ecological impacts. These bi- and tri-objective problems call for multi-criteria optimization (cf., Chapter 3). Several optimal alternatives are made available, depending on the preferences of the stakeholders for different objectives. For example, a conservationist may prefer a road with no ecological disturbance whereas the forest landowner would rather have a cost-minimal solution. A solution is deemed *Pareto-optimal* if it is not possible to decrease one objective without increasing another. We call the set of all Pareto-optimal solutions the Pareto set or Pareto frontier. Depending on the shape of the trade-off between different objectives, there is a subset of Pareto-optimal solutions located on the convex hull in the criterion space. The mathematical formulation for this specific subset of Pareto-optimal solutions is described in Chapter 4. For practical applications, these solutions can be considered the most interesting. Whereas in Chapter 3 we attempt to find Pareto-optimal solutions for bi-objective functions, in Chapter 4 we also examine tri-objective functions.

The model framework was tested in different project areas over steep terrain. We assumed the mandatory access points for the road network were known, and we limited our focus to harvesting via cable-yarding. Only two penalties were applied for ecological disturbance: to capercaillie, an endangered breeding bird (*Tetrao urogallus*), and to rare ecotypes (marshland). The following are our major findings:

(1) A cost-estimating procedure that incorporates slope gradient and geotechnical properties of the subsoil results in an optimal road network that incurs about 25% less in construction costs.

However, its total length is about 10% longer compared with state-of-the-art models where construction costs are assumed to be homogenous over the entire project area. Furthermore, a model that includes slope gradient but neglects the geotechnical subsoil results in 17% higher costs compared with our newly proposed model.

(2) The representation of a forest road is the crucial qualification for accurate network planning. The steeper the terrain, the more important it is to choose a model that is able to handle turning constraints and several different road directions. State-of-the-art models, which have a limited set of directions and do not map turning constraints, cannot find a feasible solution in areas where the average slope gradient is $> 35\%$. Furthermore, models that do include different road directions but neglect turning constraints will project network costs that are about 50% over the optimum.

(3) Using our methods, we have found it possible to determine Pareto-optimal solutions. The criteria of these solutions are located on a convex trade-off surface, as predicted by the multi-criteria optimization theory. These evaluations show that not only do economic objectives interact with ecological goals but also different ecological goals operate inversely. In one test area, a road network that can minimize one of our two ecological impacts encumbers two to three times higher costs, and increases other ecological disturbances by 20% to 40%.

The preferences for various objectives (i.e., weighting factors of the objective function) by the stakeholders greatly influence these solutions. Even relatively small changes in those preferences may cause the decision to jump from one Pareto solution to a completely different one. Knowing the trade-offs associated with these individual objectives helps the stakeholders make the final Pareto-optimal decision.

Our approach for solving the road network problem through a graph representation and SMT is very favorable when the graph is static and the weight of an edge (road link) can be assigned by a weighted sum of the different objectives. This is indisputably correct for road construction costs. For our two chosen ecological impacts, those assumptions seem to be reasonable as well. However, they are no longer valid when we incorporate forest harvesting-attractiveness. If a particular road link is chosen, the attractiveness for neighboring links may decrease. Applying our approach has one large shortcoming in that we are unable to handle the dynamic weights of a graph. Nonetheless, for low-weighting factors of harvesting-attractiveness, this model produces reasonable and nearly optimal solutions.

Zusammenfassung

In fast allen Waldgebieten, in welchen aus ökonomischen oder ökologischen Gründen, oder zur Abwehr von Naturgefahren eingegriffen wird, sind Forststrassen die Grundvoraussetzung für eine effiziente Bewirtschaftung. Die Planung eines forstlichen Erschliessungsnetzes ist nach wie vor eine herausfordernde Aufgabe, beispielsweise für den Entwurf eines neuen Strassennetzes, für den Ausbau bestehender Strassen oder für den Rückbau von Teilen des existierenden Strassennetzes. Computergestützte, vollautomatische Strassennetzwerkplanung ist ein sehr komplexes räumliches Problem, welches die Topographie, den geotechnischen Untergrund, verschiedene Holzerntesysteme und die Auswirkungen auf die Umwelt einschliessen muss.

Die meisten existierenden Optimierungsprogramme für die Planung forstlicher Erschliessungen sind ungeeignet für die Anwendung im steilen Gelände, da sie folgende Schwächen aufweisen: (1) die Annahme, dass die Baukosten im gesamten Projektgebiet gleich sind, (2) Vernachlässigung der massgebenden Restriktionen für Richtungsänderungen der Strassenlinie und stark limitierte mögliche Strassenrichtungen und (3) Optimierung des Strassennetzwerkes für nur eine Zielgrösse. Die vorliegende Arbeit hat zum Ziel, diese Schwächen zu beheben und stellt ein Komponentenmodell vor, welches für ein Projektgebiet von bis zu 50 km^2 vollautomatisch ein optimales forstliches Erschliessungsnetz mit einer Genauigkeit von 10 m entwerfen kann.

Das Problem wird auf einem mathematischen gewichteten Graphen abgebildet. Ein Graph (G) besteht aus einer Menge von Knoten (V, Punkte) und einer Menge von Kanten (E, Strassenabschnitte) zwischen zwei Knoten. Jede Kante wird mit einem positiven Wert gewichtet, der beispielsweise den Baukosten oder dem ökologischen Einfluss eines Strassenabschnittes entspricht. Angenommen, die positiven Fixpunkte einer Strasse sind bekannt, so kann das Problem als minimaler Steinerbaum (engl. Steiner Minimum Tree, SMT) formuliert werden. So führt ein SMT mit dem Gewicht "Baukosten" zum kostenminimalen Strassennetzwerk, welches alle Fixpunkte verbindet. Leider ist kein Algorithmus bekannt, der dieses Problem in polynomialer Zeit deterministisch lösen könnte, das Problem ist daher $\mathcal{NP}$-hart. Die vorliegende Arbeit zeigt intelligente heuristische Ansätze, wie das Problem nahezu optimal gelöst werden kann.

In einem ersten Schritt wird versucht, ein baukostenminimales Strassennetzwerk zu finden. Es werden die gesamten Lebenszykluskosten einer Strasse betrachtet, welche die Baukosten im ersten Jahr sowie die laufenden und periodischen Unterhaltskosten der gesamten Lebensdauer der Strasse umfassen. Um das Problem zu lösen, ist ein Modell erforderlich, welches sowohl diese Kosten zuverlässig schätzen kann (vgl. Kapitel 1) als auch die Linienführung der Strasse korrekt abbildet (vgl. Kapitel 2). In einem zweiten Schritt wird versucht, weitere Zielgrössen, wie die Güte für die Holzernte und Straffunktionen für negative ökologische Einflüsse zu berücksichtigen. Multikriterielle Optimierungstechniken erlauben, diese Zwei- und Dreizielprobleme zu lösen (vgl. Kapitel 3). Je nach den Prioritäten der Entscheidungsträger resultieren unterschiedliche optimale Lösungen. Beispielsweise bevorzugt ein Naturschützer eine Strasse mit möglichst geringem negativen Einfluss auf die Umwelt, während eine Waldbesitzerin eine kostengünstige Strasse bevorzugt. Eine Lösung ist *Pareto optimal*, wenn es nicht mehr möglich ist, eine Zielgrösse zu verbessern, ohne andere Zielgrössen zu verschlechtern. Die Menge aller Pareto optimalen Lösungen wird Paretomenge oder Paretogrenze genannt. Abhängig von der Form der Wechselwirkung dieser Zielgrössen gibt es eine Untermenge der Paretomenge, die auf einer konvexen Hülle der Zielmenge liegt. Die mathematische Formulierung für diese Paretomenge ist in Kapitel 4 beschrieben. Für praktische Anwendungen sind fast immer nur Lösungen dieser Paretomenge von Interesse. In Kapitel 3 wird versucht, die Paretomenge zwischen zwei Zielgrössen zu finden, in Kapitel 4 werden zusätzlich die optimalen Lösungen zwischen drei Zielgrössen untersucht.

Das Komponentenmodell wurde in verschiedenen Projektgebieten im steilen Gelände angewandt. In dieser Arbeit wird davon ausgegangen, dass die Fixpunkte bekannt sind und nur ein Holzerntesystem mit Seilkran zur Anwendung kommt. Zudem werden nur zwei negative ökologische Auswirkungen betrachtet: (1) das vom aussterben bedrohte Auerhuhn (*Tetrao urogallus*) und (2) seltene Feuchtgebiete.

Aus den Ergebnissen lassen sich folgende Haupterkenntnisse ableiten:

(1) Eine Baukostenfunktion welche die Hangneigung und die geotechnischen Eigenschaften des Bodens berücksichtigt führt zu einem optimalen Strassennetzwerk, welches etwa 25% kostengünstiger jedoch etwa 10% länger ist, verglichen mit herkömmlichen Modellen, welche die Strassenbaukosten im Projektgebiet als konstant voraussetzen. Ein Modell, welches nur die Hangneigung berücksichtigt, jedoch den geotechnischen Untergrund vernachlässigt, führt zu einer Lösung mit etwa 17% höheren Kosten, verglichen mit dem neu entwickelten Modell.

(2) Die Art und Weise, wie eine Forststrasse in einem Modell abgebildet wird, ist der entscheidende Faktor für die Güte der daraus resultierenden Erschliessungsplanung. Je steiler das Gebiet, desto entscheidender ist es, ein Modell zu wählen, welches Richtungsänderungen und mehrere verschiedene Strassenrichtungen abbilden kann. Herkömmliche Modelle, welche nur eine beschränkte Anzahl möglicher Richtungen aufweisen und Richtungsänderungen nicht korrekt berücksichtigen, sind nicht in der Lage, machbare Lösungen in Projektgebieten mit durchschnittlichen Hangneigungen von über 35% zu finden. Modelle, welche viele verschiedene Strassenrichtungen einschliessen, jedoch die Richtungsänderungen vernachlässigen, führen zu Lösungen, welche 50% über den optimalen Kosten liegen.

(3) Mit den in der vorliegenden Arbeit vorgestellten Methoden ist es möglich, Pareto optimale Lösungen zu finden. Die Zielgrössen der Paretomenge liegen auf einer konvexen Hüllkurve, so wie dies in der multikriteriellen Optimierungstheorie vorhergesagt wird. Die Auswertung zeigt, dass nicht nur ökonomische Ziele gegenläufig zu ökologischen Zielen sind, sondern dass sich auch verschiedene ökologische Ziele gegenseitig konkurrenzieren. Im vorliegenden Untersuchungsgebiet führt ein Strassennetz, welches eine der zwei Zielgrössen minimiert, zu zwei– bis dreimal höheren Kosten und erhöht die negative Auswirkung der anderen ökologischen Zielgrösse um 20% bis 40%.

Die Lösung ist stark abhängig von den Prioritäten der Entscheidungsträger für die einzelnen Zielgrössen (d.h. die Gewichtung der einzelnen Zielfunktionen). Eine kleine Änderung der Zielgewichtung kann zu völlig unterschiedlichen optimalen Lösungen führen. Die Lösung springt an jener Stelle von einem Pareto Optimum zu einem völlig andern Pareto Optimum. Sind die Wechselwirkungen verschiedener Zielgrössen bekannt, so ist es für die Entscheidungsträger viel einfacher, die gewünschte Pareto optimale Lösung auszuwählen.

Der in dieser Arbeit vorgestellte Ansatz, das Strassennetzwerkproblem mit Hilfe eines Graphen und eines SMT zu lösen, ist sehr vorteilhaft, wenn es sich dabei um statische Gewichte der Kanten (Strassenabschnitte) handelt, die mittels einer gewichteten Summenfunktion verschiedener Zielfunktionen hergeleitet werden können. Für Strassenbaukosten ist dieser Ansatz zweifelsfrei korrekt. Für die ökologischen Auswirkungen scheint dieser Ansatz ebenfalls vernünftig zu sein. Dieser Ansatz ist jedoch nicht mehr gültig, wenn die Attraktivität für die Holzernte abgebildet wird. Wenn ein Strassenabschnitt gewählt wird, so kann die Holzernteattraktivität von benachbarten Strassenabschnitten stark abnehmen. Der gewählt Ansatz ist nicht fähig, dynamische Veränderungen der Kantengewichte zu verarbeiten. Dies ist der grösste Schwachpunkt des Modells der vorliegenden Arbeit. Dennoch führt das Modell zu fast optimalen Lösungen, so lange kleine Gewichtungsfaktoren für die Holzernteattraktivität gewählt werden.

Résumé

Les dessertes forestières sont la base d'un aménagement du territoire efficace pour la plupart des régions où l'activité forestière est importante. La conception d'un réseau de dessertes demande une grande réflexion pour planifier de nouvelles routes, améliorer ou redimensionner des routes existantes. L'automatisation de la conception d'un réseau est un problème spatial très complexe qui doit tenir compte de plusieurs paramètres tels que la topographie, la géotechnique du sol, les systèmes d'exploitation du bois et les contraintes écologiques.

La plupart des logiciels existants pour l'optimisation des réseaux de dessertes forestières sont inappropriés pour les terrains à forte pente, parce qu'ils présentent les désavantages suivants: (1) Les coûts de construction sont homogènes pour toute une surface; (2) ils négligent les contraintes liées aux virages et les directions potentielles pour la route sont très limitées; (3) il n'est possible d'optimiser la route qu'en fonction d'une seule variable.

Le présent travail a pour but de contrer ces désavantages et propose un modèle à plusieurs composantes qui est capable de générer automatiquement un réseau de dessertes forestières pour une surface de 50 km^2 avec une précision de 10 mètres.

Le problème est représenté sur un graphe mathématique (G). Le graphe consiste en un ensemble de sommets (V, nœuds ou points de la desserte) et un ensemble d'arêtes (E, connections ou sections de la desserte) entre deux sommets. Chaque arête a un poids qui représente par exemple les coûts de construction ou les contraintes écologiques d'une section. Supposant que les points fixes sont connus, le problème peut alors être formulé par l'arbre de Steiner de poids minimal (angl. Steiner Minimum Tree, SMT). Par exemple, si les arêtes représentent les coûts, le SMT donnera le réseau connectant les points fixes avec les coûts minimaux. Malheureusement, il n'existe pas d'algorithme connu qui puisse résoudre le problème en temps polynomial. On parle alors de problème $\mathcal{NP}$-dur. Ce travail présente des approches heuristiques intelligentes qui permettent de résoudre le problème de façon quasi optimale.

En premier lieu, on recherche le réseau de dessertes aux coûts minimaux. Tout le cycle de vie de la desserte est considéré, c'est-à-dire que non seulement les coûts de construction sont pris en compte, mais également les coûts de maintenance et d'entretien sur toute la durée de service de la desserte. Pour cela, il est nécessaire d'avoir un modèle qui estime les coûts avec fiabilité (Chapitre 1). Dans un deuxième pas, on considère d'autres paramètres tels que les besoins pour l'exploitation du bois ou les contraintes écologiques. Pour résoudre ce problème plus complexe, des techniques d'optimisation multicritère sont utilisées (Chapitre 3). Le résultat sera entièrement lié aux choix et préférences des décideurs. Par exemple, un écologiste va favoriser une desserte forestière avec un minimum d'impact sur l'environnement tandis qu'un propriétaire va se soucier essentiellement des coûts. Les solutions obtenues sont appelées *optima de Pareto*, s'il n'est pas possible d'améliorer le résultat d'un paramètre sans empirer le résultat d'un autre paramètre. L'ensemble des optima de Pareto est l'ensemble de Pareto ou la frontière de Pareto. Selon l'interaction entre les paramètres, il existe un sous-ensemble de Pareto qui se trouvent sur une enveloppe convexe. La formulation mathématique est indiquée au Chapitre 4. Pour la pratique, seules les solutions de cet ensemble des optima de Pareto sont intéressantes. Dans le Chapitre 3, des solutions des optima de Pareto sont trouvées pour deux paramètres et dans le Chapitre 4 pour trois paramètres.

Les différents composants du modèle ont été testés pour plusieurs régions à forte pente. On suppose toujours que les points fixes sont connus. On ne considère qu'un seul système d'exploitation de la forêt; ici la grue à câble et seulement 2 contraintes écologiques; la présence du grand tétras (*Tetrao urogallus*) et la présence de marais. On trouve les résultats principaux suivants:

(1) D'un modèle qui considère la pente et les propriétés géotechniques du sol résulte un réseau de dessertes forestières qui est environ 25% meilleur marché, mais 10% plus long que les résultats des modèles développés jusqu'à ce jour, qui calculent avec des coûts de construction constants. D'un modèle qui considère la pente, mais néglige la géotechnique du sol résulte des solutions environ 17% plus chères que le nouveau modèle présenté.

(2) La manière dont un modèle représente les dessertes forestières est cruciale pour la qualité de la planification du réseau de dessertes. Plus raide est le terrain, plus il est important d'utiliser un modèle qui considère plusieurs directions de route et qui peut traiter les changements de directions correctement. Les modèles traditionnels qui ne considèrent que peu de directions et ne peuvent pas traiter les changements de direction, ne sont donc pas capables de trouver une solution réalisable sur un terrain ayant une pente supérieure à 35%. Les modèles qui tiennent compte de plusieurs directions, mais qui ne traitent pas correctement les changements de direction donnent des solutions environ 50% plus chères.

(3) Avec la méthode présentée ici, il est possible de trouver des optima de Pareto. Les paramètres de l'ensemble des optima de Pareto se trouvent sur une courbe convexe comme prédit par la théorie d'optimisation multicritère. L'analyse montre qu'il n'y a pas que les contraintes écologiques qui sont en concurrence avec les contraintes économiques, mais que les différentes contraintes écologiques sont concurrentes entre elles. Pour une surface test, un réseau de desserte qui minimise les impacts pour une contrainte écologique donne des coûts environ deux à trois fois plus élevés et défavorise une autre contrainte écologique de 20% et 40%. Les solutions sont fortement liées aux poids que les décideurs attribuent aux paramètres (c.-à-d. pondération). De petits changements de pondération peuvent résulter des solutions complètement différentes. La solution saute en fait d'un optimum de Pareto à un autre optimum. Si les interactions entre les différents paramètres sont connues, il est plus facile de définir l'optimum de Pareto à atteindre.

L'approche présentée dans ce travail, qui est de formuler le problème avec un SMT dans un graphe est très avantageuse, si les segments de routes ont des poids constants qui peuvent être définis par une somme des fonctions pondérées des différents paramètres. Cette approche est sans aucun doute correcte pour obtenir un réseau de desserte aux coûts minimaux ou pour minimiser les impacts écologiques. Si par contre, on ajoute le paramètre "exploitation du bois", cette approche n'est plus correcte. Le choix d'une méthode d'exploitation du bois ne sera pas valable pour tous les segments de route et le modèle présenté ici n'est pas capable de traiter des changements de poids entre les segments. C'est d'ailleurs le point le plus faible de ce modèle. Cependant, ce désavantage est moindre si la pondération de l'exploitation du bois est petite et le modèle donne alors des solutions quasi optimales.

General introduction

Goals

In most regions that support forest activities, such as harvesting and silvicultural practices, roads are the backbone of efficient management. These roads are costly infrastructures, have a lifespan of several decades or even centuries, and often bring adverse effects to the environment. Switzerland, for example, has a forest road network of about 32'000 km (Brassel & Brändli, 1999), which corresponds to a total investment of about 8 to 10 billion Swiss francs (about $6 \cdot 10^9$ USD) for replacement. To reduce the maintenance costs for this infrastructure, the trend has been to decrease density while improving standards for the existing roads. Worldwide total forest cover is $3.9 \cdot 10^9$ ha (FAO, 2007). If managers were to increase this density by an additional $5\frac{m}{ha}$, at a cost of 3 USD per meter, the overall investment volume would be about 60 billion USD.

Therefore, road network planning is a crucial activity that should strive for optimal solutions. It is a challenging task for engineers, whose goals are simultaneously to find routes with the lowest construction and maintenance costs, the least adverse impact, and the maximum benefit. Mathematical optimization is a widely used approach to solve such complex problems, requiring the formulation of an objective function and several constraints. Forest engineers and scientists have been searching for computer-aided techniques and tools that will considerably improve the effectiveness and efficiency of road-network layouts. However, the existing tools have some critical shortcomings: (1) they assume road construction costs to be homogenous throughout the project area; (2) they neglect the turning constraints for a road centerline, and limit the directions for discrete road segments to 8 or 16 only; and (3) they optimize the road network for only one objective, primarily the lowest cost. Although the currently available methods may provide useful results in flat and homogenous areas, they do not work well over steep terrain.

The goal of this thesis project was to develop techniques that help engineers locate an optimal road network within a specific project area, whether planning new routes or evaluating the existing networks. This novel approach is designed for mountainous regions, of up to 50 km^2, with different geological subsoils. It provides an optimal forest road network with a precision of about 10 m. Its main improvements are in: (1) estimating the spatial variability of road construction costs by considering the geometry of the road cross section, terrain slope, and geotechnical properties of the subsoil; (2) mapping various turning constraints on a mathematical graph, so that 40 different directions are possible for each road segment leaving a single node; and (3) implementing optimization for multiple objectives (i.e., life-cycle costs, harvesting-attractiveness, and ecological penalties).

History and state of the art

Forest road planning

Until the 1960s, the main emphasis in this field of research was related to such technical problems as road embankments and retaining and pavement structures. In modern times, the first studies were conducted by the "Ecole Nationale des Ponts et Chaussées" in Paris, founded in 1747, and by John Loudon McAdam, a Scottish engineer in the late 18$^{\text{th}}$ century. Most contemporary engineering problems in forest road construction have been solved and recorded in standard books, including those by Kuonen (1983), Walbridge et al. (1984), and AASHTO (1993).

Although some research is on-going into the materials and methods for forest road building, the principles of road construction are now well-established.

The challenging task today is to find an optimum road network layout. General road planning has it roots in the 1860s. Wilhelm Launhardt, a German road engineer, started to formulate general rules for locating a cost-minimal network (Launhardt, 1869, 1872). His approach was driven by planimetry, and his focus was on determining the shortest connections between different villages. The first rules for identifying the best layout for forest road networks were derived by K. Jägerschmid, a German engineer in the early 19$^{\text{th}}$ century, at a time when roads had to lead to a good rafting location at the riverbank. However, Jägerschmid's approach was limited to general guidelines for road gradients and spacing, and did not provide optimization techniques. In the early 20$^{\text{th}}$ century, planning for forest roads was not considered as crucial as for forest railways. After the second World War, those railway systems became less significant while forest roads and, therefore, their network planning became more important because of the rapid spread of truck transportation. Until the 1970s, road network layout was a cognitive, time-consuming task that required both engineering skills and practical experience. Computer-aided design arose in the 1970s, when automatic algorithms were developed by Kirby (1973), Mandt (1973), and Dykstra (1976). However, computing power and the availability of digital terrain data limited the capacity and usefulness of those programs. Nevertheless, spatial resolution decreased continuously, from about 200 m (Tan, 1999) to 10 m (Heinimann et al., 2003), while accuracy increased.

Tools for automatic road network design improved simultaneously with advancements in computing performance and the emerging availability of digital terrain data. A first stream was the introduction of decision-support tools, from simple spread sheet applications to integrated software packages running together with GIS-applications. A second stream of research was aimed at developing fully automated tools that – for given terrain and design specifications – could apply mathematical optimization techniques to produce an optimal or near-optimal solution without any decisive influence from an operator. Seminal work in this regard was done by Twito et al. (1987), Epstein et al. (1994), Chung & Sessions (2001a), and Chung et al. (2007). The software tool PLANEX (Epstein et al., 1999) is probably the most widely used in forest management. However, it does not provide acceptable results for steep terrain. Anderson & Nelson (2004) have recently presented a technique for finding the shortest path between two locations, even in steep terrain, assuming that an accurate digital elevation model (DEM) is available. The approach described in the following chapters presents further improvements, mainly by considering the spatial variability of construction costs, turning constraints, and optimization for multiple objectives.

Graph optimization

The theory of graphs has its roots in work by Leonard Euler, as revealed in the problem of the "Seven Bridges of Königsberg" in 1746 that had first been published by Euler (1741). That topology involved edges, nodes and edges, and nodes and areas. Later, Sylvester (1878) introduced the mathematical term *graph* for chemical algebra. Now, the general formulation of a graph (G) is defined as follows: $G = (V, E)$, where V is a finite, non-empty set of vertices (nodes) and E is a finite set of edges (links between a pair of vertices $E \subset V \times V$). Furthermore, a weighted graph, which is relevant to our current study, is defined as $G = (V, E; w)$, where w is an attribute for each edge that represents the weight (cf., e.g., Jungnickel, 2005). Graph theory is widely used for modeling practical problems, including those pertaining to forest road network design (Sakurai et al., 2002). With such an application, the problem can be solved

with a specific graph optimization algorithm. In the thesis presented here, the most important methods incorporate Dijkstra's shortest path algorithm (Dijkstra, 1959) and the minimum spanning tree algorithms of Kruskal (1956) and Prim (1957), both of which have been utilized for a wide variety of challenges in operations research. The Steiner Minimum Tree (SMT), a subgraph that connects a subset of given nodes with a minimum weight, has been used as well. This tool was developed from studies conducted in the 1820s by Jakob Steiner, a Swiss mathematician who solved the problem of determining the Euclidean minimum connection of any three and four points in the plane. Launhardt (1872) then formulated this Steiner approach to find the cost-minimal lines of communications in Germany. As formulation of the SMT problem in graphs has become increasingly important, Karp (1972) has been able to prove that this problem is $\mathcal{NP}$-complete. Unfortunately, that means the problem is up to now not solvable with an algorithm within polynomial time deterministically. Nevertheless, different heuristics are known to provide a near-optimal solution in keeping with that time constraint.

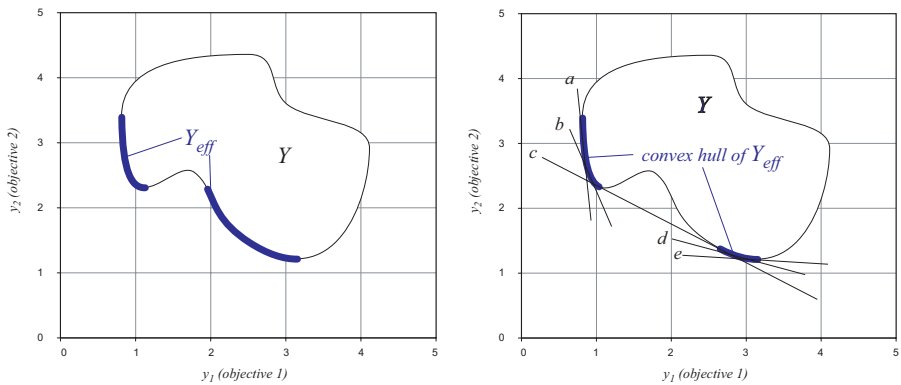

Figure 1: Efficient set (Y_{eff}) and convex hull around Y_{eff} in the criterion space. a, ..., e represent the tangents around Y_{eff}.

Multi-criteria optimality

The theory of optimality and the economical formulation of multiple, conflicting objectives had its start at the end of the 19$^{\text{th}}$ century. Edgeworth (1881), (1889), and Pareto (1896–1897) introduced the effects of feasible and unfeasible solutions in welfare economics. The border line for solution space between feasible and unfeasible alternatives is now known as the Pareto frontier and Pareto border, respectively. Solutions at the Pareto frontier are *Pareto-optimal*. There, it is impossible to enhance one objective without diminishing at least one other objective. Since the 1950s, Pareto-optimality has become an important notion in neoclassical economics, with broad applications in game theory, engineering, and the social sciences. Together with economical and technical applications, fundamental work has been conducted in mathematical science. However, the terminology may differ across disciplines. Here, we have followed the definitions of Ehrgott (2000), which are state-of-the-art for mathematical multi-criteria optimization. They present x as the solution and x^* as the *Pareto-optimal solution*. The set of feasible solutions is called the solution space X; the set of Pareto-optimal solutions, X_{Par}. "Decision" is a synonym for "solution"; "decision space", a synonym for "solution space". Every feasible x has a vector y that consists of a finite set of criteria $(y_1, y_2, y_3, ...)$, $y = f(x)$, where $f(x)$ is the objective function.

The set of feasible criterion vectors is Y, i.e., the "criterion space". The criteria for a Pareto-optimal solution x^* is called an *efficient point* y^*. Mapping X_{Par} on the criterion space leads to the *efficient set* Y_{eff}.

Solutions which are not Pareto-optimal are definitively not sensible for real world applications. However, we can not say that every Pareto-optimal solution leads to a sensible solution. For example, all Pareto-optimal solutions not located on the convex hull of Y_{eff} leads to an unfavorable ratio between the increase of one objective and the decrease in another one. Therefore, our main goal is to find all Pareto-optimal solutions which are located on the convex hull of Y_{eff} (Fig. 1).

Problem definition and scope

The ideal forest road network must be able to access different points within an area, e.g., good landing locations or the existing forest infrastructure. The most important locations should be accessible from two directions in order to provide some redundancy if road segments become temporarily blocked. Whereas sites with a higher priority should be reached directly, it does not matter whether sites with low priority have a long access distance. Our approach is based on the following assumptions:

- the location for the set of mandatory access nodes (K) is known,
- redundant access to the mandatory nodes is not needed,
- all locations have the same priority.

If the problem can be modeled as a mathematical graph (G), we then look for the weight (w)-minimal subset of this graph (G') that connects all mandatory nodes ($K \subset V$) minimally. This is known as an SMT problem.

The result of such optimization is a road network layout in the form of a digital geo-referenced vector file. The data format is compatible with ArcGIS, and its accuracy of 10 m is adequate for preliminary planning. Additionally, our program provides detailed cost and impact information for each road segment.

Here, we describe a forest road as a sequence of straight lines, curves, and switchbacks. The width of the roadway is defined by different cross sections. Even though a particular cross section in steep terrain may necessitate the movement of a lot of earth, the model is strictly attached to the terrain surface. This model does not consider the design of bridges and tunnels for crossing extremely difficult units. However, it is possible to add potential bridges and tunnel locations manually before the optimization process begins.

Outline

Our road network optimization framework can tackle mountainous project areas up to a size of about 50 km^2, assuming a resolution of 10 m. In steep terrain, the resolution of the underlying DEM should be at least 10 m if the model is to be useful for recognizing uneven terrain. The framework consists of four major clusters of components (Fig. 2): (I) a model to estimate spatial variability in road construction and maintenance costs; (II) a concept that defines discrete road segments and geometric constraints, and then is mapped on a mathematical graph; (III) an objective function for multiple objective dimensions; and (IV) the optimization procedure itself.

For this thesis, the four component clusters are presented as separate papers that have been or will soon be published in scientific journals:

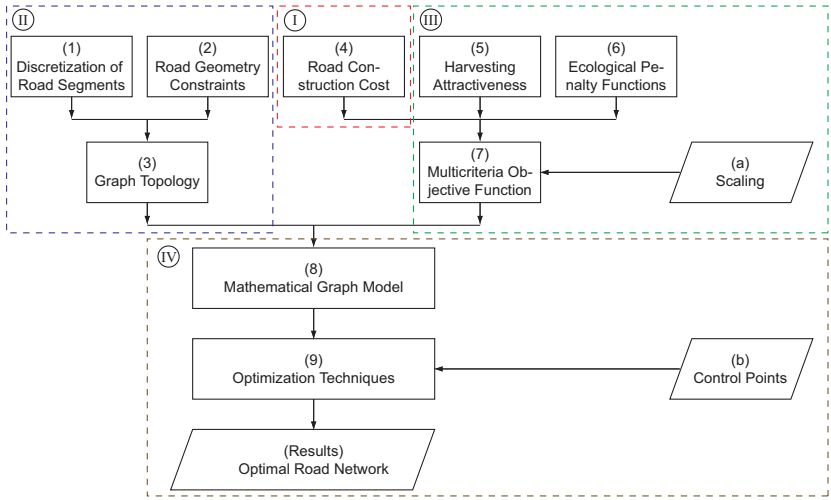

Figure 2: Framework of the automatic road network design model

Paper I – "Modeling spatial variability in the life-cycle costs of low-volume forest roads"[1]. This describes a generic model for road construction and maintenance costs (Component 4). A cost estimation model has been developed for mountainous areas, and this paper shows the effect of introducing a DEM and a layer for the geotechnical unit of the road network design.

Paper II – "Improved road network design models with the consideration of various link patterns and road design elements"[2]. Horizontal and vertical road alignment constraints are mapped on a mathematical graph (Components 2, 3), and the effect of different link patterns is evaluated in order to discretize the road (Component 1).

Paper III – "Automatic road-network planning for multiple objectives"[3]. Themes include the integration of construction costs, harvesting-attractiveness (Component 5), and adverse ecological impacts (Component 6) into the same optimization (Component 7). For harvesting-attractiveness, we have selected the cable yarder system; as our two examples for analyzing ecological impacts, we have chosen the capercaillie (*Tetrao urogallus*), the largest mountain grouse in Europe, and which is now threatened with extinction, plus marshlands, which are very rare in Switzerland. Here, we succeed in finding Pareto solutions and trade-offs among these different objectives. However, this paper does not follow the terminology defined by Ehrgott (2000). Instead, we use standard definitions common to the economics discipline, which do not distinguish between solution space (X) and criterion space (Y). Our diagram of a Pareto frontier is, in fact, the mapped criterion vectors for Pareto-optimal solutions within the criterion space, Y_{eff}. With the chosen method, we are able to identify only the Pareto-optimal solutions,

[1]Stückelberger, J.A., Heinimann, H.R. and Burlet, E.C. (2006). European Journal of Forest Research, 125: 377–390.

[2]Stückelberger, J.A., Heinimann, H.R. and Chung, W. (2007). Canadian Journal of Forest Research, 37: 2281–2298.

[3]Stückelberger, J.A., Heinimann, H.R., Chung, W. and Ulber, M. (2006). In: Chung, W. and Han, H.S. (Eds.): Proceedings of the 29th Council on Forest Engineering, pp. 233–248. July 30 – August 2, 2006, Coeur d'Alene, ID, USA. This report received the Council on Forest Engineering 2006 Student Communications Award for the best paper.

which are located on the convex hull of (Y_{eff}, and not all Pareto-optimal solutions (X_{Par}). Nevertheless, this precision does not change our conclusions.

Paper IV – "Multi-criteria optimization procedures for designing a forest road network"[4]. The main focus is on the mathematical formulation of a graph model (Component 8), the optimization technique (Component 9), and the results of our model evaluation. This paper also provides an overview of the entire framework for Components 1 to 9. We specify the incomplete definition of Pareto optimality, and we explore the efficiency presented in Paper III. A case study in the area of "Wägital", on the northern slopes of the Swiss Alps, demonstrates the trade-offs within a tri-objective optimization.

[4]Stückelberger, J.A., Heinimann, H.R., Schwartz, J., Steger, A. and Chung, (submitted October 2007).

Chapter 1

Modeling spatial variability in the life-cycle costs of low-volume forest roads

Jürg Andreas Stückelberger, Hans Rudolf Heinimann,
Edouard Charles Burlet

Received: July 22, 2005 / Accepted: December 12, 2005 /
Published: May 6, 2006

European Journal of Forest Research (2006)125: 377–390

Abstract

Cost estimation is probably the most decisive factor in the process of computer-aided, preliminary planning for low-volume road networks. However, the cost of construction is normally assumed to be route-independent for a specific project area, resulting in sub-optimal layouts. This is especially true for mountainous terrain and in areas with unstable subsoil. Here, we present a model for more accurately estimating spatial variability in road life-cycle costs, based on terrain surface properties as well as geological properties of the subsoil. This parametric model incorporates four structural components: embankment, retaining structures, pavement, and drainage and stream-crossing structures. It is linked to a geodatabase that allows users to derive location-specific parameter values as input. In applying this model, we have demonstrated that variability in costs ranges widely for mountainous areas, with the most expensive construction being approximately five times greater there than on more favorable sites. This variability strongly affects the optimal layout of a road network. First, when location-specific slope gradients are considered, costs are reduced by about 17% from those calculated via currently available engineering practices; when both slope gradient and geotechnical formations are included, those costs are decreased by about 20%. Second, the length of theroad network is increased by about 4% and 10% respectively, compared with current practices.

1.1 Introduction

Computer-aided engineering approaches for the layout of low-volume forest road networks have been in development since the 1970s (Kirby, 1973, Mandt, 1973, Dykstra, 1976), resulting in software packages such as PLANS (Twito et al., 1987), PLANEX (Epstein et al., 2001), or NETWORK 2001 (Chung & Sessions, 2001b). Each formulates the problem in terms of combinatorial optimization, which comprises three main components: (1) a finite set of possible road segments for a specific project area, (2) an objective function, and (3) an optimization mechanism. The objective function represents both construction and transportation costs, which must be minimized by considering specific constraints. Accuracy of this cost information is a decisive factor in identifying an optimal or at least near-optimal solution. However, construction-cost estimates very often rely on expert judgments, and are assumed to be route-independent. Because high costs are increasingly becoming a major concern when building low-volume roads, engineers urgently need to develop an effective, more highly accurate procedure for estimating route-dependent costs.

Three methodological streams of cost estimating are available: (1) direct rule-of-thumb estimating, (2) estimating relationships, and (3) bottom-up parametric modeling. The first method employs a judgmental estimate by an expert familiar with the current task. Such direct estimations rely more or less on data from past projects or programs, with readily available data. This approach has historically been dominant in preliminary road-network planning, serving as the basis for software packages such as PLANEX or NETWORK 2001.

The second approach, using estimating relationships and formulae, calculates the cost of either individual components or the entire system, and is based on cost-driving technical parameters. Markow & Aw (1983) have identified relationships to predict the volume of earthwork needed, as well as the numbers of culverts and bridges per unit length. Those relationships estimate physical construction quantities, which are then multiplied by respective unit prices and summed to determine the total cost of construction. In contrast, Anderson & Nelson (2004) have devised an estimating relationship that uses only road gradient as an input parameter.

The third method – bottom-up parametric modeling – starts with a work-breakdown structure (WBS) that represents the subsystems, components, or elements of a whole project. Here, similar deliverables are grouped into classes and a physical measure is then used as an indicator for cost within each class. Durston & Ou (1983) have developed an approach that considers the following subsystems: earthwork, clearing area, grubbing area, seeding area, ditch relief culverts, drainage crossings, and the aggregate volume for surfacing. This particular model, run on a hand-held computer, has been demonstrated to be more effective and accurate than previously used techniques. Heinimann (1998) has developed a similar approach that has been proven useful for cost-modeling under steep-slope conditions.

Here, we report the development and analysis of a model for estimating the life-cycle costs of forest roads, using location-specific parameters within a given project area. Our emphasis is on low-volume routes through mountainous regions. In addition, we present validation results, and discuss the influence of different cost-modeling options on both construction cost estimations and road network layouts.

1.2 Methods and model development

1.2.1 Cost estimation framework

Understanding how the design elements of road and terrain features can influence life-cycle costs is a challenging task. A cost-estimating procedure for predicting spatial variability must be able to automatically derive the cost-driving characteristics of road components for any specific location within a project area, and to analyze cost per unit of road length based on their unit-cost information.

Identification of the building components for low-volume roads follows a standardized WBS (Westney, 1997) within the construction industry, i.e., the cost classification by elements (CCE) approach (CCE, 1991). This method consists of three hierarchical levels: (1) the macro element, (2) the element group, and (3) the element level. For preliminary planning, Level 2 is an appropriate decomposition that accommodates four element groups: embankment structure, supporting and retaining structures, pavement structure, and drainage and stream-crossing structures. A standard design cross-section defines the structural dimensions in terms of crown, surface, ditch, and shoulder width, cut- and fill-slope angles, and retaining wall specifications (Fig. 1.1). To verify how those element groups affect construction costs, we assessed five low-volume projects carried out under different slope conditions in Switzerland (Fig. 1.2). There, the cost for the embankment structure (A) depended heavily on the slope gradient, whereas the cost for supporting and retaining structures (B) seemed to be relevant for slope gradients $> 50\%$. The costs for pavement (C) and drainage structure (D) were somewhat variable, as explained by the bearing capacity of the subsoil and by the design standard. For example, our second study site, "Prabé Sud", is situated in limestone in the central Swiss Alps with heavy rainfalls, where its asphalt concrete surface course incurred high construction costs. This preliminary, approximate analysis clearly indicated that slope gradient is the leverage factor for an analytical cost model. Additionally, the shear strength of the subsoil is critical to the design of cut-and-fill slopes (Coulomb, 1776, Terzaghi, 1944), as well as for the design of the pavement structure (AASHTO, 1993). Therefore, spatial information about geotechnical soil properties must be included if road engineers are to improve the accuracy of cost modeling.

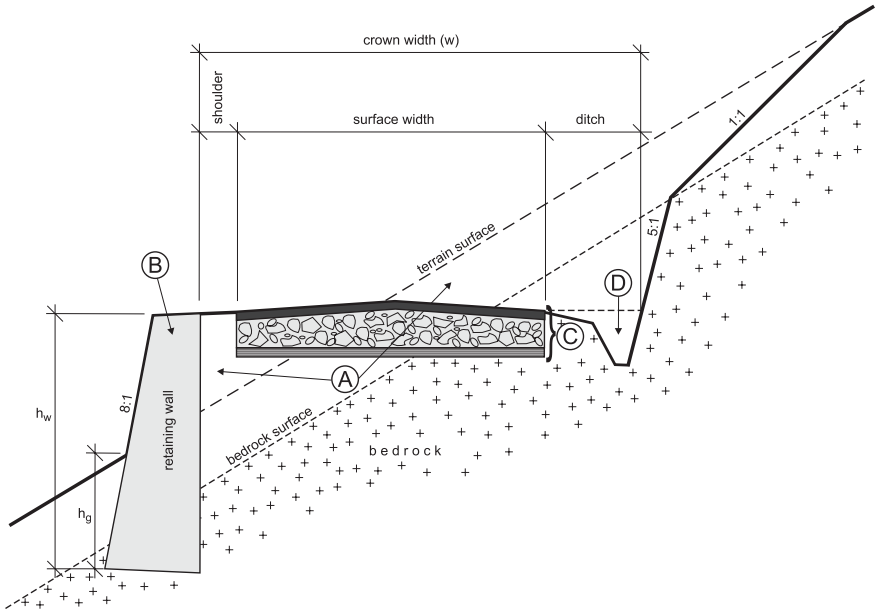

Figure 1.1: Standard design cross-section with four element groups: (A) embankment structure, (B) retaining structures, (C) pavement structure, and (D) drainage and stream-crossing structures. h_w: height of retaining wall, h_g: depth of foundation of retaining wall, w: crown width (surface + shoulder + ditch). Figure is not drawn to scale, especially in shoulder and ditch dimensions.

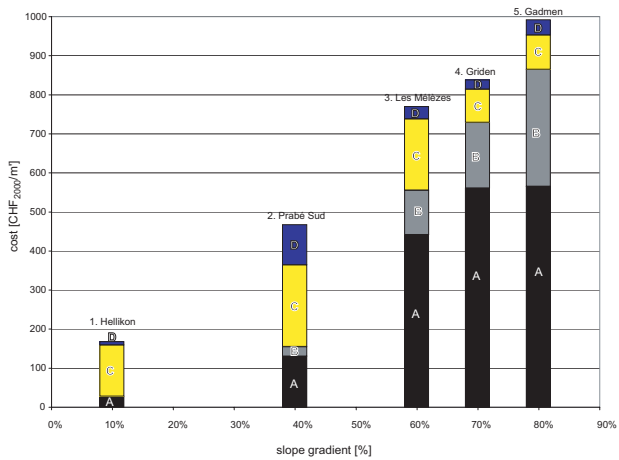

Figure 1.2: Cost of element groups in relation to slope gradient. All values are in Swiss francs (CHF), adjusted to price level for Year 2000.

1.2.1.1 Embankment model

Design engineers can choose among full-bench, self-balanced, or retaining-wall cross-sections. Therefore, our current analysis combined the element groups "embankment" and "retaining" structures. The embankment model was aimed at calculating the excavation volume of a standard cross-section at any location within a project area (Fig. 1.3). This model assumed: (1) the slope angle of the terrain (η) to be constant for the whole cross-section,(2) the cut- and fill volume to be self-balanced, (3) the angles for cut-and-fill slopes to be determined by the geotechnical properties of the subsoil, (4) consolidation of cut-and-fill slope material to differ, and (5) the bedrock surface to be parallel to the terrain surface. Loosening and loss of fill-slope material was assessed with a shrinking factor (f_{shr}) that depended on subsoil geotechnical properties. Because the cut-slope angle (ϕ_{cut}) is most often higher than that of the fill slope (ϕ_{fill}), the

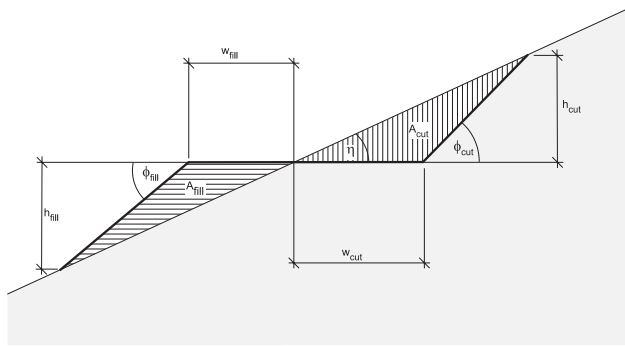

Figure 1.3: Standard design cross-section of low-volume road. A_{cut}: cut-slope area; A_{fill}: fill-slope area; h_{cut}: cut-slope height; h_{fill}: fill-slope height, uphill side; w_{cut}: road width, uphill side; w_{fill}: road width, downhill side; η: slope angle, depending on terrain surface; ϕ_{cut}: cut angle, depending on geotechnical properties; and ϕ_{fill}: fill angle, depending on geotechnical properties.

self-balanced design required the axis to be shifted horizontally in uphill direction (Fig. 1.3). However, if the slope angle had become equal to or larger than the fill-slope angle, the road would then have needed to be built according to a full-bench design. Heinimann (1998) has devised Equations 1.1, 1.2 and 1.3 to calculate excavation volumes for the conditions and constraints mentioned above; these equations are valid only for positive slope angles. Nevertheless, on a digital elevation model (DEM), values for slope gradient may also be negative. Therefore, our algorithmic implementation had to be robust, which required a more detailed model formulation as follows:

$$A_{cut} = \frac{w_{cut}^2 \cdot \tan(\phi_{cut}) \cdot \tan(\eta)}{2\big(\tan(\phi_{cut}) - \tan(\eta)\big)} > 0 \tag{1.1}$$

$$A_{fill} = \frac{(w - w_{cut})^2 \cdot \tan(\phi_{fill}) \cdot \tan(\eta)}{2\big(\tan(\phi_{fill}) - \tan(\eta)\big)} > 0 \tag{1.2}$$

$$f_{shr} = \frac{A_{fill}}{A_{cut}} \leq 1 \tag{1.3}$$

$$w_{cut}^2 \cdot \underbrace{\left(\frac{\tan(\phi_{cut}) \cdot f_{shr}}{\tan(\phi_{cut}) - \tan(\eta)} - \frac{\tan(\phi_{fill})}{\tan(\phi_{fill}) - \tan(\eta)}\right)}_{a}$$

$$+ w_{cut} \cdot \underbrace{\frac{2w \cdot \tan(\phi_{fill})}{\tan(\phi_{fill}) - \tan(\eta)}}_{b}$$

$$+ \underbrace{\frac{w^2 \cdot \tan(\phi_{fill})}{\tan(\eta) - \tan(\phi_{fill})}}_{c} = 0 \tag{1.4}$$

$$w_{cut} = \frac{-b \pm \sqrt{b^2 - 4ac}}{2a} \tag{1.5}$$

To make the analytical explanation easily understandable, only positive slope gradients were considered in Equations 1.1, 1.2, 1.3, 1.4, 1.5, 1.6, 1.7, 1.8 and 1.9. Cut-slope and fill-slope angles (ϕ_{cut} and ϕ_{fill}) had to be greater than ground slope (η) because of geometrical constraints. Here, we examined three different cases in terms of variable a (Eqs. 1.5, 1.6): (1) fill-slope angles larger than cut-slope angles, (2) cut-slope angles greater than fill-slope angles, and (3) fill-slope angles equal to cut-slope angles. In the first case, the resulting value was less than zero ($a < 0$). Therefore, the root term of Equation 1.5 was the limiting factor, and the discriminate d had to be positive (Eq. 1.6), thereby resulting in Equation 1.7.

$$d = b^2 - 4 \cdot a \cdot c > 0 \tag{1.6}$$

$$d = \frac{4 \cdot \ w^2 \cdot \tan(\phi_{fill}) \cdot \tan(\phi_{cut}) \cdot f_{shr}}{\big(\tan(\phi_{fill}) - \tan(\eta)\big) \cdot \big(\tan(\phi_{cut}) - \tan(\eta)\big)} > 0 \tag{1.7}$$

All factors in the numerator of Equation 1.7 were positive, and both ϕ_{cut} and ϕ_{fill} were always greater than η. Hence, the formulation was correct for any possible case. Likewise, because the negative branch of the root term in Equation 1.5 led to values greater than w, only the positive branch of the root term was feasible.

The second case dealt with fill angles smaller than cut angles ($a > 0$). In most case, however, geotechnical stability required the latter to exceed the former. Assuming that, in some cases, the fill angles were smaller, the root term in Equation 1.5 become smaller than b. As a consequence, only the positive branch of the root term resulted in feasible solutions.

The third case considered fill angles equal to cut angles ($a = 0$). The conditions for this case follow from Equation 1.8. Furthermore, for a self-balanced design the cut-road width was equal to the fill-road width Equation 1.9.

$$f_{shr} \cdot \tan(\phi_{cut})\big(\tan(\phi_{fill}) - \tan(\eta)\big) - \tan(\phi_{fill})\big(\tan(\phi_{cut}) - \tan(\eta)\big) = 0 \tag{1.8}$$

$$w_{cut} = w_{fill} = -\frac{c}{b} = \frac{w}{2} \tag{1.9}$$

Equations 1.1, 1.2, 1.3, 1.4, 1.5, 1.6, 1.7, 1.8 and 1.9 are analogously applicable for negative slope gradients ($\eta < 0$). However, in these cases cut-slope and fill-slope angles (ϕ_{cut} and ϕ_{fill}) had to be more negative than ground slope angle (η) because of geometrical constraints.

When one knows the relation of w_{cut} to w_{fill}, one can then calculate self-balanced cut-and-fill volumes for each location in the project area. However, such a cross-section design is not always the most appropriate. Full bench is a second option for cross-section design, increasing

embankment stability in steep terrain or unstable subsoil conditions by shifting the road structure horizontally in the uphill direction. As the third option for cross-section, the retaining-wall design locates those structures on either the uphill or downhill side of the road. We used a lookup table to define the critical terrain slope figures for each geotechnical unit as well as to discriminate among these three cross-section design solutions (cf., Tab. 1.1).

In difficult terrain conditions, part of the excavation volume may be of rock. Practical experience in Switzerland has shown that the unit cost for its excavation is approximately 4 to 5 times greater than for the removal of soil alone. Inaba et al. (2001) have developed an empirical model to estimate the share rock excavation as a function of slope, a coefficient for each geological unit ($coef_{rock}$), and crown width for low-volume roads Equation 1.11. For the current study, we determined the share of rock for cut-slope areas in three groups of geological formations, all with crown widths of 4.10 m (Fig. 1.4). The first group comprised mesozoic and tertiary sediment formations, typical of the northern slopes of the Alps, and included conglomerate, sandstone, limestone, and flysch. The second group consisted of intrusive and the metamorphic rock formations – granite and gneiss – that are typical for the central and southern slopes of the Alps. The third group consisted of quaternary formation such as moraine and alluvial deposit. For slope gradients of up to approximately 40%, the necessary volume of rock excavation was of minor importance and could be easily neglected. At gradients of 70%, about one-third of the volume was rock; at gradients of about 90%, two-thirds consisted of rock. In general, the rock excavation volume was calculated as the product of the cut-slope volume multiplied by the rock share factor (Fig. 1.4).

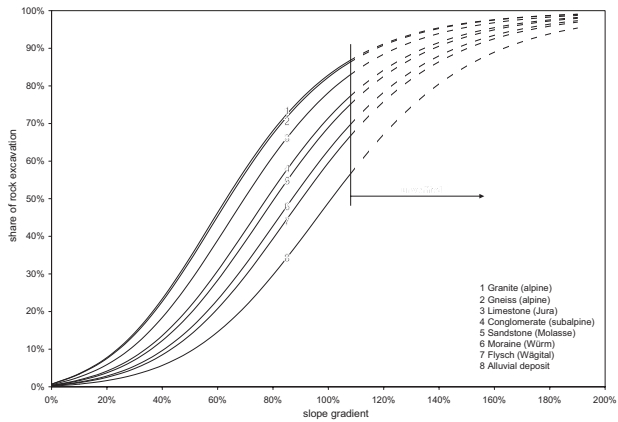

Figure 1.4: Share of rock excavation for low-volume road (crown width = 4.10 m), as a function of slope gradient and type of geological formation.

$$\begin{aligned} logit &= -6.69 + coef_{rock} + (4.913 + 0.396 \cdot \tilde{w}) \cdot \tan(\eta)^{0.6} \\ p_{rock} &= \frac{e^{logit}}{1 + e^{logit}} \end{aligned} \tag{1.10}$$

where, $coef_{rock}$ = geological parameter for rock ratio estimation (cf., Tab. 1.1)
η = slope angle of the terrain
e = the Euler number (2.718...)
$logit$ = interim result for logit-function
p_{rock} = share of rock in total cut area [0...1]
$\tilde{w}$ = the dimensionless numerical value of the road crown width in meter

The total costs for earthwork and embankment preparation for a road segment depended on both the earth excavation volume (V_{cut}) and rock excavation volume (V_{rock}). Volume was approximated by the frustum of a pyramid (Eq. 1.11), whereas the total embankment cost was determined with Equation 1.12.

$$V = \frac{l}{3} \cdot \left(A_0 + \sqrt{A_0 \cdot A_1} + A_1\right) \tag{1.11}$$

where, A_0 = area (either fill or cut) of the initial cross-section
A_1 = area (either fill or cut) of the following cross-section middle length
l = middle length of the arc of the segment
V = volume (either fill or cut)

$$C_{emb} = V_{fill} \cdot c_{comp} + V_{cut} \cdot \left(c_{exc} + p_{rock} \cdot c_{rock}\right) \tag{1.12}$$

where, c_{comp} = cost for compaction per volume unit
C_{emb} = embankment cost
c_{exc} = excavation cost per volume unit
c_{rock} = extra cost for rock excavation per volume unit
p_{rock} = share of rock in total cut area [0...1]
V_{cut} = cut volume
V_{fill} = fill volume

1.2.1.2 Retaining structure model

In difficult terrain conditions (e.g., steep slopes, unstable soil conditions), retaining structures are necessary to provide safe embankments. Assuming that the slope gradient could be extracted automatically from a digital elevation model, and that preference rules indicated a retaining-wall cross-section design, we then calculated the height (h_w) (Fig. 1.1) and length of the retaining wall. Additional height (h_g) used for the foundation was presumed to be constant. The cost for a retaining wall was assumed to be proportional to its height times length (Eq. 1.13), a rule that seems appropriate for heights of up to 3 m.

$$C_{wall} = (h_{w1} + h_{w2} + 2 \cdot h_g) \cdot l \cdot c_{wall} \tag{1.13}$$

where, c_{wall} = cost for retaining wall per unit area
C_{wall} = cost for retaining wall
h_{w1}, h_{w2} = height of retaining walls (uphill and downhill sides)
h_g = constant value for foundation and clearance of retaining wall (in the present model, = 1 m)
l = length of road segment

1.2.1.3 Pavement structure model

The cost of pavement structures is assumed to be proportional to numerous variables, including the surfaced road area for specific soil-bearing conditions, expected traffic volume, and the

aggregate materials used for the sub-base, the base course, and the surface course. To design the pavement structure, we adapted AASHTO procedures to the special requirements for low-volume roads in Switzerland (Burlet, 1980). In Equation 1.14, both a standard road width and widening at curves and switchbacks were considered.

$$C_{pav} = \left(w_{s0} + \frac{k_{cw}}{r}\right) \cdot l \cdot c_{pav} \tag{1.14}$$

where, c_{pav} = cost for pavement per unit area
C_{pav} = cost for pavement structure
k_{cw} = constant value for road widening in curves (in the present model, = 26 m)
l = length of road segment
r = curve radius
w_{s0} = standard road surface width

1.2.1.4 Drainage and stream-crossing structures

The cost for drainage structures, such as ditches or culverts, was assumed to be proportional to road length (l) (Eq. 1.15). Ditch relief culverts ideally are arranged at constant 50-m intervals, but would be unnecessary on flat terrain ($\eta < 12\%$). Three principal types of stream-crossing structures are available: bridge, culvert, and ford, the last type being the only one automatically considered in the present model. Its construction incurred a higher cost due to the hardening measures of the surface, extra drainage (e.g., a culvert at the vertex location in the channel), and additional retaining structures. The unit cost for a ford presumably depends on geology and size of the area defined by its location.

$$C_{drain} = \begin{cases} 0 & \text{if } \tan(\eta) < 12\% \\ \frac{C_{culvert}}{d} \cdot l & \text{else} \end{cases} \tag{1.15}$$

where, $C_{culvert}$ = cost for single culvert
C_{drain} = cost for drainage structure
d = distance between ditch relief culverts (in the present model, = 50 m)
l = length of road segment

1.2.1.5 Life-cycle cost model

Life-cycle costs entail those for construction, routine and periodic maintenance, rehabilitation, and decommissioning. The model analyzed here did not consider the last two factors, and assumed the maintenance cost to be dependent only on road gradient and geology. This assumption, however, differs from practices in the USA and in Canada, where thresholds for total traffic volume trigger periodic maintenance. To make these cost components comparable, they must be normalized in time. Net present value (NPV), annual equivalent rate (AER), and internal rate of return (IRR) are measures commonly used for obtaining the time value of money. Our model followed the NPV approach, assuming a project life cycle of 50 years, an interest rate of 2%, and a constant share in maintenance costs per year. Equations 1.16 and 1.17 are widely applied in engineering economics (Heinimann, 1998, Park & Sharp-Bette, 1990).

$$C_{ann} = C_{reg} + \frac{C_{peri}}{n} \tag{1.16}$$

$$C_{tot} = C_{con} + C_{ann} \cdot \left(\frac{1-(1+i)^{-N}}{i} \right) \quad (1.17)$$

where,
C_{ann} = average annual maintenance cost
C_{con} = construction cost
C_{per} = periodical maintenance cost
C_{reg} = regular maintenance cost
C_{tot} = total cost for a single road segment
i = annual interest rate (in the present model, = 2%)
n = periodical-maintenance interval (in the present model, = 5 years)
N = amortization period of the road (in the present model, = 50 years)

1.2.1.6 Curve and switchback model

Detailed road engineering defines the horizontal layout of a road as a consecutive set of straight lines and curves, whereas computer-aided preliminary planning tools usually use a traverse representation, consisting of a continuous series of lines. The latter approach has two shortcomings (Heinimann et al., 2003). First, the road length for curves is shorter than the tangent distance, and the road does not widen (cf., Eq.Equations 1.14). Second, a change in direction of $> 135°$ requires a "hairpin bend" embankment structure, called a switchback. Constructing a switchback always involves considerable additional earthwork and surfacing, resulting in significantly higher total cost. The balancing of cut-and-fill volumes is not possible for a single cross-section of a switchback, but must be achieved between the beginning and the end of the switchback curve. Figure 1.5 shows that, depending on the central angle (γ), our procedure for calculating switchback costs required several intermediate cross-sections. The best possible volume balance was then identified by shifting the switchback center orthogonally to the contour lines, at a step width of 0.5 m and within an interval of -5 m to +5 m. This procedure was similar to one proposed by Aruga et al. (2004).

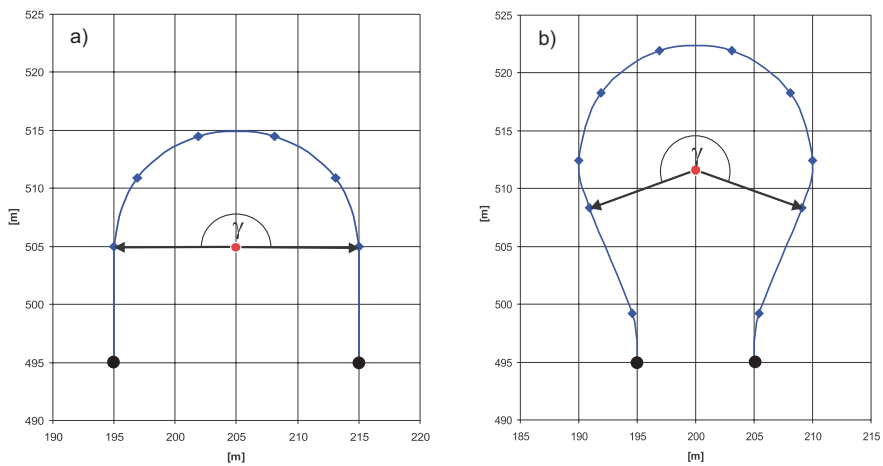

Figure 1.5: Road segments of switchbacks, **(a)** γ central angle = 180°, **(b)** γ central angle = 220°. Each switchback starts and ends at regular nodes (*bold point symbols*). The centerline is subdivided into 6 **(a)** or 10 **(b)** respectively, intermediate sections (*slim point symbols*). Regular nodes are fixed whereas locations of intermediate nodes depend on the location of the center as well as γ.

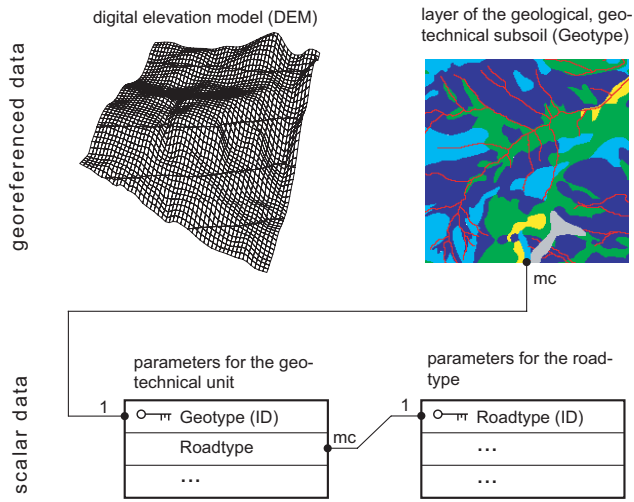

Figure 1.6: Entity-relationship model for the input data

1.2.2 Organization of input data

1.2.2.1 Data model

One purpose of the present model was to derive cost-driving features automatically from a geographical database. This database, represented by 10 $m \times 10$ m cells, had two layers: (1) a digital elevation model (DEM) of the terrain surface, and (2) a geotechnical classification of the subsoil. A first lookup table (Tab. 1.1) specified the engineering and cost properties for each geotechnical unit. A second lookup table (Tab. 1.2) defined the design elements of a standard cross-section for each geotechnical unit. Figure 1.6 shows an entity-relationship model of the data. This data structure makes it possible to adapt the model to any area specific conditions in the world as long as the road can be modeled by the four element groups explained in Subsection 1.2.1.

1.2.2.2 Geotechnical parameters

Engineering and cost properties are specific for each geotechnical unit. Site specific parameters are stored as a record in a data base table consisting of five engineering properties (cut-slope inclination ($\tan(\phi_{cut})$), fill-slope inclination ($\tan(\phi_{fill})$), inclination of retaining wall ($\tan(\phi_{wall})$), shrinking factor (f_{shr}), and a coefficient for rock ratio estimation ($coef_{rock}$), cf., Eq. 1.10), six parameters for construction costs (excavation cost (c_{exc}), cost for emplacement and compaction of the filling material (c_{comp}), additional cost for rock excavation (c_{rock}), cost for pavement structures (c_{pav}), cost for retaining walls (c_{wall}), and cost for drainage structures (c_{drain})), and two parameters for maintenance (constant cost per road length ($c0_{ann}$), and variable cost proportional to the road gradient ($c1_{ann}$) and road length). Special terrain types (e.g. landslides, stream crossings, rehabilitation of existing roads) may require additional cost parameters. These parameters can be defined by flat cost per link or flat cost per length. Sites where construction is impossible (e.g. lake, marshland) are represented by negative values. Construction processes

(full mechanized, low mechanized, labor intensive) are represented by cost values only that may be obtained by analyses of contractor bids, engineering estimation, or final costing analysis. Table 1.1 shows all geological parameters used in the area of Wägital (cf., Subsection 1.3.2).

1.2.2.3 Road parameters

The model assumes one predominant road type for a specific project area. However, the designer may specify different design parameters, e.g. a smaller road width in rocky terrain are, or a less maximum, road gradient in instable subsoil. The road type is linked to the geotechnical unit and defined by the parameters maximal allowable road gradient (η_{max}), minimal radius in curves (r_{min}) and switchbacks (r_{SB}), standard road surface width (w_{s0}), width for ditch and shoulders (w_{d+s}), road widening in curves (k_{cw}), and minimal excavation depth for pavement structures (z_{min}). Table 1.2 shows all road design parameters used in the area of Wägital (cf., Subsection 1.3.2).

1.2.3 Model implementation

Our procedures were implemented via Borland Delphi 7.0 software (Object Pascal language), which produced approximately 3700 lines of code. Input and output data consisted entirely of text files that could be easily imported from or exported to commercial geographical information systems, such as ESRI ArcGIS. At present, this implementation can handle areas of up to 100 km^2, with 10 $m \times 10$ m raster cells. The model split the road route into 10-m segments for straight lines and curves, and 2-m sections for switchbacks. Procedures for optimizing the road network were implemented in a separate program unit, which was previously described by Stückelberger et al. (2004).

1.3 Validation and evaluation

1.3.1 Model validation

Validation was aimed at demonstrating that our model reasonably represented the cost of low-volume road projects. It required high-quality cost data normally available only after a project is completed. However, a full validation that investigates assumptions, input parameters, and output values is difficult to achieve. Therefore, compromises were necessary, resulting in a preliminary validation approach.

In this current study, validation was performed for projects on two different geological formations. The first covered an area in the molasse zone; the second, in limestone. Both were located on the northern slopes of the Swiss Alps. The first part of the validation compared the excavation volumes produced by the model with those values obtained from actual, detailed road projects, as engineered by students in the molasse zone. The second part occurred in the limestone zone, and was mainly focused on investigating rock excavation volumes and costs. Decisive figures from real-world cases were extracted from engineering documentation, especially technical reports and cost estimates. Application of the model required us to specify the design element and the unit-cost parameters, both of which were stored in a lookup table linked to the geology layer of the spatial database (Fig. 1.6).

The first part of the validation demonstrated that our model accurately estimated the excavation volume. However, it also showed that a 10 $m \times 10$ m representation resulted in inaccu-

Geotechnical unit			engineering parameters				cost parameters									flat cost
ID	name	road type	tan (φ_{cut})	tan (φ_{fill})	tan (φ_{wall})	f_{shr}	$coef_{rock}$	c_{exc} $\frac{CHF}{m^3}$	c_{comp} $\frac{CHF}{m^3}$	c_{rock} $\frac{CHF}{m^3}$	c_{pav} $\frac{CHF}{m^2}$	c_{wall} $\frac{CHF}{m^2}$	c_{drain} $\frac{CHF}{m}$	$c0_{ann}$ $\frac{CHF}{m \cdot a}$	$c1_{ann}$ $\frac{CHF}{m \cdot a}$	link CHF	length $\frac{CHF}{m}$
10	standard subsoil	1	1	0.8	10	0.8	1	6.8	4	12	28	80	18	1.2	2	0	0
21	moraine	1	1	0.8	10	0.8	0.68	6.8	4	12	28	80	18	1.2	2	0	0
22	alluvial deposit	1	1	0.8	10	0.8	0.11	6.8	4	12	28	100	18	1.2	2	0	0
31	conglomerate	1	1	0.8	10	0.8	1.07	6.8	4	12	28	80	18	1.2	2	0	0
32	sandstone	1	1	0.8	10	0.8	0.95	6.8	4	12	28	100	20	1.2	2	0	0
33	flysch	2	0.8	0.67	10	0.8	0.54	6.8	10	5	52	200	85	2.5	5	0	0
34	limestone	1	1.25	0.8	10	0.8	1.43	6.8	4	15	28	80	15	1	0	0	0
41	granite	1	1.25	0.8	10	0.8	1.73	6.8	4	15	28	80	18	1	0	0	0
42	gneiss	1	1.25	0.8	10	0.8	1.69	6.8	4	15	28	80	18	1	0	0	0
51	landslide, low active	2	0.8	0.67	10	0.8	0	6.8	10	0	80	200	85	4.5	5	0	12
52	landslide, active	2	0.8	0.67	10	0.8	0	6.8	10	0	80	200	85	7.5	5	0	12
53	landslide, very active	2	0.8	0.67	10	0.8	0	6.8	10	0	80	200	85	10	5	0	12
61	stream, stable subsoil	1	1	0.8	10	0.8	1	6.8	4	12	41	200	20	3	5	1000	0
62	stream, instable subsoil	1	0.8	0.67	10	0.8	0.54	6.8	10	5	64	200	85	4	5	5000	0
81	existing road, good	3	1	0.8	10	0.8	1	0	0	0	0	0	0	1.2	2	0	0
82	existing road, poor	1	1	0.8	10	0.8	1	0	0	0	0	0	0	1.2	2	0	45
91	marshland	-1	-1	-1	-1	-1	-1	-1	-1	-1	-1	-1	-1	-1	-1	-1	-1
92	lake	-1	-1	-1	-1	-1	-1	-1	-1	-1	-1	-1	-1	-1	-1	-1	-1

Table 1.1: Engineering and cost parameters for each geotechnical unit. The data were calibrated for the area of Wägital (Switzerland).

Road type ID	name	η_{max}	r_{min} m	r_{SB} m	w_{s0} m	w_{d+s} m	k_{cw} m^2	z_{min} m
-1	no go	-1	-1	-1	-1	-1	-1	-1
1	standard road	0.12	20	10	3.4	0.6	26	0.30
2	road in instable	0.10	20	10	3.4	0.6	26	0.50
3	existing road	0.20	10	5	3.4	0.6	13	0.30

Table 1.2: Design parameters for each road type used in the area of Wägital (Switzerland)

rate estimates for stream channel or terrain edge locations. For the second part, data obtained from the engineering documentation were compared with the model output (Tab. 1.3). Here, the model overestimated the total embankment volume by about 16%, seemingly favoring a full-bench cross-section design. In contrast, the road engineers preferred a retaining-wall cross-section design, which was represented by a much higher cut-slope volume predicted by the model. Cost figures showed that the model estimate for the embankment structure was within the range of accuracy (+/-10%), while the engineer's estimate for the pavement structure was about 20% higher. Although the road engineer planned for additional turnouts and other areas to be surfaced with aggregate material, if those factors were neglected, costs for the pavement structure were more or less identical. The usefulness of our validation results was limited because they were based on a comparison of estimates from an engineer versus a model. A more reliable validation would have required accurate post-construction information on design-element unit quantities and unit cost, which is usually not available.

	Item	Unit	Project bid	Model	Difference
earth work	Cut volume	m^3	1'929	2'720	+41%
	Fill volume	m^3	1'042	7'21	-31%
	Total volume	m^3	2'971	3'441	+16%
cost	Embankment and retaining structures	CHF	78'465	85'648	+9%
	Pavement structure	CHF	59'200	45'900	-23%
	Drainage and stream-crossing structures	CHF	13'180	17'880	+36%
	Total cost	CHF	150'845	149'428	-1%

Table 1.3: Comparison of excavation and cost figures for two alternatives: (1) results of engineering project design and contractor bid versus (2) model results. Costs, in Swiss francs (CHF), are adjusted to price level for Year 1997.

1.3.2 Model evaluation

The objectives of our model evaluation were (1) to investigate the influence of terrain parameters, e.g., slope and geology, on the spatial variability in construction costs; and (2) to assess the effect of cost-estimating strategies on optimal road network layout.

Figure 1.7: Spatial variability in road life cycle costs for Scenario III, based on slope gradient and geotechnical soil properties. The lake "Wägital" is at eastern boundary and watershed is at western boundary. (5 $km \times 7$ km)

1.3.2.1 evaluation of road network layout

The "Wägital" project site is located on the northern slopes of the Swiss Alps, in flysch and limestone zones. This area is characterized by extremely difficult geotechnical conditions, such as low soil-bearing capacity (CBR values $< 3\%$), unstable terrain with many landslides, and a dense channel network. Evaluation was based on three cost-estimating scenarios:

1. Scenario I, which assumed construction costs to be route-independent (240 $\frac{CHF}{m}$) and constant for the entire project area. The design parameters (minimum curve radius (r_{min}), maximal allowable road gradient (η_{max}), etc.) correspond to road type #1 "standard road" of Tabel 1.2.

2. Scenario II, in which slope gradient was considered the only parameter affecting the spatial variability of construction costs. The geotechnical parameters correspond to geotechnical unit #10 "standard subsoil" of Tabel 1.1.

3. Scenario III, which considered both slope gradient and geotechnical information as decisive parameters as well as different road types for cost variability. All design and cost parameters are shown in Tabels 1.1 and 1.2.

Scenario I served as a reference for the engineering practices currently used to estimate costs at a preliminary planning stage.

	10%-quantile ($Q_{0.1}$)		median (50%)		90%-quantile ($Q_{0.9}$)		difference ($Q_{0.9} - Q_{0.1}$)	
	CHF	EUR	CHF	EUR	CHF	EUR	CHF	EUR
Scenario I	240.0	155.8	240.0	155.8	240.0	155.8	0.0	0.0
Scenario II	160.1	104.0	179.0	116.2	234.2	152.1	74.1	48.1
Scenario III	139.5	90.6	238.0	154.5	441.6	286.8	302.1	196.2

Table 1.4: Quantiles of cost estimation after Scenarios I, II, III

1.4 Results and discussion

1.4.1 Spatial variability of construction costs

The 35-km^2 project area included the lake "Wägital" at the eastern boundary and a watershed at the western boundary. For each of these 3 scenarios we calculated in each grid cell the potential road life-cycle cost for a unit length of 1 m, assuming a straight alignment of the road parallel to the contour line. Figure 1.7 illustrates the spatial variability in road life cycle costs for Scenario III, which considered both slope gradient and geotechnical soil properties. Figure 1.8 presents the variability of life-cycle cost per unit for the three model scenarios as cumulated frequency curves.

Scenario I assumed a route independent cost of 240 $\frac{CHF}{m}$. Therefore the variability is zero, resulting in a vertical straight line of cumulated frequency curve.

Scenario II, which considers terrain slope gradient as the only factor influencing construction cost resulted in a median cost of about 180 $\frac{CHF}{m}$ with a range of about 75 $\frac{CHF}{m}$ between the 10%-quantile ($Q_{0.1}$) and 90%-quantile ($Q_{0.9}$) (Tab. 1.4). The cumulated frequency curve represents more or less the distribution of the slope gradients in the project area.

Scenario III represents a cost estimating procedure that considers terrain, slope, and different road types resulted in a cumulative frequency curve with median cost of about 240 $\frac{CHF}{m}$ and a variability range of about 300 $\frac{CHF}{m}$. The huge cost variability is a result of different subsoil that was represented by three classes (A) stable subsoil in limestone and moraine, (B) instable subsoil in flysch formation and high landslide activity, and (C) stream crossing sites with laborious construction work.

The cumulative frequency curves of Scenario II and III asymptotically converge to the 100% line. However, values above the 98%-quantile should be excluded from analysis due to model limitation for very steep terrain conditions.

Assuming that Scenario III is closest to reality and the most accurate procedure, the results depicted in Figure 1.9 clearly demonstrate that conventional cost-estimation practices (which are route- and location independent) are inappropriate for difficult terrain conditions.

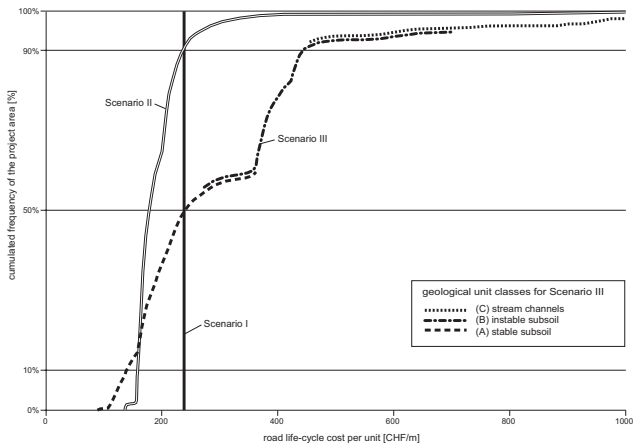

Figure 1.8: Variability of life-cycle cost per unit for Scenario I, II, and III. The curves show the cumulated frequency of the project area to the construction and maintenance costs for each scenario.

1.4.2 Influence of cost-estimating procedures on road network location

A minimum spanning tree problem was used to evaluate how various cost-estimating strategies affect the optimal layout of road networks. In this study, 10 mandatory access points were linked by a minimum-cost network (Fig. 1.9). Access points 000, BRH, and AU are at lake level (about 900 mNN), ROW, SBU, ALP, and OBO have a intermediate elevation between 1000 mNN and 1200 mNN, and EGS, TAS, and STO have a high elevation of about 1300 mNN. We first devised a finite set of vertices that corresponded to the centers of all 10 $m \times 10$ m grid cells. Second, a set of road links was defined from each vertex to its adjacent vertices. Third, we formulated a set of design constraints, e.g., minimum curve radius, maximum road gradient, and turning constraints for the combination of incoming and outgoing road links (Tab. 1.1 and 1.2). We then calculated the first- and second-order Steiner points (Prömel & Steger, 2002). Finally, we identified the minimum cost spanning tree by combining Dijkstra's (Dijkstra, 1959) shortest path (SP) and Prim's (Prim, 1957) minimum spanning tree (MST) algorithms (see also Stückelberger et al., 2004).

Criterion	Unit	Scenario I	Scenario II	Scenario III
Network length	m	17'406	18'176	19'001
Embankment and retaining structures	1000 CHF	3'098	1'972	1'847
Pavement structure	1000 CHF	3'337	3'062	2'871
Drainage and stream-crossing structures	1000 CHF	207	298	167
Total construction cost	1000 CHF	6'642	5'332	4'885
Avg. construction cost	$\frac{CHF}{m}$	382	293	257
Maintenance cost per year	1000 $\frac{CHF}{a}$	50.1	67.7	50.9
Net present value (50 years)	1000 CHF	8'196	7'430	6'464
Relative difference		reference	-17%	-21%
		+27%	+15%	reference

Table 1.5: Key values calculated for road network, based on three different cost-estimation scenarios

Figure 1.9 presents the evaluation results for the three scenarios. A visual assessment of the map demonstrates that the three strategies greatly affected the spatial layout of the road network. Scenario I has two connections from lake level to high level (BRH-SBU-ROW-EGS and AU-ALP-STO). Because the costs are route independent, the model tried to keep the road network at minimal length. Both effects resulted in a lot of switchbacks and therefore high life-cycle cost. Scenarios II and III shows nearly identical road routes in 000-BRH-SBU-AU and EGS-ROW-TAS. However, Scenario II connects the high level via access points AU-SBU-STO in less stable subsoil where as Scenario III made a connection via AU-OBO-ALP-STO in limestone layer, which is stable and therefore favorable.

Table 1.5 contains key data for the scenarios. Again, Scenario I depicted current modeling practices, which assumed route-independent costs. Optimization for this scenario resulted in the shortest road length (17.4 km), but the highest life-cycle cost (+27%) compared with the minimum cost alternative. Scenario II (slope gradient only) produced a total network length of 18.2 km. Compared to the minimum cost alternative, this scenario resulted in life-cycle costs of 15% above the minimum but 17% below the conventional practice. Finally, Scenario III, with both slope gradient and geotechnical information as major decisive parameters, was most cost-effective, with a minimum road network tree and life-cycle costs 21% lower than those incurred by standard, current practices.

1.5 Conclusions

We have developed a model for estimating forest road construction costs. This system considers location-specific terrain and subsoil parameters, and can be used to evaluate how various

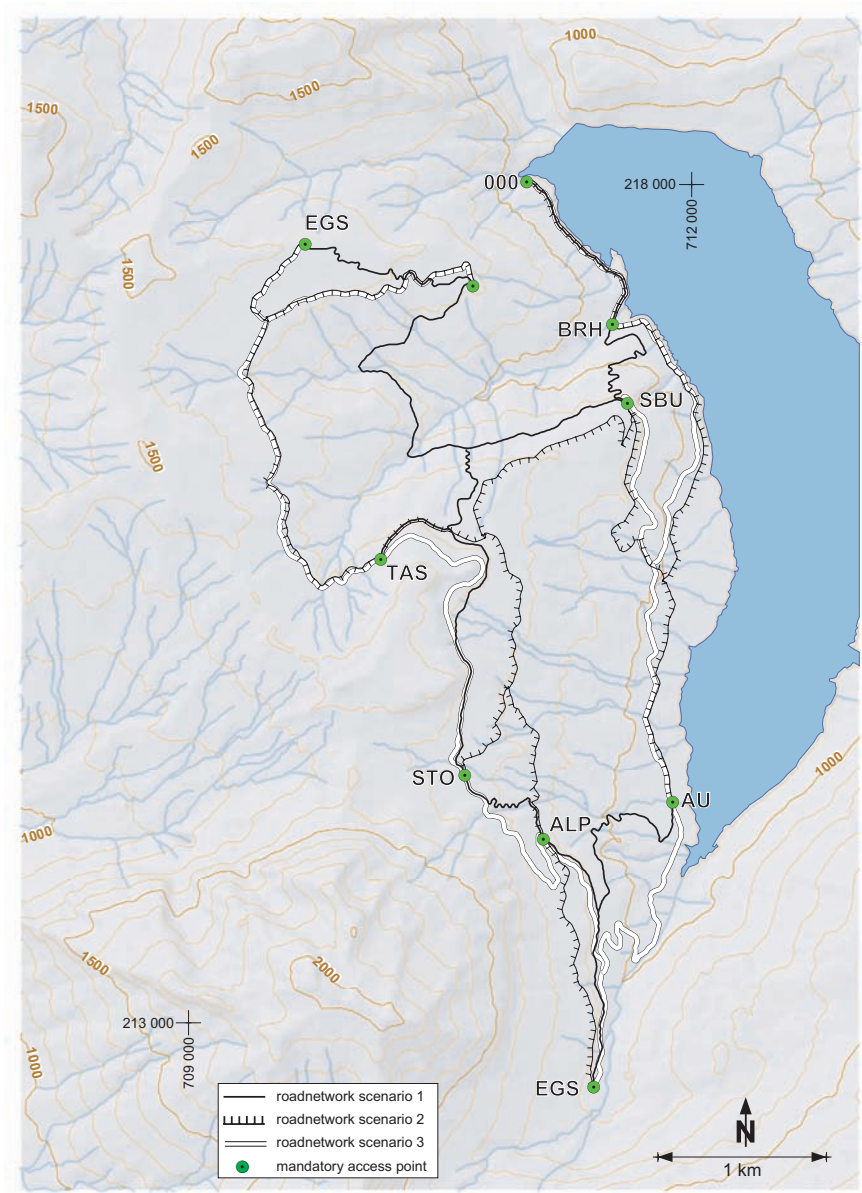

Figure 1.9: Model-designed road network for Scenarios I, II, and III, based on cost-estimating strategies defined in evaluation layout. Background: hill shade of relief, streams, and lake. Area ($5\ km \times 7\ km$) at Wägital, Switzerland

cost-estimating strategies affect the optimal layout of road networks. Our model consists of four element groups – embankment, retaining, pavement, and drainage structures – their dimensions and quantities being defined in terms of topographic, subsoil, and cross-sectional parameters. A spatial database that comprises a digital elevation model (10 $m \times 10$ m resolution) and specifications for geotechnical formations is a prerequisite if one is to derive location-specific terrain parameters. Our validation and evaluation of this model demonstrated that: (1) under difficult terrain conditions, construction costs can range from 140 (10%-quantile) to 440 CHF (90%-quantile) per unit of length, thereby typically requiring a factor of about 3 between minimum and maximum costs; (2) a cost-estimating procedure that incorporates both slope gradient and geotechnical properties of the subsoil results in an optimal road network in which, compared with current modeling practices, construction costs are reduced by about 25% and life-cycle costs by about 20%, all while road lengths increase about 10%; and (3) a cost-estimating procedure that considers only slope gradient can still produce an optimal road network with 20% lower construction costs and 17% lower life-cycle costs. Therefore, based on these results, we believe that spatial variability in construction costs decisively affects the identification of an optimal road network, and that an improved strategy for cost estimations should become a matter of course for engineering practices.

Our approach may be used in any case for which site specific life-cycle cost information is available for element groups (1) embankment, (2) supporting and retaining, (3) pavement, and (4) drainage structures. However, the model is restricted to terrain conditions with slope gradient below 150%, where height of retaining structures is less than 3 m, and where no bridges and tunnels are required. Nonetheless, our validation also revealed some uncertainty that requires further investigation. A first problem consists of stream crossings for which we implemented only the ford-case. In some sites bridges may be more appropriate. A second problem is the road location near sharp terrain edges and small channels for which a 10 $m \times 10$ m grid resolution is inappropriate to map these small-scale terrain features. Finally protective structures against natural hazards (rock fall, mudflow, avalanches) which result in additional cost, is a third problem to be investigated for extreme area conditions.

Chapter 2

Improved road network design models with the consideration of various link patterns and road design elements

Jürg Andreas Stückelberger, Hans Rudolf Heinimann, Woodam Chung

Submitted: October 2, 2006 / Accepted: February 17, 2007 /
Published: November 23, 2007

Canadian Journal of Forest Research 37: 2281–2298

Abstract

The success of an automatic road network layout over steep terrain mainly depends on the model design. Most previous models have used a grid representation that considers only eight adjacent cells when evaluating feasible road links. Here, we present improved models and alignment constraints mapped on a mathematical graph for better designs that are more applicable under field conditions. We have refined the link pattern by considering up to 48 neighboring cells, and have introduced 16 directional classes per grid cell. Optimization techniques, such as shortest path, minimum spanning tree, and Steiner minimum tree algorithms, are used on the graph to derive a road network that is optimal in terms of its construction costs. These improved models have been applied to different mountainous project areas. Our results show that, by considering various link patterns and alignment constraints, one can determine more appropriate and cost-effective locations for road networks, especially in steep terrain.

Résumé

Le succès de la conception automatisée d'un réseau routier en terrain montagneux dépend principalement du type de modèle utilisé. Pour représenter des liaisons de routes possibles, la plupart des modèles développés jusqu'à ce jour utilisent une représentation en trame et ne considèrent que les 8 cellules voisines. Cette publication présente un modèle qui permet d'améliorer la conception des routes forestières et rurales et qui représente toutes les conditions sur un graphe mathématique. Le modèle de routes est affiné en tenant compte de 48 liaisons d'une cellule aux cellules voisines et en introduisant 16 classes de directions. Avec les techniques d'optimisation, par exemple les algorithmes du chemin le plus court, de l'arbre couvrant de poids minimal et de l'arbre de Steiner de poids minimal, on peut déterminer le réseau routier optimal du point de vue des coûts de construction. Le modèle amélioré est évalué en trois régions différentes. Les résultats montrent que le nouveau modèle permet d'obtenir un meilleur emplacement du tracé vertical et horizontal de la route – spécialement en terrain forte pente – et réduit substantiellement les coûts de construction.

2.1 Introduction

Designing an optimal forest road network across a varying landscape is a challenging task (Scaparra & Church, 2005b). Several engineering problems, such as an overwhelming amount of terrain and environmental data, the uncertainty of cost figures, a lack of explicit constraints, and fuzzy and contradictory goals, make this task even more complicated. Computer-aided engineering approaches for solving road network layout problems have now emerged (Kirby, 1973, Mandt, 1973, Dykstra, 1976). The development of such approaches has been accelerated by the widespread availability of digital elevation models. Initially limited by computing power, they have been continuously improving, resulting in software packages for optimal road network design such as PLANS (Twito et al., 1987), PLANEX (Epstein et al., 1999, Epstein et al., 2001), and CPLAN (Chung et al., 2004). In addition, road centerline optimization techniques have been evolving (Chew et al., 1989, Aruga et al., 2004) to optimize detailed engineering design of both highways and low-volume forest roads. However, even the most sophisticated methods may have the following shortcomings: (1) they often ignore the road cross section when estimating road construction costs, (2) they limit the number of possible links from a specific network node to its adjacent nodes, and (3) they assume the road centerline to be a chain of consecutive straight lines without considering curve or switchback constraints. Automatic design

approaches that overlook these shortcomings may result in impractical road network locations, especially in steep terrain.

Previously, we addressed the first shortcoming and presented a route-dependent cost estimation model (Stückelberger et al., 2006a). Here, we introduce a new approach to forest road layout that overcomes the last two shortcomings: limited link patterns and the lack of gradient and curvature constraints. In our approach, we determine the minimum-cost path between two control points in a geographical area, as well as the minimum-cost spanning tree that connects multiple control points. Our approach aims to (1) improve the formulation of road link patterns, (2) enhance the formulation of horizontal and vertical alignment constraints by considering realistic design elements, and (3) evaluate the improved formulation solved by standard graph optimization algorithms. We first describe the mathematical formulation of the location problem, including link pattern representation and design constraints. We then describe the adaptation of network optimization algorithms. Finally, we present and discuss model validation.

2.2 Mathematical formulation of the road network location problem

Laying out a road network is a complex location problem (Church et al., 1998), especially over steep terrains. This problem can be solved by finding the shortest path (the least-cost path) or minimum spanning tree that connects control points within a specific geographical area, subject to horizontal and vertical alignment constraints. Such an approach requires representation of the solution space as a graph, while mathematically formulating the alignment constraints.

2.2.1 Link pattern representation

Road engineers control the geometry of a layout by following a sequence of vectors, known as a 'traverse'. The road is then designed as a series of curves inside the angles between consecutive straight segments along vectors, plus curves outside the angles between successive vectors that define hairpin bends (Ervin & Gross, 1987). A geographical area is the continuous physical entity on which we can define an infinite number of points for use as the start- and end-points of vectors. However, graph optimization algorithms require a finite set of nodes (vertices) and links (edges). Therefore, the specification of all possible alternatives follows the concept of discretization, i.e., splitting a continuous physical system into a discrete set of simple shapes. The prevailing approach uses a grid consisting of squares. Although the resolution of such a grid for different road layout models varies with the computing capacity and the area of interest (Liu & Sessions, 1993, Dean, 1997, Chung & Sessions, 2001a), we have used a 10 $m \times 10$ m node resolution in this study. Each node represents the center of a grid cell. We believe this resolution is appropriate for forest road design (Heinimann et al., 2003, Stückelberger et al., 2004) because it equals the lower limits of the elements that define the centerline of a road, especially the minimum lengths of curve tangents, the straight segments between curves, and the minimum radius for switchbacks (Kuonen, 1983).

Because the finite set of all possible start-points and end-points is defined, the next task is to identify which connections (links) between any two points are feasible. The predominant approach is to determine the links from a start-node to its adjacent nodes (Fig. 2.1a), a process that results in eight links per node, i.e., a Moore neighborhood of Range 1 (Barile & Weisstein, 2002). A Moore neighborhood of Range 2, which provides 24 possible links and has 16 unique directions (Fig. 2.1b), has previously been used by Heinimann et al. (2003). However,

that extension of 24 links results in only eight additional directions. Because one of our goals is to evaluate the effect of different link patterns on the road layout, we have also defined and assessed a 48-link pattern (Fig. 2.1c), which consists of the full Range 2 neighborhood, 16 links of Range 3, and eight links of Range 5. This pattern results in a nearly homogenous distribution of 40 directions.

A rectangular grid representation may cause an angular and, therefore, unrealistic road alignment because its location is represented by a series of connected grid cells. Anderson & Nelson (2004) have described an approach that prevents this risk by shifting the coordinate values for each point randomly. They have generated 30 nodes per hectare, at an average node spacing of 18.25 m. However, a rectangular grid representation requires less memory than a vector that represents the same level of node density because it is not necessary to store the coordinates of individual points when a grid is used. For this reason, and to facilitate systematic analysis of the alternative road links, we have used a 10 $m \times 10$ m grid to identify road nodes, and have combined it with the link pattern described for Figure 2.1c.

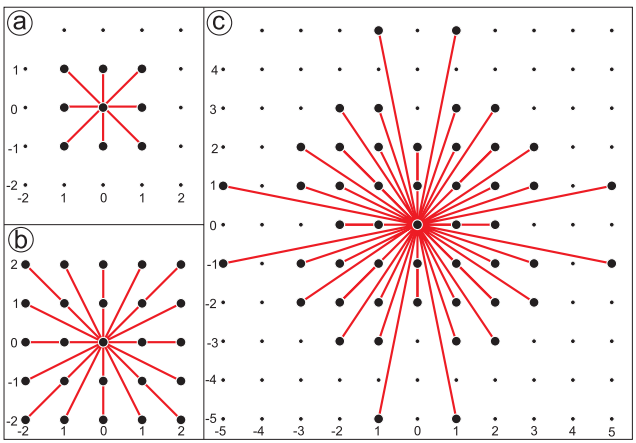

Figure 2.1: Neighborhood patterns for Models 8- (a), 24- (b), and 48-link (c)

2.2.2 Road curvature constraints

In steep terrain, where a road must accommodate considerable differences in elevation, a shortest-path algorithm used on a grid often produces a zigzag sequence of straight lines and excessive switchbacks. Under real conditions, such patterns should be limited for two reasons. First, roads have to maintain a certain minimum-curve radius for driving comfort. Second, the construction of switchbacks entails additional cost. One approach for preventing this has been to penalize dramatic directional changes in road alignment (Anderson & Nelson, 2004). Another has been to check the horizontal road alignment feasibility (curvature) of combining incoming and outgoing links for each node, and allow only feasible links to be considered (Chung & Sessions, 2001a, Epstein et al., 2001). However, none of these previous tactics has actually been used to map curvature constraints on a mathematical graph.

For the link pattern in Figure 2.1b, 16 different directions are considered in the model. At each outgoing and incoming node, the model checks all possible directional combinations. Consequently, the solution space increases by a factor of $16^2 = 256$. A minimum radius is the criterion

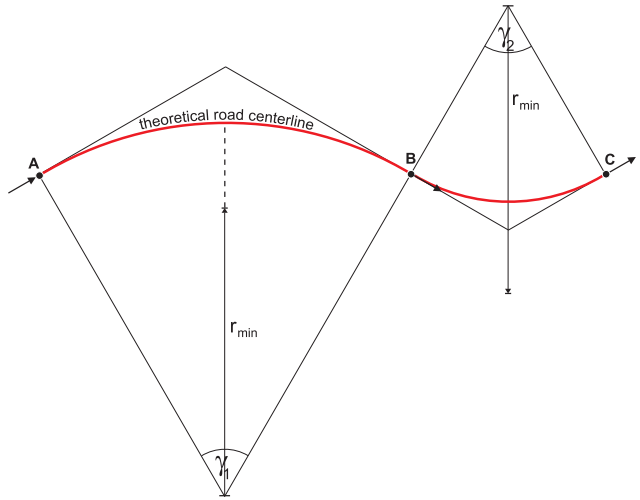

Figure 2.2: Curvature constraints in graph model. Link A-B is feasible whereas link B-C is not, because its road radius would be smaller than the minimum radius (r_{min}).

for determining whether a link is feasible or not (Fig. 2.2). In this study, the minimum radius has been set at 20 m for regular curves and 10 m for switchbacks.

Representation of such constraints requires one physical node to be split into 16 virtual nodes. Thus, the corresponding mathematical graph can be displayed three-dimensionally (3-D), consisting of 16 virtual layers, each of which maps one directional class. Figure 2.3 illustrates this 3-D approach for turnings of different road links. Node O represents an incoming node, while Nodes A, B, C, and D represent potential intermediate control points, depending on the road direction. The 0-layer represents the link direction, from west to east, whereas the 4-layer indicates the south-to-north link. The 8- and 12-layers represent link directions from east to west and from north to south, respectively. A link with a 180° turn (for example, from Node O to Node D in Figure 2.3 results in a left-turn switchback. In this representation of the solution space, any chains of links (walk) result in a feasible alignment of the road. Graph optimization takes place in this 3-D graph, and the result can then be mapped back to the 2-D grid, which represents the x, y-surface area of the real world.

Although a total of 40 possible road directions exists in the 48-link model, we have regrouped them into 16 directional classes to reduce the problem size. All links connecting to the nodes in the Moore neighborhood of Ranges 1 and 2 can be assigned to one of 16 directions without errors. However, some links connecting nodes in the Moore Neighborhood of Ranges 3 and 5 (Fig. 2.1c) do not fit exactly to the 16 directions of Figure 2.1b. So, the effective direction is rounded toward the nearest of the 16 given directions. In our analysis, we have assumed that this angular difference (max. 18° distributed over 51 m) does not affect practical applications.

2.2.3 Road gradient constraints

Road gradient must be less than or equal to a maximum allowable value for safe truck operations. The gradient of a single road segment is calculated by dividing the elevational difference by the segment's horizontal length. If the gradient is too high, the link becomes infeasible. Each node

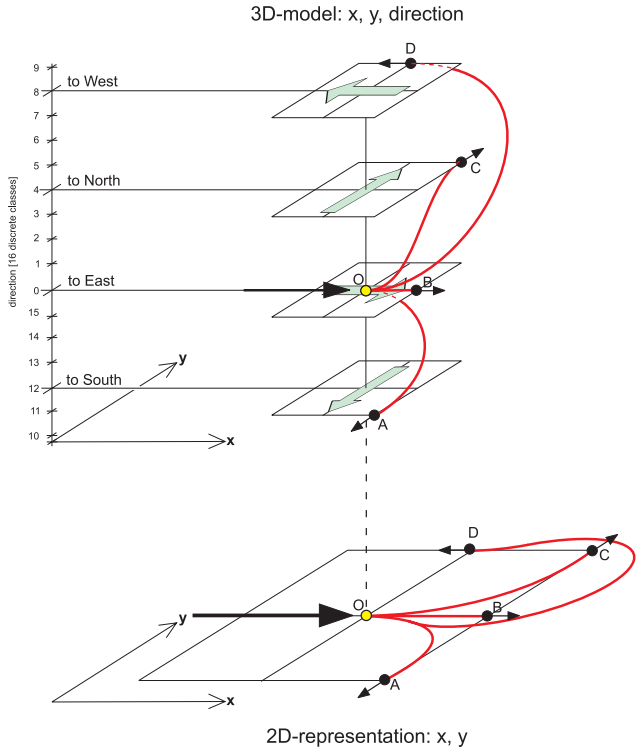

Figure 2.3: Representation of directional change constraints, illustrated by 4 directions. Combinations of outgoing and incoming links represent right-hand curve (OA), straight line (OB), left-hand curve (OC), and left-hand switchback (OD).

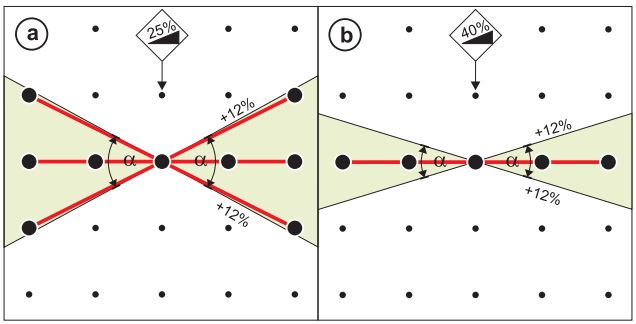

Figure 2.4: Sector of feasible link gradients (-12% < road gradient < +12%) in slope gradient of 25% (a) or 40% (b)

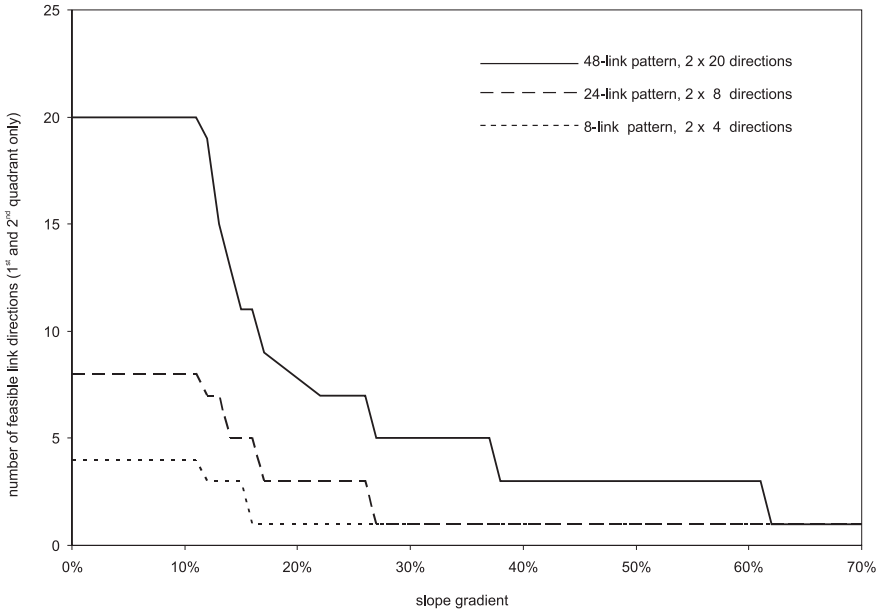

Figure 2.5: Number of feasible links (-12% < road gradient < +12%), depending on link pattern and slope gradient

located in steep terrain has a feasible sector of allowable link-gradients. The steeper the terrain, the smaller the sector and the fewer the links that are feasible (Figs. 2.4, 2.5). Because of this, the link pattern used in road network models becomes important, especially in steep terrain.

In order to connect two terminals (mandatory access nodes) with a large elevational difference, one should find the road route with a centerline gradient (n_{road}) nearest the maximum allowable value ($n_{road} = n_{max}$). Then again, the strict application of gradient constraints ($n_{link} \leq n_{max}$) to each single link gradient (n_{link}) often results in the average gradients of the centerline (n_{road}), which are usually below the maximum allowable link gradient ($n_{road} < n_{max}$). This is a consequence of the regular node structure, where most outgoing links have a gradient lower than the maximum allowable link gradient ($n_{link\_max} < n_{max}$). To overcome this problem, we have developed and introduced a relaxation rule into our model to accept link gradients that are slightly above the maximum (n_{max}). If the gradient (n_t) of a link is higher than the maximum allowable gradient but smaller than the maximum gradient plus a tolerance ($n_{max} + c$), a probability (p) is calculated according to Equation 2.1. The closer n_t is above n_{max} and the farther n_0 (i.e. presenting n_{link_max}) is below n_{max}, the greater the probability for accepting this link. This procedure then calculates a random number (r) and compares it to the calculated probability. If the random number is smaller than the probability, the link is classified as "feasible"; otherwise, it is "infeasible" (Eq. 2.2). This relaxation provides some link over the maximum allowable road gradient for preliminary planning. During the field survey and detailed planning, the vertical road alignment must then be adjusted so that the average road gradient does not exceed n_{max}. Although some links may have a gradient above the maximum allowable limit, it is unlikely that the overall gradient between the start-terminal and the end-terminal will be larger than the allowable gradient due to a small tolerance. With this relaxation rule it is possible to find centerlines that use, on average, nearly the entire capacity of the maximum road gradient.

$$p = \begin{cases} \frac{n_{max}-n_0}{n_t-n_0} & \text{if } n_0 \leq n_t \leq n_{max}+c \\ 0 & \text{else} \end{cases} \quad (2.1)$$

$$b = \begin{cases} 1 & \text{if } r \leq p \\ 0 & \text{else} \end{cases} \quad (2.2)$$

where, b = Boolean value, 0: infeasible, 1: feasible
c = maximum tolerance for a relaxed link gradient (about 4%)
n_0 = maximum gradient among the previous links of the same outgoing node
n_{max} = maximum allowable road gradient (about 12%)
n_t = link under investigation
p = probability
r = random number [0...1]

Additional rules exist for special cases. The first exception is a switchback. To ensure safe truck operations and driving comfort, the road gradient in switchbacks must be much lower than the maximum allowable road gradient. Therefore, only links with a gradient less than half the maximum allowable link gradient are considered feasible ($\leq \frac{1}{2} \cdot n_{max}$). The second exception is a ford, which is a type of stream crossing where the planned road must fulfill additional design criteria, i.e., the gradient must decline toward the stream and incline after the ford. Therefore, our model only accepts, within a buffer of 30 m from a stream, those links that either have a negative gradient toward the stream or are leaving the stream with a positive gradient.

2.2.4 Road construction cost and weight function

Using graph optimization algorithms requires that each link (edge) be weighted. In the present case, the weight of each link corresponds to the cost of the road segment. Dean (1997) has assigned the cost value using a given cost layer and the length of the link, while O'Neal et al. (2006) have presented a spread sheet tool to estimate the construction cost for a specific road segment. Anderson & Nelson (2004) have estimated that cost as a function of road length and gradient. Previously, we introduced a model for accurately estimating road construction and maintenance costs based on terrain surface properties as well as the geological properties of the subsoil (Stückelberger et al., 2006a, Stückelberger, 2006). That model followed an approach of cost classification by elements (CCE, 1991). For example, forest roads comprise four structural components: (1) embankment, (2) retaining structures, (3) pavement, and (4) drainage and stream-crossing structures. Our cost model considered road widening in curves and switchbacks, and aimed for – if geotechnically possible – a balanced design for cut-and-fill volume in each cross section.

In the applications presented here, we have applied that cost model (Stückelberger et al., 2006a) to estimate construction and maintenance costs for each road link identified as feasible. That cost is considered the weight of the link. The parameters for engineering, cost, and road design used with these applications are shown in Tables 2.1 and 2.2.

2.3 Optimization procedures

Once a mathematical graph of vertices (nodes), edges (road links), and weights (road construction and maintenance costs) is built, graph optimization techniques are applicable.

Geotechnical unit		Engineering parameters					Cost parameters							flat cost
ID		$\tan(\phi_{cut})$	$\tan(\phi_{fill})$	$\tan(\phi_{wall})$	f_{shr}	$coef_{rock}$	c_{exc} $\frac{CHF}{m^3}$ $\frac{USD}{CY}$	c_{comp} $\frac{CHF}{m^3}$ $\frac{USD}{CY}$	crock $\frac{CHF}{m^3}$ $\frac{USD}{CY}$	c_{pav} $\frac{CHF}{m^2}$ $\frac{USD}{ft2}$	c_{wall} $\frac{CHF}{m^2}$ $\frac{USD}{ft2}$	c_{drain} $\frac{CHF}{m}$ $\frac{USD}{ft}$	CHF USD	link length $\frac{CHF}{m}$ $\frac{USD}{ft}$
Parameters for Switzerland														
21	Moraine	1	0.8	10	0.8	0.68	6.8	4	12	28	80	18	0	0
22	alluvial deposit	1	0.8	10	0.8	0.11	6.8	4	12	28	100	18	0	0
31	conglomerate	1	0.8	10	0.8	1.07	6.8	4	12	28	80	18	0	0
32	Sandstone	1	0.8	10	0.8	0.95	6.8	4	12	28	100	20	0	0
33	Flysch	0.8	0.67	10	0.8	0.54	6.8	10	5	52	200	85	0	0
34	Limestone	1.25	0.8	10	0.8	1.43	6.8	4	15	28	80	15	0	0
41	Granite	1.25	0.8	10	0.8	1.73	6.8	4	15	28	80	18	0	0
42	Gneiss	1.25	0.8	10	0.8	1.69	6.8	4	15	28	80	18	0	0
51	landslide	0.8	0.67	10	0.8	0	6.8	10	0	80	200	85	0	12
61	stream crossing	1	0.8	10	0.8	1	6.8	4	12	41	200	20	1000	0
91	marshland / lake	not feasible												
Parameters for Idaho														
11	silt-sand	2	1	10	0.8	0	1.4	0	0	0.18	120	1.2	0	0.21
12	silt-clay	1.5	1	10	0.8	0	1.4	0	0	0.18	120	1.35	0	0.21
13	Schist	2	1	10	0.8	1	1.4	0	1.6	0.18	120	1.2	0	0.21
61	stream crossing	1	1	10	0.8	0	1.4	0	0	0.18	120	1.35	2300	0.21

Table 2.1: Engineering and cost parameters for each geotechnical unit. The data were calibrated for the areas of Uetliberg, Wägital, and Giswil (Switzerland), and for the Mica Creek Watershed (Idaho, USA). $\tan(\phi_{cut})$: cut-slope inclination, $\tan(\phi_{fill})$: fill-slope inclination, $\tan(\phi_{wall})$: inclination of retaining wall, f_{shr}: shrinking factor of earth volume fill : cut, $coef_{rock}$: coefficient for rock ratio, c_{exc}: excavation cost, c_{comp}: emplacement and compaction of the filling material, c_{rock}: additional cost for rock excavation, c_{pav}: cost for pavement structures, c_{wall}: cost for retaining walls, c_{drain}: cost for drainage structures. $1\ CHF \approx 1\ CAD \approx 0.85\ USD$, $1\ CY \approx 0.764\ m^3$, $1\ ft \approx 0.308\ m$

	n_{max}	r_{min}	r_{SB}	w_{s0}	w_{d+s}	k_{cw}	z_{min}
Switzerland:		$[m]$	$[m]$	$[m]$	$[m]$	$[m^2]$	$[m]$
- Uetliberg (ZH)	12%	20	10	3.4	0.6	26	0.30
- Giswil (OW)	10%	20	10	3.6	0.6	30	0.50
- Wägital (SZ)	12%	10	10	3.4	0.6	26	0.30
Idaho:		$[ft]$	$[ft]$	$[ft]$	$[ft]$	$[ft^2]$	$[ft]$
- Mica Creek (ID)	12%	100	60	14	3	250	1

Table 2.2: Design parameters for each road type used in design projects. n_{max}: maximum road gradient, r_{min}: minimum radius for standard curves, r_{SB}: minimum curve radius for switch backs, w_{s0}: standard road surface width, w_{d+s}: additional width for shoulder and ditch, k_{cw}: road curve widening factor (x/radius), z_{min}: minimum excavation depth (i.d. topsoil material not usable for embankment), $1\ m = 3.24\ ft$

The problem-solving procedure can be subdivided into the following steps:

1. Identify t terminal nodes that must be accessed.
2. Find all $t-1$ shortest paths (SPs) from one starting node to all other terminals.
3. Find all $\frac{t}{2} \cdot (t-1)$ SPs, connecting each terminal with the others.
4. Find $t-1$ edges to define a minimum spanning tree (MST) that connects all terminals.
5. Find additional nodes in the area where the road can branch out, and determine the Steiner minimum tree (SMT).

2.3.1 Gradient-sensitive shortest-path algorithm

Determining the shortest path in a graph is a $\mathcal{P}$-problem ($\mathcal{P}$: polynomial, meaning that the problem is solvable within a polynomial time, n^k, where n is the number of nodes and k is any positive real number). Dijkstra (1959) earlier introduced an algorithm to identify the SP from any node to all other nodes. This algorithm, widely used to locate the shortest route (Anderson & Nelson, 2004), is applicable for positive link weights only. The source code is available on the Internet (e.g., www.cprogramming.com, 2005a). This algorithm guarantees the mathematical optimum; by running it $t-1$ times, we can obtain all $\frac{t}{2} \cdot (t-1)$ SPs.

However, Dijkstra's algorithm considers only the link weight, and is incapable of simultaneously analyzing multiple link attributes, such as link weight and gradient. Because frequent and large fluctuations in gradient reduce traffic comfort and contradict engineering practices, changes in those link gradients are penalized depending on the difference between the gradients of the incoming and outgoing links. Therefore, the weight of a link is the sum of the construction cost and its penalty. This penalty function aims to prefer a solution where the gradients of several consecutive road links are nearly identical and to prevent excessive gradient changes along the road centerline. However, this penalty function does not affect the actual cost of the links. In the current model, the penalty function is set as linear and corresponds to the cost of four additional meters per 1% change in gradient. Due to this penalty, the modified Dijkstra's algorithm used in our model does not provide the "shortest path", but it most likely identifies the least-cost path with less frequent gradient changes.

2.3.2 Network optimization algorithms

To find the minimum spanning tree between all terminals, we have created a very simple graph, where only terminals exist as vertices. This new graph is completely independent of the 10 $m \times$ 10 m graph-model, which covers the entire project area presented in Subsection 2.2.1. To avoid confusion, we call the 10 $m \times 10$ m-graph the "1st order graph", and the new graph, the "2nd order graph". The edges between the vertices in the latter are the shortest paths, which result from the iterative SP algorithm in the former. The weight of an edge in the 2nd order graph corresponds to the total cost between two terminals in the 1st order graph, which is also gained through the SP algorithm. Kruskal (1956) and Prim (1957) have introduced algorithms to determine the MST. Both algorithms lead to the mathematical optimum and solve the problem in the polynomial time of the number of vertices ($\mathcal{P}$-problem). For example, a 128-node problem – which is far above the presented cases of a 2nd order graph – is solved almost instantly (< 1 *sec*) with a modern PC. These algorithms are very common; their source codes are well described on the Internet (e.g., www.cprogramming.com, 2005b). Prim's MST algorithm is used in our current model.

Nevertheless, the MST in the 2nd order graph may not result in the least-cost road network. Good branch-out points for roads often exist in a 1st order graph, and are known as Steiner points (Fig. 2.6). Finding such points in a graph is very complex, and up to now cannot be solved exactly within the polynomial time deterministically ($\mathcal{NP}$-hard problem). The processing time for an exact solution is k^n where n = number of nodes, and k = any positive real number (Garey & Johnson, 1977, Garey et al., 1977). However, as the values for n increase, such problems soon become unsolvable within a limited time span. Methods to obtain nearly optimal solutions have been described by Prömel & Steger (2002), Polzin (2003), and Rosenwein & Wong (1995). We have previously applied these to find SMTs for low-volume forest roads (Stückelberger et al., 2004). These algorithms, which usually require a large amount of computing time even though optimality is not reached, have an expected error of about 2 to 4% (Ghanwani, 1998).

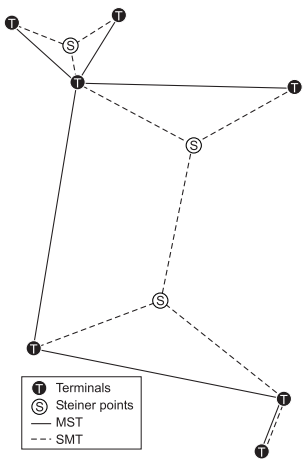

Figure 2.6: Example of Minimum Spanning Tree (MST) and Steiner Minimum Tree (SMT) with 7 mandatory access nodes (Terminals) and 3 good branching points (Steiner points), respectively

2.3.3 Implementation

The current program has been developed in Object Pascal (Borland Delphi 7.0); the source code for calculating the road cost of all the links and building a graph consists of 3'700 lines. In contrast, the source code for finding the MST comprises only a few hundred lines.

One complication is memory management. A project area of 36 km^2, with a 10 $m \times 10$ m resolution, is nearly the limit for a modern PC with 2 GB RAM. Such a problem leads to 5.8×10^6 nodes, or a maximum of 276×10^6 links. Each link contains 60 bits of information; for all links we have used 16.6×10^9 bits, or approximately 2 GB. However, not all the theoretical links are feasible because of curvature and gradient constraints, as well as soil bearing capacity. Depending on the slope gradient and the geology of the subsoil, only a subset of one-quarter to one-half of the theoretical links is usually feasible, which greatly frees up computer memory.

2.4 Link model specification

The more neighbor nodes that are involved in the road link pattern, the more complex the graph model becomes, and the longer the process takes to find the optimum solution. However, a more complex and realistic link pattern usually better represents the real world, provides more alternatives, and, therefore, results in a better solution. We have tested and compared nine models that use different link patterns in order to identify their influence on road layouts (Tab. 2.3).

Model	Neighborhood			Road gradient		Road radius		Penalty[b]	
	8-link-pattern	24-link-pattern	48-link-pattern	any link $\leq n_{max}$	link $\leq n_{max}+$ tolerance [a]	min. curve $[m]$	min. switchback $[m]$	$[m]$ per switchback	$[m]$ per % change in road gradient
a) Zigzag 8	•			•		0	0	0	0
b) Zigzag 24		•		•		0	0	0	0
c) Lazy Zigzag		•			•	0	0	100	0
d) 8-link	•			•		20	10	0	0
e) 24-link		•		•		20	10	0	0
f) 48-link			•	•		20	10	0	0
g) Relax			•		•	20	10	0	0
h) Ramp			•	•		20	10	0	4
i) Combined			•		•	20	10	0	4

Table 2.3: Nine models and their constraints. [a] In the present study: tolerance = 4%; [b] The penalty increases the weight of a link by the value of the construction cost for the indicated distance, but does not affect either the road length or the road cost

Model (a) "Zigzag 8" considers only 8 direct links to adjacent nodes and no curvature constraints, so it allows zigzagging without any penalties. Many road network models and GIS software (e.g., ESRI ArcGIS 9) utilize this approach in their least-cost path algorithms. Model (b) "Zigzag 24" is similar to Model (a), but it also connects the nodes in the Moore neighbor-

hood of Range 2 (cf., Fig. 2.1b). SCAPARRA & CHURCH (2005a) have used this layout for finding corridor locations. Model (c) "Lazy Zigzag" has the same link pattern as Model (b) but penalizes switchbacks. Due to this penalty, the alignment is expected to be less zigzagging than with Model (b). Model (c) also allows links to be slightly above the maximum road gradient (n_{max}), with tolerance set at 4%. Model (d) "8-link", Model (e) "24-link", and Model (f) "48-link" all have curvature constraints, as described in Section 2.2. The link pattern follows Figure 2.1a for Model (d), Figure 2.1b for Model (e), and Figure 2.1c for Model (f). For these models, the gradient of each link (n_{link}) is set to be always below the maximum allowable gradient (n_{max}).

As explained in Subsection 2.2.3, we have tried here to relax the constraints in order for maximum link gradients to approach n_{max}. Model (g) has the same link pattern as Model (f), but allows for values above the maximum road gradient (n_{max}). Because a constant road gradient is preferred over a long section (cf., Subsection 2.3.1), Model (h) "Ramp" penalizes the gradient change between two consecutive road links. It is based on the link pattern of Model (f) as well. Finally, Model (i) "Combined" is the aggregation of Models (g) and (h). The goal is to find a constant road gradient near n_{max}.

2.5 Results

2.5.1 Link model comparisons

These nine different models (Tab. 2.3) have now been applied to a 1-km^2 area in the research forest of ETH Zurich (Fig. 2.7). The southwestern portion of that area is flat terrain, with an average downhill slope of 40% to the northeast. Various student project results and expert opinions have been analyzed and compared with model outputs.

Three terminals (control points) have been located: (A) at the bottom of the hill (in the northeast, elevation 492 mNN), (B) on the upper ridge of the hill (in the middle, elev. 619 mNN), and (C) in the flat area (in the south, elev. 643 mNN). Terminal (B) is positioned between terminals (A) and (C), so that no Steiner Point is necessary. This project results in two road sections – one in steep terrain (from A to B), and the other in the flat area (B to C). The input data include a digital elevation model and a grid-layer for the geological subsoil, both in the resolution of 10 $m \times 10$ m.

The results of each model are summarized in Table 2.4, in terms of road length and cost, and road locations (Fig. 2.7). Because the zigzag models (a, b, c) develop road locations without considering switchbacks, we have also calculated construction costs with the additional expense for switchbacks based on the road alignments of these model results. Model (g) "Relax", which considers realistic curvature constraints and relaxes the gradient constraint, provides the least cost path among the nine models. Therefore, we have used this one as a base model for our further comparisons.

Model (a) "Zigzag 8" is incapable of determining a solution for a road route through steep terrain (A-B), and the proposed route B-C is unreasonable, based on field verification.

Model (b) "Zigzag 24" does identify a feasible solution for both sections. However, its section A-B is very zigzagging, resulting in 18 switchbacks, which is not a practical design in that project area. According to our field verification, section B-C is feasible except for the very last switchback near point C. The road cost is 13% higher than from the base model. Model (c) "Lazy Zigzag" produces only two switchbacks between A and B, which seems realistic in this terrain.

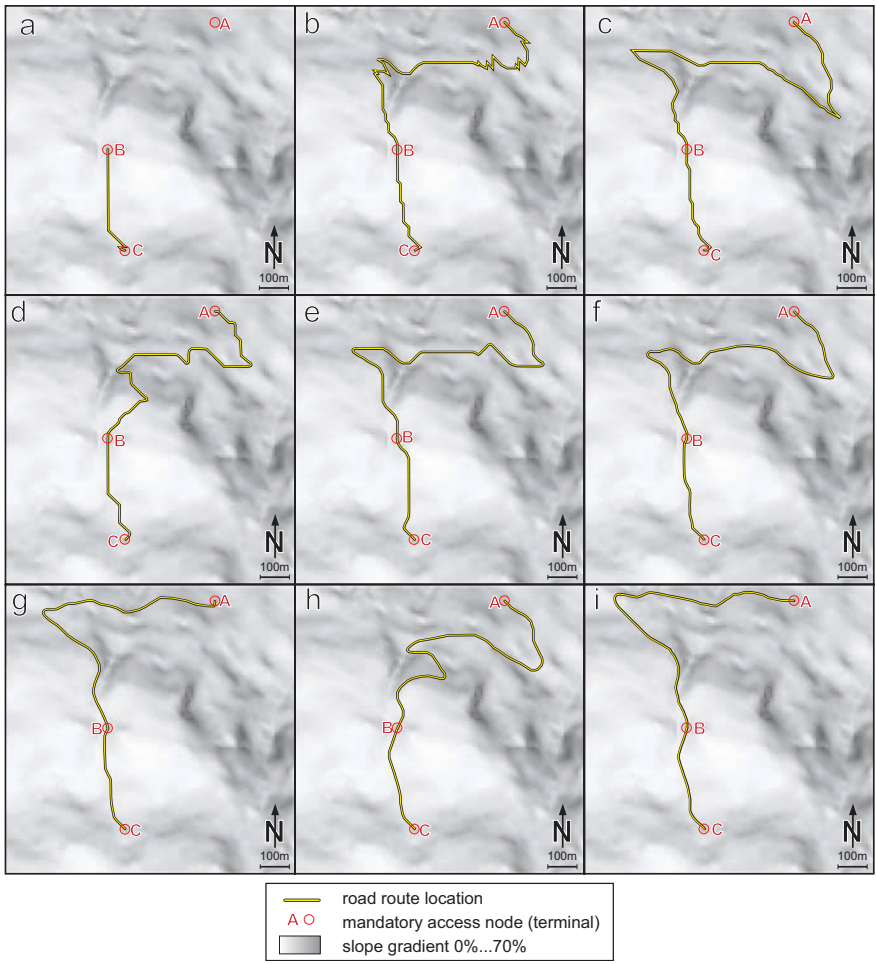

Figure 2.7: Road route locations for 9 different model alternatives (a, ..., i) between 3 mandatory access points (A, B, C). Background: slope gradient of project area, Research Forest ETH-Zurich (Switzerland), 1 $km \times 1$ km

Model	Road segment A-B					Road segment B-C					Processing time[a]
	$length$		$cost_{model}$	$cost_{effective}$		$length$		$cost_{model}$	$cost_{effective}$		
	$[m]$	$[\%]^b$	$[kCHF]$	$[kCHF]$	$[\%]^b$	$[m]$	$[\%]^b$	$[kCHF]$	$[kCHF]$	$[\%]^b$	$[s]$
(a) Zigzag 8	-	-	-	-	-	402	103	62.4	91.7[c]	148	15
(b) Zigzag 24	1'080	85	188.7	321.6[c]	126	375	96	56.3	69.6[c]	113	13
(c) Lazy Zigzag	1'007	80	356.1	428.4[c]	168	370	95	62.1	62.4[c]	101	13
(d) 8-link	1'530	121		385.5	151	407	105		67.5	109	33
(e) 24-link	1'477	117		306	120	394	101		64.2	104	31
(f) 48-link	1'428	113		291.3	114	389	100		61.8	100	31
(g) Relax	1'266	100		254.9	100	389	100		61.8	100	31
(h) Ramp	1'468	116		305.6	120	395	102		64.4	104	31
(i) Combined	1'396	110		289.4	114	391	101		64.1	104	31

Table 2.4: Comparisons of road lengths, costs, and processing times among the nine models. [a] Processing time with a PC Pentium IV, 2.66 GHz, 1 GB physical RAM, and 1 GB virtual RAM for SP road route location. The processing time for data-reading and graph-building is not included. [b] Percent ratio to the base model (g). [c] The effective cost is the sum of the model cost plus the cost of constructing switchbacks. Model (g) "Relax" is used as the base model. $kCHF = 1000\ CHF \approx 1000\ CAD$

However, the field verification shows that their proposed locations would be suboptimal because they require a huge excavation volume and/or high retaining structures. Section B-C from Model (c) seems similar to that of Model (b), but just a slight difference in road alignment makes its cost 10% less than for Model (b). Model (c) also provides for a minimum road length that is 5% less than the base model for Section B-C.

Model (d) "8-link" includes curvature constraints and switchbacks, but the result seems to be less desirable than with the base model. A total of four switchbacks is located in section A-B. Although their proposed locations appear reasonable, the road length and cost are much higher than for the base model. Even in flat terrain (B-C), this model calls for 5% more length and 9% higher cost than does the base model. Models (e) "24-link" and (f) "48-link" achieve similar solutions, but the former seems to follow grid structures, while the latter better fits the terrain, producing a less expensive route. The average road gradient from Model (f) is 9%, or 3% less than the road gradient limit of 12%. In steep terrain (section A-B), both models produce routes that are 10% to 20% higher in road length and cost than the base model. In flat terrain, Models (e) and (f) differ very little, and their routes are similar to that from the base model.

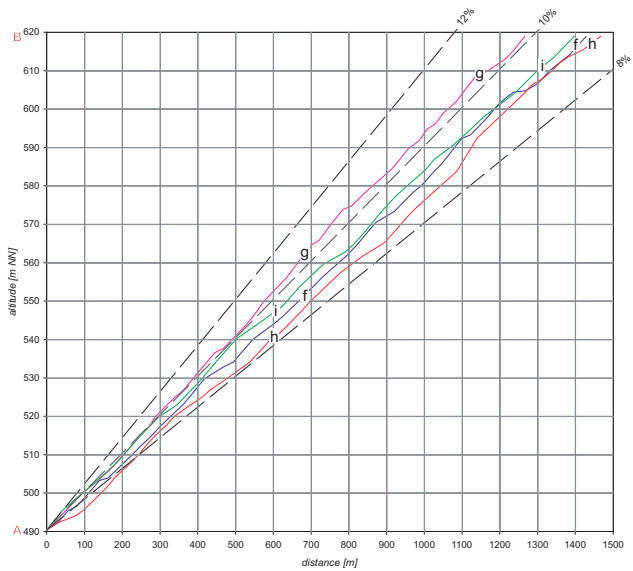

Figure 2.8: Profile in length (10×super-elevated) for 4 model alternatives (f, ..., i)

When the strict limit of a maximum road gradient is eased, Model (g) "Relax" is able to connect A and B with one switchback only, leading to an approximately 10% reduction in both length and cost compared with Model (f). The average road gradient is about 1% higher than for Model (f), but is clearly within the limit of 12% (Fig. 2.8). The road location for section B-C is identical to that from Model (f).

Models (h) "Ramp" and (i) "Combined" attempt to obtain a homogenous road gradient. Their length profiles show that both are slightly smoother than those of Models (f) and (g) (Fig. 2.8). The proposed penalty for changes in road gradient reduces the average gradient by about 0.5% when comparing (f) to (h) and (g) to (i). In steep terrain, the constraints of having constant road gradients increases cost and length by about 10%.

The computation times required for models that include curvature constraints (i.e., d through i) are about twice as long as those calculated with the zigzagging models (a, b, c) (Tab. 2.4).

2.5.2 Model validation

In order to validate our models, we have chosen three obviously different models – ((a) "Zigzag 8", (c) "Lazy Zigzag", and (f) "48-link") – and have applied them to two forest areas where roads have previously been developed. Those model results have also been compared with the current road locations. Model (a) "Zigzag 8" was selected to represent most existing grid-based models. Model (c) "Lazy Zigzag" represents a contemporary state-of-the-art in road network optimization, incorporating the need for penalties for switchbacks Anderson & Nelson (2004) and the neighborhood link patterns Scaparra & Church (2005a). All segments are assumed to be straight lines. It includes no penalties for horizontal or vertical alignment. The costs are calculated after the geotechnical subsoil and digital elevation model and includes additional costs for stream crossings. To show the benefit of the enhanced link pattern, we have selected Model (f) "48-link", which is deterministic. Even though Model (g) "Relax" may provide the least-cost road locations, we have not selected it because it may produce a different solution in each run due to a probabilistic component in the model that makes further analysis more difficult.

The comparisons we have made here with the existing roads may not provide perfect validation due to the following drawbacks: (1) the models consider construction costs only, although actual road networks are often built for multiple objectives (e.g., timber harvesting, recreation access, minimized expense); (2) existing road locations and alignments may not be optimal; and (3) road alignment alternatives may exist that have nearly similar construction costs, but with totally different spatial alignments. Keeping those shortcomings in mind, the comparisons here have been done only qualitatively and not quantitatively.

Project	Model (a) "Zigzag 8"	Model (c) Lazy Zigzag	Model (f) "48-link"	Existing road
Giswil:				
- length $[m]$	-	6'606	2'864	3'021
- model cost $[CHF]$	-	2'725'700	1'180'400	1'244'800
- cost per length $[\frac{CHF}{m}]$	-	413	412	408
Mica Creek:	(n_{max}= 15%)			
- length $[ft]$	(25'144)	16'239	15'889	18'758
- model cost $[USD]$	(300'117)	90'474	80 662	9'716
- cost per length $[\frac{USD}{mile}]$	(63'021)	29'413	26'800	26'097

Table 2.5: Model evaluation results in the project areas "Giswil" and "Mica Creek".
$1\ USD \approx 1.23\ CHF$, $5280\ ft \approx 1\ mile \approx 1.609\ km$

Our first area for validation is located in Giswil, in the northern slopes of the Swiss Alps (Fig. 2.9). With an average slope gradient of about 39%, this site was formerly used for cost-benefit analysis of road investments (Stückelberger et al., 2006a), which have now provided us with numerous data for engineering and cost parameters. Three control points (A, C, and D) are given, and we have built the SMT connecting those points. However, real costs for the existing roads (built in the 1960s) are not available. Therefore, we have estimated construction costs for the existing road by using our cost model and the actual road centerline (Tab. 2.5).

Model (a) "Zigzag 8" is inadequate for finding a feasible solution at this particular site, even though the maximum allowable road gradient has been set to 20%. Likewise, the result from

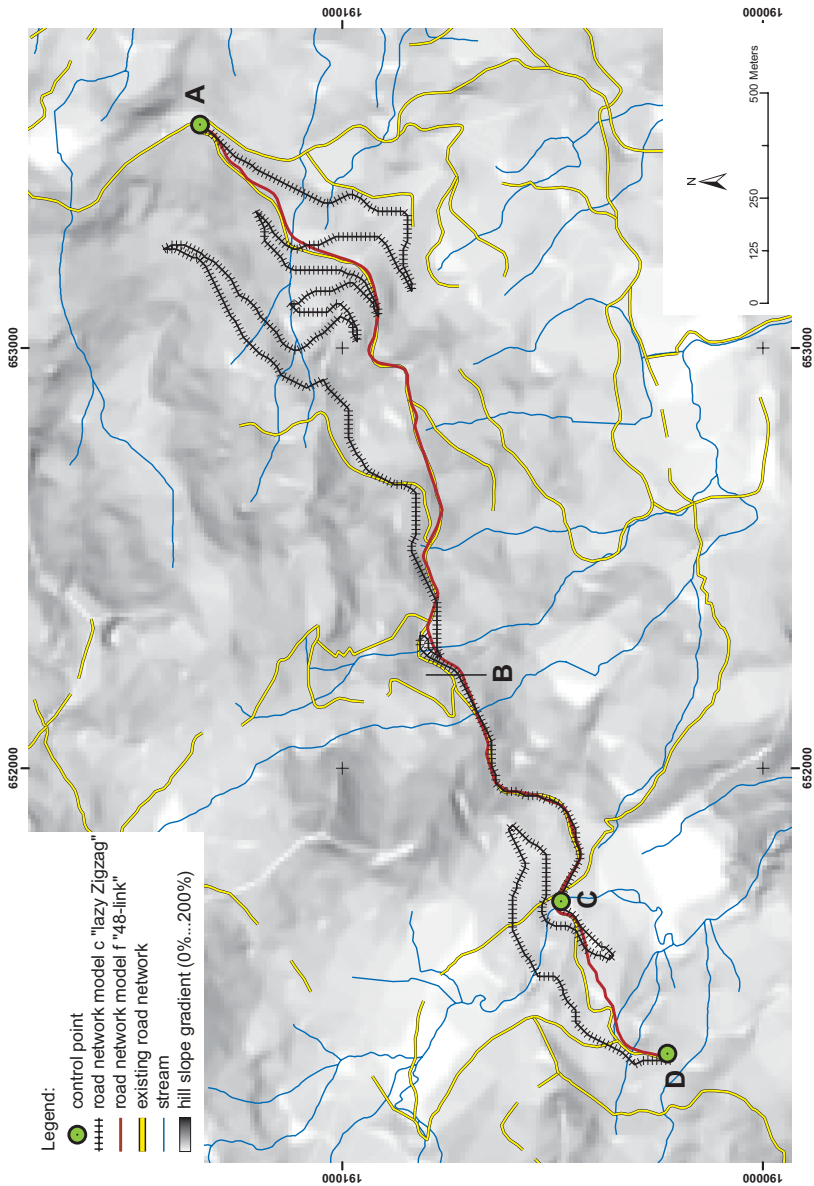

Figure 2.9: Model-designed road network for Models "Lazy Zigzag" (c) and "48-link" (f), and existing road network. Background: slope gradient and streams. Giswil project area (Switzerland)

Model (c) "Lazy Zigzag" does not match well with the existing road (Fig. 2.9). Although nine switchbacks are called for with that model, the current road has none. The road length and cost are more than twice as great compared with the existing conditions, even though section B-C is similar to the actual road. Model (f) "48-link" describes nearly the same alignment as the real road, with only a minor variation near site B, where the current road must connect with another. The existing road follows the contour lines in the area between C and D, whereas the model suggests slight road gradient changes. The model result is less expensive, but the existing road may provide better traffic comfort. Road lengths and costs are similar in both cases.

Our second area for validation is in the Mica Creek watershed in Northern Idaho, USA (Fig. 2.10). The average slope gradient is 30% and the node spacing used is 75 ft (22.9 m). Engineering and cost parameters (cf., Tab. 2.1) for this site were obtained from the USDA Forest Service cost guide for road construction (US Forest Service, 2006). As with the Giswil site, four control points (A, B, C, and D) have been identified in this area (Fig. 2.10).

Model (a) "Zigzag 8" does not provide a feasible solution here except when the maximum allowable gradient (n_{max}) is increased to 15%. Moreover, the network design for this solution is far different from the existing roads. In contrast, Model (c) "Lazy Zigzag" produces a road alignment similar to actual conditions, and both designs are nearly identical along section A-B. The model results, however, present different road locations along section C-D, where two stream crossings are required in the model result, compared with the current avoidance of such crossings. Model (f) "48-link" produces road alignments similar to the existing road in sections A-B and C-D. Section B-C, however, differs in that the current road is located farther away from another parallel road than the model result would indicate, perhaps because road spacing accommodates timber harvesting purposes. Finally, the existing road crosses streams three times, whereas the model calls for only one stream-crossing, resulting in a less expensive road.

2.5.3 Model application

For further evaluation of our models, we have applied them to a large, unroaded area, Wägital, which is located on the northern slopes of the Swiss Alps in the geological zones of flysch and limestone (Fig. 2.11). The road network layout in this region is challenging because of the steep terrain (average slope gradient of approximately 45%), difficult geotechnical conditions, and a dense water channel network. Our evaluation task is to find a Steiner minimum tree and connect 10 terminal nodes that have been identified by road engineers. The area is 35 km^2, and its graph representation consists of 5.6×10^6 nodes and 95.3×10^6 links. This problem size nearly reaches the capacity limit of a PC with 2.66 GHz and 2 GB RAM.

The purpose of such a model application is to answer the following questions:

- Can the model solve the road network location problem, and how much computing time is required?
- What is the benefit of the 48-link model over other models?
- Does the model result seem reasonable when compared with expert opinion?

Similar to the model validation introduced above, we have again used Model (c) "Lazy Zigzag" as a current state-of-the-art approach, and Model (f) "48-link" as the new approach. Model (a) "Zigzag 8" has not been included because of its inability to find any feasible solutions. The quantitative results from each model are presented in Table 2.6, and the network layouts are

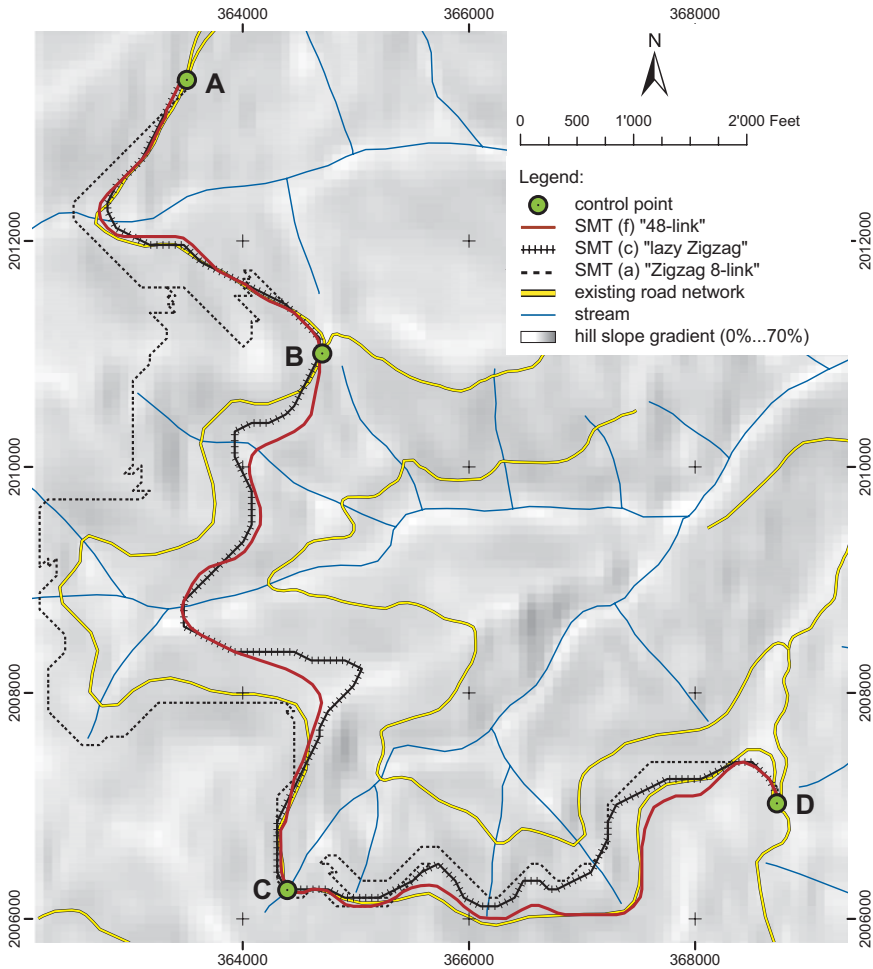

Figure 2.10: Model-designed road network for Models "Zigzag 8" (a), "Lazy Zigzag" (c) and "48-link" (f), and existing road network. Background: slope gradient and streams. Mica Creek watershed (Idaho, USA)

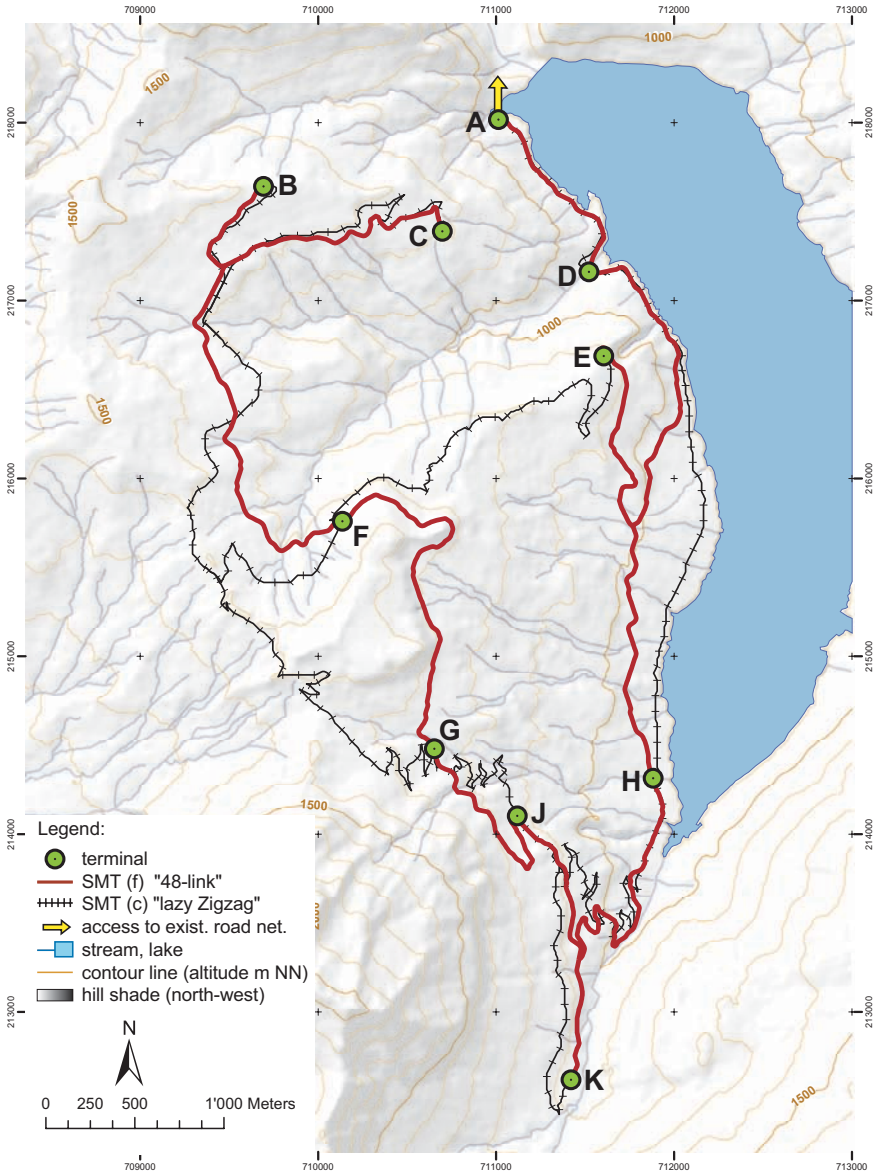

Figure 2.11: Model-designed road network for Models "Lazy Zigzag" (c) and "48-link" (f), based on road construction cost estimations. Background: hill shade of relief, streams, and lake. Wägital project area (Switzerland); 5 $km \times 7$ km

Model	Processing time for graph-building [min]	Optimization approach	Processing time for optimization [min]	Length [m]	Number of switchbacks	Construction cost [1000 CHF]	[%][b]
Lazy Zigzag[a]	113	MST	31	24'292	40	8'028	118%
		SMT	38	22'931	35	7'623	112%
48-link	164	MST	301	20'358	10	7'295	107%
		SMT	746	18'769	6	6'802	100%

Table 2.6: Results of Models "Lazy Zigzag" (c) and "48-link" (f) in the Wägital project area.
1 $CHF \approx 1\ CAD$. [a] This model does not include additional costs for curve-widening and switchbacks.
[b] Percent ratio to the SMT of the 48-link model.

shown in Figure 2.11. The Steiner minimum tree that has resulted from the 48-link model is used as the base reference in these comparisons.

With a personal computer (2.66 GHz, 2 GB RAM), both models can find a solution after 0.5 hours or 12 hours of computation time for Model (c) or Model (f), respectively. The difficulties associated with the former arise because too many switchbacks are proposed when connecting nodes in steep terrain, especially near terminals G, H, J, and K. Although both models connect the 10 terminals in a similar sequence, their road network layouts are not congruent. Terminal E is connected from Terminal F in Model (c), whereas Model (f) connects Terminal E from Terminals D and H. Both models locate two Steiner points in similar areas (one for B, C, and F; the other, for H, J, and K).

Our field verification, conducted with road engineers, has revealed that the location of road routes in Model (c) is not practical because too many switchbacks are involved. In contrast, the road locations resulting from Model (f) seem feasible, although one potential problem is noted in section H, J, K, where the engineers have suggested the possible elimination of two of the three switchbacks.

2.6 Conclusions and discussion

The objective of this study has been to increase the effectiveness of automatic route location layouts for forest roads in steep terrain by (1) refining the road link pattern from one node to its adjacent nodes, and (2) improving the formulation for road curvature constraints.

Our investigation of the various models demonstrates that the link pattern specification heavily influences road network locations and alignments. Standard 8-link models that have been widely used may not be adequate for finding field-applicable road networks, even over moderate terrain. Our results indicate that a "24-link" pattern model, with switchback penalties but without curvature constraints, represents the lower limit of link pattern specifications for moderate conditions with slope gradients of up to 30%. Increasing the steepness of the terrain demands the improvement of link patterns (e.g., 48 links per node) as well as the introduction of curvature constraints, although such enhanced link models require more processing time than do simple 8-link models.

By modifying the link pattern from 8 to 24 and penalizing switchbacks, one can improve the cost of proposed road network solutions in moderate terrain by at least three-fold, while increasing the computing time by only about 20%. In this model, the penalties for switchbacks are constant and may be very low for steep terrain. A higher switchback penalty or a penalty as a function of the slope gradient, additional penalties for vertical and horizontal road alignment would presumably improve the penalty model and may lead to more accurate results. However, a 24-link pattern is very limited in steep terrain (cf., Fig. 2.4 and Fig. 2.5). Instead of improving enhanced penalty models we mapped the curvature constraints on the graph model. The introduction of curvature constraints increases the size of the graph representation by a factor of 256, resulting in a 2- to 20-fold longer computing time. For moderate terrain, this addition of curvature constraints improves a solution by about 10% in cost savings, whereas for steeper conditions, such constraints become mandatory when identifying reasonable road network alignment designs. However, those curvature constraints only make sense together with an enhanced link pattern.

This improved approach has some limitations, including, first, the size of the project site. For example, an area of 35 km^2 with a node spacing of 10 $m \times 10$ m and 10 terminal points seems to define the maximum for both problem size (6×10^6 nodes and 3×10^8 links) and processing time (about 12 hours) for personal computers currently available. Second, our new approach considers only a single objective function (i.e., minimizing road construction costs). Most real-world problems, however, deal with multiple objectives, such as minimizing road and harvesting costs as well as ecological impacts. Although our approach can be modified to consider those multiple objectives (Stückelberger et al., 2006b), the efficiency of the current problem-solving techniques may remain questionable as the problem becomes more complicated. Third, the improved approach may not always provide "optimal" road networks. Some modifications to the proposed link-pattern and node spacing may be necessary for better results, depending on the road design specifications. Those results must then be field-verified before they can be implemented.

Further study of any automatic road layout should include improving network optimization algorithms, e.g., SMT. The Steiner Tree problem is $\mathcal{NP}$-hard, and up to now no algorithm can find the real mathematical optimum within a short solution time. When combined with exact network algorithms, intelligent heuristic search methods may be a promising path toward such improvements. Other research should involve the formulation and scaling of multiple objective functions in order to better represent real-world problems. Not only the economic efficiency of forest roads, but also other considerations such as ecological impacts, soil disturbance, and scenic values, often must be incorporated into road decision-making.

Chapter 3

Automatic road-network planning for multiple objectives

Jürg Andreas Stückelberger, Hans Rudolf Heinimann, Woodam Chung, Marcus Ulber

Abstract accepted: February 15, 2006 / Submitted: Mai 30, 2006 /
Published: July 29, 2006

Nominated for the COFE Student Communication Award: June 12, 2006 /
Elected for the best paper: July 31, 2006

The 29th Council on Forest Engineering Conference. July 30 – August 2, 2006. Coeur d'Alene, Idaho. W. Chung and H.S. Han, editors.
pp. 233–248

Abstract

Automatic planning of forest road networks is an on-going, challenging task. Advances have been triggered by the increased availability and accuracy of digital terrain models, greater computing power, and improvements in optimization techniques. Defining one's objective functions is a crucial step in guiding the design process and controlling optimization. However, the problem still exists for mapping the fitness of design alternatives to valuable, spatially explicit figures for one or more of those functions. This paper aims (1) to present system models that map the spatial variability of three objective functions (construction and maintenance costs, negative ecological effects, and the suitability, or attractiveness, for cable-yarding landings); and (2) to evaluate the effects of this multi-objective problem on Pareto-optimal solutions. We have taken two approaches for articulating our objective preferences (*a priori* "choice before search" and *a posteriori* "search before choice") as well as two optimization methods (graph algorithms and a heuristic search). Our results show that (1) the Steiner minimum tree solutions are located on convex trade-off surfaces, as expected from the multi-objective optimization theory; (2) single-point solutions are clustered on the Pareto frontier, such that small changes in the relative weights of objective-function components can trigger movement from one cluster to the next; and (3) allocation of relative weights to those components greatly affects the solution.

3.1 Introduction

Designing the optimal road network is difficult to do across a varying landscape (Scaparra & Church, 2005a). Engineers must consider several related problems: (1) an overwhelming amount of terrain and environmental data, (2) a lack of explicit constraints, and (3) unclear and contradictory goals. Computer-aided engineering approaches have been developed for solving these layout problems (Kirby, 1973, Mandt, 1973, Dykstra, 1976, and their utility has been accelerated by the widespread availability of digital elevation models. Initially limited by computing power, they have been improving continuously, resulting in software packages such as PLANS (Twito et al., 1987), PLANEX (Epstein et al., 1999, Epstein et al., 2001), and CPLAN (Chung & Sessions, 2002). However, even the most sophisticated methods have some shortcomings: (1) they assume road-building costs to be route-independent, (2) they limit the number of possible links from a specific network node to its adjacent nodes, (3) they assume the road centerline to be a chain of consecutive straight lines without considering curve or switchback constraints, and (4) they rarely analyze systematically the trade-offs between different objective functions. Previously, we reported improvements on the first three shortcomings, and presented a route-dependent cost estimation model (Stückelberger et al., 2004, Stückelberger et al., 2006a) and an improved link-pattern. Here, we introduce an approach to forest road layout that overcomes the last shortcoming – the lack of systematic analysis for trade-offs in multiple objectives.

Real-world engineering optimization problems are inherently multi-objective because they normally have several, possibly conflicting, goals that must be satisfied simultaneously (Stadler, 1988). Rarely is there a single point that optimizes all the objective functions concurrently. Most optimization algorithms rely on a scalar fitness function to guide the search. The most intuitive approach is to combine the multiple objectives into a single function via the "weighted sum of objective functions methods" (Coello, 2000), (Coello, 2001). Weighting factors map the preferences of a decision maker, and can be allocated in two ways: (1) *a priori*, where the trade-offs to be applied are defined before the optimization methods are run, and (2) *a posteri-*

ori, where the decision maker chooses the solution by examining possible options computed by optimization methods (Collette & Siarry, 2004). *A posteriori* methods produce, at the end of the optimization process, a trade-off surface. Most previous approaches to road layouts used a mono-objective configuration that minimized some cost functioning. Only a few contributions were based on a bi- or multi-objective problem, and were implemented very efficiently by the "weighted sum of objective functions" approach. Nevertheless, it is possible, by varying the value of the weights, to approximate the trade-off surface. One obvious problem with this approach, however, is that it may be difficult to generate a set of weights that properly scales the objectives when little is known about the problem. Another, more serious, drawback is that this approach cannot generate proper members of the Pareto (1896–1897) optimal set when the frontier is concave (Coello, 2001, Collette & Siarry, 2004). The goals presented here include: (1) the development of a system model that maps the spatial variability of three objective functions (life-cycle costs, concurrent ecological effects, and the suitability, or attractiveness, of cable-yarder landings; and (2) an evaluation of the Pareto frontier for this objective configuration at specific test sites. We first describe the methodology and then provide an assessment of optimal road layouts for different mono- and multi-objective configurations.

3.2 Methods

3.2.1 Objective functions

The resolution of problems concerning realistic road-route layouts requires the simultaneous optimization of more than one objective function. Solutions must be (1) physically feasible, (2) economically efficient, (3) environmentally sound, and (4) institutionally acceptable. Physical feasibility is usually guaranteed by constraint formulations on the solution space, whereas economic efficiency and environmentally soundness have to be simultaneously maximized. Our aim is to solve the following problem: find a minimum spanning tree that connects mandatory points in mountainous terrain. Here, "minimum" refers to simultaneously and efficiently reducing life-cycle costs and the likelihood of selecting attractive landing locations, as well as minimizing the disturbances to habitat and rare ecotopes. The four components of this objective function are specified below.

3.2.1.1 Estimating construction costs

Cost estimation is the most decisive factor when planning the layout of low-volume forest road networks. We (Stückelberger et al., 2006a) have developed a model that estimates the spatial variability of road life-cycle costs. This overall model has five components: (1) a digital elevation model (DEM), (2) classification for geotechnical properties of the subsoil, (3) the specification of road design parameters, (4) unit costs for structural components, and (5) a rock-excavation share model (Fig. 3.1). Historically, this method has been superior to estimates based on expert knowledge, and is believed to be the only procedure for modeling the spatial variability of roading costs in large, mountainous areas.

3.2.1.2 Estimation of adverse ecological effects

It is a normative decision to select a set of adverse ecological effects. Decision preferences also vary in space and time, making it difficult to compare different approaches. In our investigation, we have considered two types of environmental impacts – habitat quality for the capercaillie

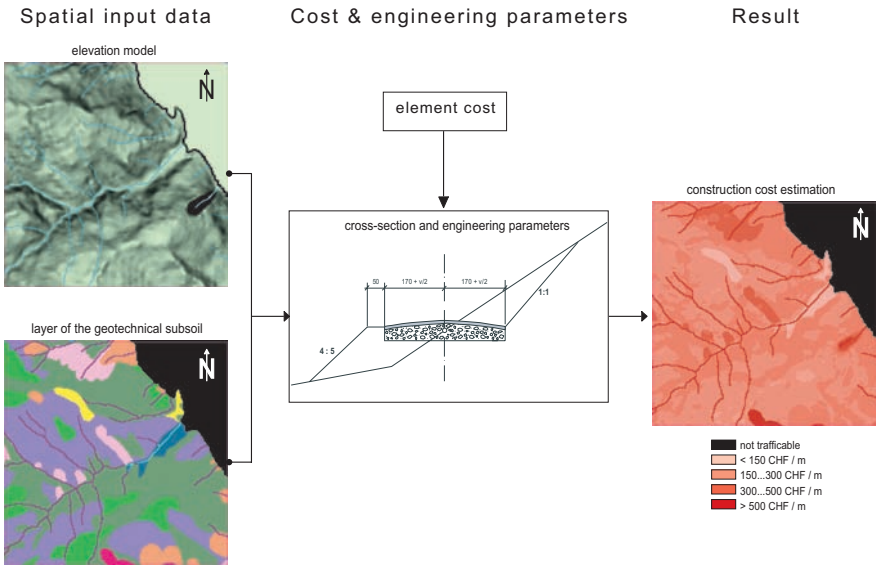

Figure 3.1: Flowchart for potential road construction cost estimation. Area of Wägital (Switzerland), 2 $km \times 2$ km

(*Tetrao urogallus*) and marshland biotopes. Capercaillie, the largest mountain grouse in middle Europe, is threatened with extinction (Keller et al., 2001). Its requirements for forage, cover, reproduction, and comfort are crucial variables that define habitat suitability (Bollmann, 2003). We have used Graf's (Graf et al., 2002) habitat suitability index (HSI, cf., USDI Fish and Wildlife Service, 1981) to measure capercaillie habitat quality. Disturbances are assumed to be proportional to road length and HSI (Ulber, 2004). For example, a 100-m-long road segment that crosses a capercaillie habitat with a suitability index of 0.2 results in an impact cost of 20, which is considered equivalent to a 20-m road segment that might cross a habitat with an HSI of 1.

Marshland areas, including upland moors, reeds, and wetlands, are important ecotopes that are protected by Swiss legislation. Determining their ecological value is difficult. Government agencies have established a standard evaluation procedure that considers the size of the area, the number of different vegetation types, and diversity (BUWAL, 1991). Several adverse effects on marshlands must be weighed. First, road construction directly disturbs such areas due to sealing of the surface. Second, it can cause indirect disturbance by influencing the flow of groundwater (Marti et al., 1997). Third, a road can dissect a marshland biotope, leading to fragmentation (Jaeger, 2002). Therefore, we have introduced outside and inside buffer zones, each 100 m wide (Fig. 3.2). The inside buffer zone and the center zone are assumed to have habitat values based on the considered worth of the ecotope (Ulber, 2005), whereas the habitat value of the outside buffer zone is assumed to decrease from that value to zero. Marshland disturbance is presumed to be proportional to road length and ecological value. If a road enters the center zone, an additional penalty is added to the disturbance factor, thereby representing the fragmentation effect.

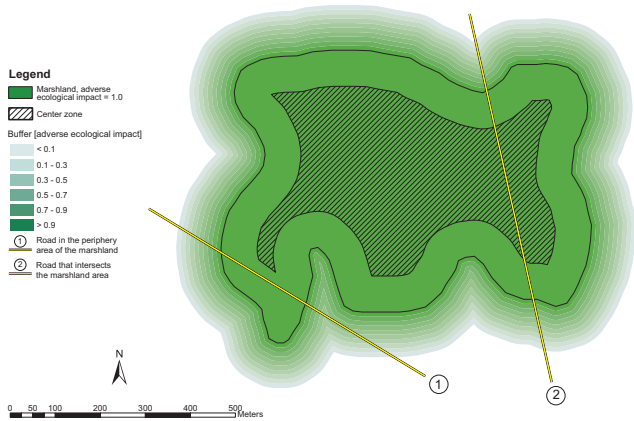

Figure 3.2: Marshland area with buffer and central zones. Road (1) affects the marshland in the buffer zone and periphery only, whereas Road (2) additionally influences the marshland because of the intersection effect (schematic draft).

3.2.1.3 Attractiveness of cable-yarder landings

Positioning of the landing locations influences the efficiency of off-road transportation, especially for cable-based extractions. A road should not only connect mandatory access points, but also reach favorable landings. We, therefore, have introduced a landing-attractiveness factor that considers both effectiveness and efficiency of the cable yarder in operations (Fig. 3.3). This factor is calculated according to the following procedure:

1. select a raster cell as a potential landing location (L)
2. for = 0° to 345° (in 15° increments):
3. determine the tailspar point (T) for maximal skyline length,
4. determine the terrain profile,
5. for any point between T and L:
6. calculate ground clearance of the cable road,
7. when ground clearance is ≤ 0, then
8. move T one unit in the direction of L.
9. fix location T,
10. connect all T-points,
11. calculate area bounded by T-points (Fig. 3.4),
12. weight the area with the timber volume to be harvested, and
13. repeat 1 to 12 until all raster cells are evaluated

Step 12 can also be modified slightly by weighting the potential logging volume by a factor that represents the installation and logging conditions (e.g., the number of intermediate supports (I) and logging direction).

A powerful model (CableAnalysis 1.0) is available for automatically determining the landings for cable logging (Chung, 2002, Chung & Sessions, 2003, Chung et al., 2004). We have incorporated this model into our procedure for calculating attractiveness for the cable yarder.

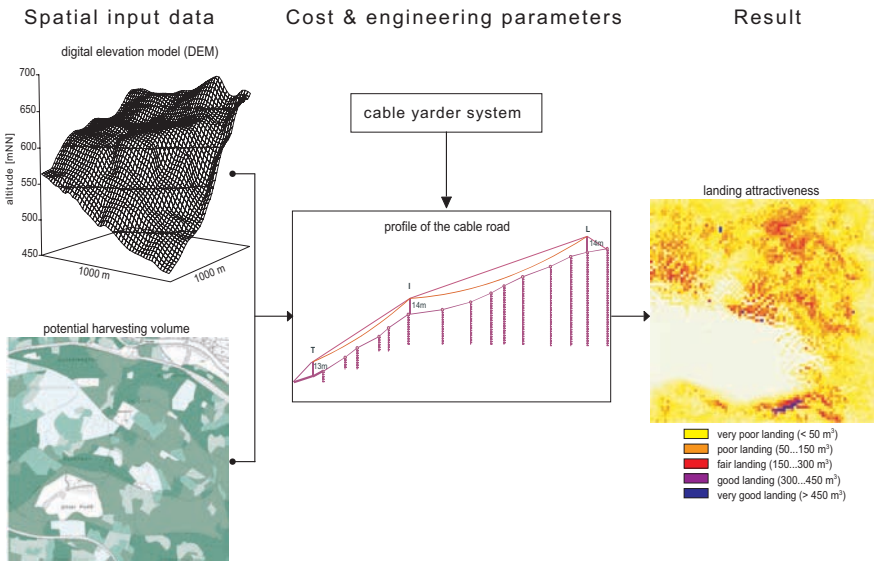

Figure 3.3: Flowchart for calculating cable-yarder attractiveness. Area of Uetliberg (Switzerland), 1 $km \times 1$ km

3.2.2 Multi-objective optimization

Multi-criteria optimization is rooted in late-19$^{\text{th}}$ century welfare economics, as described by Edgeworth (1881), (1889) and Pareto (1896–1897). A feasible solution to a multiple objective problem is considered Pareto-optimal if no other feasible solution is at least as good for every objective function or performs worse than at least one other. This means that no objective component can be improved without other components being made worse. Typically, there is an entire curve or surface of Pareto points, whose shape indicates the nature of the trade-off between different goals (Fig. 3.5). Multi-objective problems are very often solved by combining all components into one scalar objective function (Eq. 3.1). The prevailing approach consists of minimizing the weighted sum of function components, which is called an "*a priori* definition of the multiple-objective function". With this approach, the decision maker defines the trade-off to be considered and explicitly expresses his or her preferences before running the optimization model.

$$O_x = \sum_{i=1}^{k} w_i \times f_i(x) \tag{3.1}$$

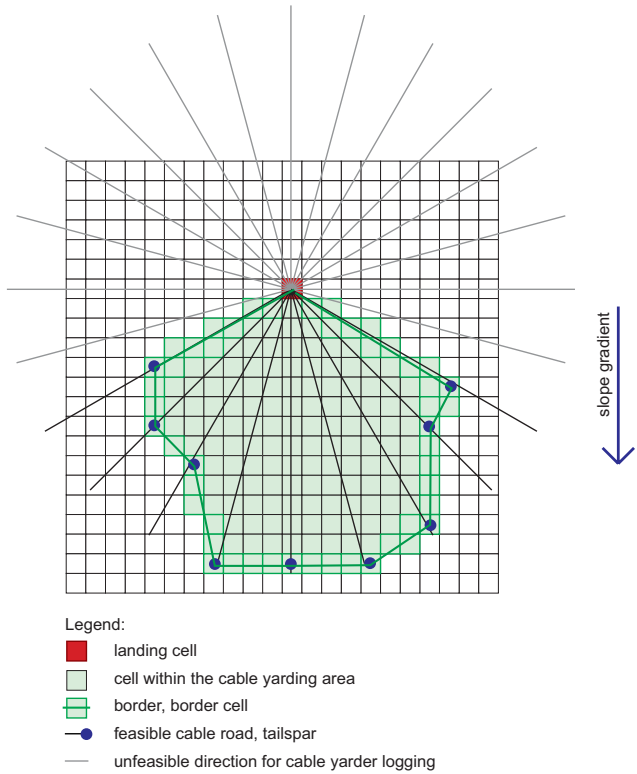

Figure 3.4: Cable-yarder landing and its overspanning harvesting area (schematic draft)

where, x = objective x
O_x = aggregate fitness of object x
k = number of different objectives
w_i = weighting factor of objective i
$f_i(x)$ = i$^{\text{th}}$ objective function for object x

It is up to the user to choose appropriate weights, which are extremely decisive for the solution that will result from the optimization process. The main shortcoming of this "*a priori*" approach is that the solution represents only one point on the Pareto frontier, and trade-offs are not evaluated and understood. In contrast, an "*a posteriori*" optimization aims at tracing the complete Pareto frontier curve for each multi-objective case, thereby producing $n(k-1)$ evaluation cases. The eventual computational effort is extremely high, necessarily restricting the analysis to only a small subset of the solution space.

"A posteriori" preference methods investigate a set of solutions that results from systematic variation in the weights of the objective-function components. At the end of the optimization, those methods produce a trade-off surface, i.e., the Pareto frontier[1]. Given two objectives, O_1 and

[1]Here we used a definition, which is common in economics but not entirely strict. In Paper IV (Chapter 4) we referred to a mathematical, more precise definition which distinguishes *solution space* and *criterion space*. We therefore used the term *Efficient Set*, i.e. the mapped Pareto Set from the *solution space* to the *criterion space* (cf. Definition 2).

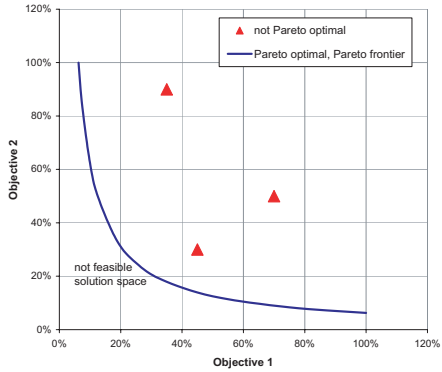

Figure 3.5: Solution space with Pareto optima of 2 objectives

O_2, that must be minimized simultaneously, many Pareto frontiers in real-case studies describe a hyperbolic function derived with Equation 3.2, and defined by parameters a, b, c, and d. Often, parameter a is set to 1.

$$y = \frac{c}{x^a + b} + d \tag{3.2}$$

where, $x = O_1$ and $y = O_2$

3.2.3 Graph model for road-network system

Road engineers control the geometry of a layout by following a sequence of vectors, known as a 'traverse'. The road is then designed as a series of curves inside the angles between consecutive vectors, straight segments along vectors, and curves outside the angles between successive vectors that define hairpin bends (Ervin & Gross, 1987). A geographical area is the continuous physical entity on which we can define an infinite number of points for use as the start- and end-points of vectors. However, graph optimization algorithms require a finite set of nodes (vertices) and links (edges). Therefore, the specification of the design space follows the concept of discretization, i.e., splitting a continuous physical system into a discrete set of simple shapes. The prevailing approach uses either grid or graph representations. Road directions in the former are limited to the eight neighboring grid cells. In contrast, a graph representation is not limited to a regular grid structure, and allows more and different road directions. The aim of a graph model is first to generate a mesh of all possible links over the entire project area, then find the best subset of the graph that represents the optimal forest road network.

Our model employs a graph representation. However, our nodes are arranged in a regular structure representing the central point of each raster cell of the DEM. In contrast to a standard grid representation, road links (edge) are not defined between neighboring grid cells only, but also are found within an enlarged neighboring area (Fig. 3.6). This extension of neighborhood is very important, especially in steep terrain (Stückelberger et al., 2004).

3.2.4 Optimization techniques

The problem here is to find the minimum spanning tree that links all mandatory control points. The solution requires a sequence of analytical tasks:

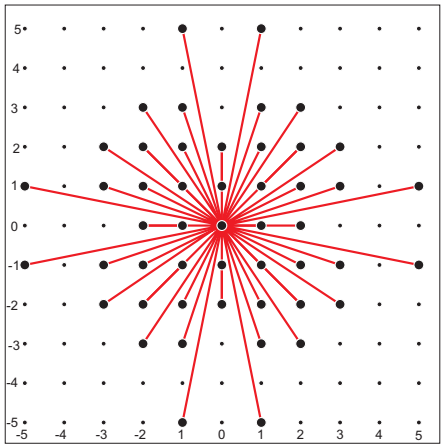

Figure 3.6: Neighborhood patterns of one center node to 48 neighboring nodes

- identify a feasible set of links,
- calculate and assign the weight for each feasible link,
- use Dykstra's algorithm (DIJKSTRA, 1959) to calculate the shortest paths (SPs) for any subset of two control points,
- find the minimum spanning tree (MST), using the SP to all mandatory control points (terminals), according to Prim's algorithm (PRIM, 1957), and improve the solution by introducing Steiner points (PRÖMEL & STEGER, 2002) to identify the Steiner minimum tree (SMT).

SP and MST algorithms are well documented (WWW.CPROGRAMMING.COM, 2005a, WWW.CPROGRAMMING.COM, 2005b). The problem of introducing Steiner points is more difficult. In a graph with n nodes, $n-2$ Steiner points may be incorporated to improve the solution and find the Steiner minimum tree. Unfortunately, there is no algorithm to locate those Steiner nodes within polynomial time, making this problem $\mathcal{NP}$-hard (i.e. Non-deterministic Polynomial-time hard). If the size of the project area and the number of terminal points are limited, it is possible to determine the mathematical optimum for the SMT by testing all combinatorial possibilities. For larger problems, however, the use of heuristics is an efficient approach to obtain at least near-optimal solutions. Simulated annealing (KIRKPATRICK et al., 1983), the heuristic we have adopted here, produces solutions that are within a couple percentage points of the optimum.

3.3 Model evaluation and results

3.3.1 Evaluation of layout

Different configurations of the multi-objective function are evaluated in order to optimize route layouts. Here, we have analyzed three configurations: (1) mono-objective, (2) Pareto frontier, and (3) bi-objective with weight variations. Although our graph model follows the 48-link pattern (Fig. 3.6), a Steiner minimum tree optimization procedure is used. Our first test site is at

"Wägital", a 35-km^2 area on the northern slopes of the Swiss Alps. This region is characterized by steep terrain (average slope gradient of approximately 35%), difficult geotechnical conditions, a dense water channel network, and high-value ecotopes and habitats. It, therefore, is an ideal model for investigating multiple, conflicting objective conditions.

3.3.2 Mono-objective optimization results

The "Wägital" area has 10 mandatory control points (Fig. 3.7). The problem to be solved is to find an SMT that minimizes costs, impacts on capercaillie habitat, and harm to marshland ecotopes. The key parameters in our cost-optimal solution (Scenario 1; Tab. 3.1) consist of a 19-km-long road network with a life-cycle cost of 6.6 million Swiss francs (CHF). Adopting eco-optimal solutions that conserve both capercaillie habitat and the marshland ecotope results in a longer road network and higher costs. When those potential impacts are evaluated separately and compared with our cost-optimal data, the capercaillie-optimal solution (Scenario 2) involves a 62% longer road network and 84% higher costs. Likewise, the marshland-optimal solution (Scenario 3) requires an additional 18% in road length and a 32% increase in costs, compared with the cost-optimal solution. These results demonstrate the conflicting nature of two ecological objectives. The capercaillie-optimal solution not only incurs longer roads and greater costs, but also increases the impact on marshland ecotopes by about 65%. Overall, the impact of the marshland-optimal solution is three-fold greater than that of the capercaillie-optimal solution. The main difference in length and cost for capercaillie-optimal versus marshland-optimal solutions, based on our Steiner minimum tree network (Fig. 3.7), arises because a long detour is required for bypassing capercaillie habitat in the northern part of the project area.

3.3.2.1 Cost versus ecology trade-offs

The determination of the Pareto frontier is based on stepwise changes in the relative weight of objective-function components[2]. Here, we have evaluated the trade-off between cost minimization and the lowest ecological impact. The eco-component is a scalarization of the two eco-objectives, minimization of capercaillie habitat impacts and minimization of marshland ecotope impacts. Relative weights of these two components change within a range from zero to 1000. Our Pareto frontier evaluation (Fig. 3.8) is bound by two extremes: (1) the cost-optimal solution (at the upper-left end), and (2) the eco-optimal solution (lower-right end). These numbers represent the relative weight between the eco- and the cost-components of the objective function. One might assume the Pareto points to be evenly distributed along that frontier. However, the Pareto-optimal solutions are concentrated on three clusters: (1) a cost-optimal cluster, with relative weights of 0 to 4, (2) a cost-eco-balanced cluster, relative weights of 5 to 350, and (3) an eco-balanced cluster, relative weights of 400 to 1000. The Pareto frontier has two discontinuities at which the solutions are "jumping": first, at the weight change from 4 to 5, and second, from 350 to 400. The Pareto points (Fig. 3.8) are located on a hyperbola (parameters $a = 1$, $b = -0.62$, $c = 0.182$, and $d = 0$ (Eq. 3.2), and the optimization results truly lie at the Pareto frontier. The spatial layouts for the cost-optimal, cost-eco-optimal, and eco-optimal solutions are shown in Figure 3.9. These evaluation results improve our understanding of the trade-offs.

[2]This approach leads to a subset of the Pareto frontier only. However, this subset contains the most interesting Pareto optimal solutions for real cases. In Paper IV (Chapter 4) we discuss this issue in detail (cf. Subsection 4.2.7).

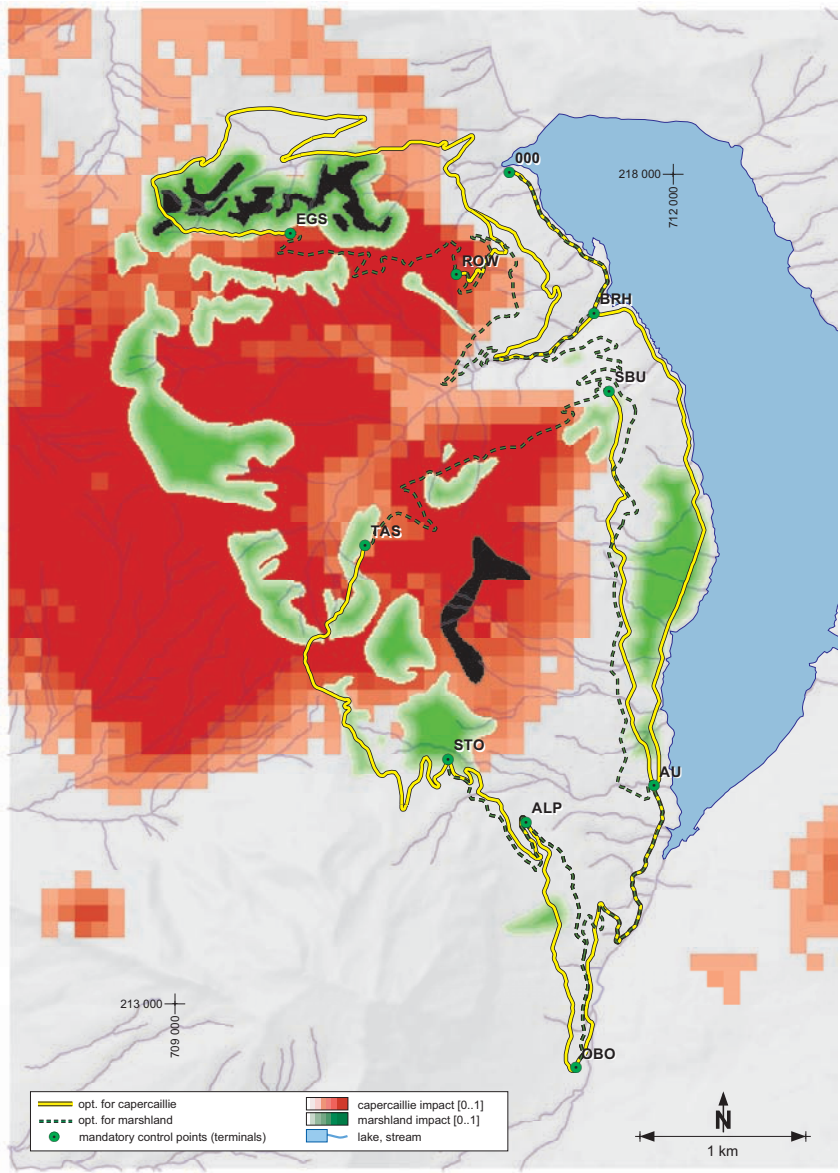

Figure 3.7: Road network (SMT) for Scenarios 2 (capercaillie-optimal) and 3 (marshland-optimal) between 10 mandatory control points. Background: ecological value of capercaillie and marshland, streams, lake, and hillside. Project area of Wägital (Switzerland), 5 $km \times 7$ km

Scenario	Road length $[m]$	Net present value $[CHF]$	relative	Capercaillie impact $[m \times I]$	relative	Marshland impact $[m \times I]$	relative
(1) Cost-optimal	19'001	6'630'831	100%	6'221	285%	1'677	80 ×
(2) Capercaillie-optim.	30'827	12'216'567	184%	2'184	100%	2'776	132 ×
(3) Marshland-optimal	22'439	8'771'925	132%	7'279	333%	21	1 ×

Table 3.1: Key parameters and their associated costs when comparing road networks among optimized scenarios

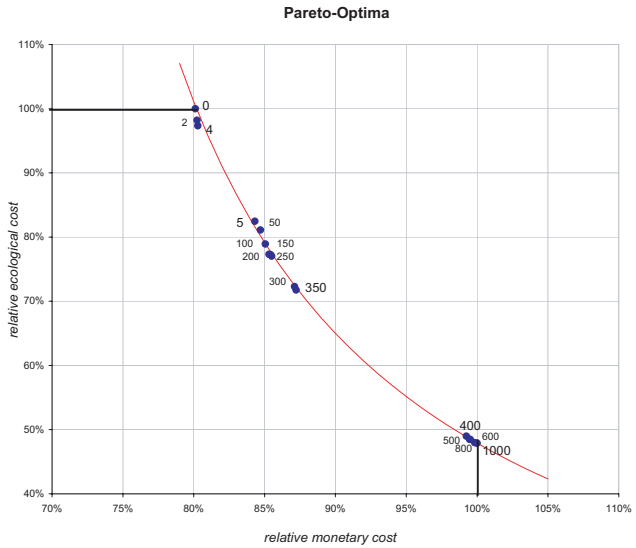

Figure 3.8: Pareto-optimal solutions and Pareto frontier of monetary and ecological costs. Area of Wägital (Switzerland)

3.3.3 Trade-offs between costs and landing attractiveness

In evaluating the trade-off between minimizing costs and maximizing of landing attractiveness for cable yarding, determination of the Pareto frontier is based on a stepwise change in the relative weights of two objective-function components. The problem to be solved here is to connect three control points in the "Uetliberg" project area (Fig. 3.11). Relative weights change between zero and two. The Pareto frontier (Fig. 3.10) is bound by the cost-optimal solution (upper left) and the attractiveness-optimal solution (lower right). One assumes that a stepwise change in relative weight would be manifested in corresponding steps on the Pareto frontier. Nevertheless, relative weights between zero and 0.65 result in a cost-optimal cluster with a road length of about 1.85 km and a landing attractiveness of about 150%. In contrast, a relative weight of 0.7 is associated with approx. 33% longer roads and a landing attractiveness of about 250%. This discontinuity is caused by a change in route location between points B and C. A further increase to 1 for relative weight alters the route between points A and B, such that relative road construction costs rise by 170% and the relative landing attractiveness is enhanced by 360%, compared with our construction cost-optimal solution. Raising the relative weight from 1 to 2 produces marginal improvement in landing attractiveness but also increases construction costs considerably. Figure 3.11 illustrates the spatial layouts of our different Steiner minimum trees.

3.4 Discussion and conclusions

This paper presents models for mapping the spatial variability of three objective functions in forest road design (life-cycle costs, adverse ecological effects, and landing attractiveness). The effects of this multi-objective problem on Pareto-optimal solutions were evaluated at various test sites. Three major findings have emerged from this investigation. (1) The Steiner minimum tree solutions are located on convex trade-off surfaces, as predicted by the multi-objective optimization theory. (2) Single-point solutions are clustered on the Pareto frontier; even small changes in the relative weights of objective-function components can trigger jumping from one cluster to the next. (3) The allocation of relative weights to those components greatly influences the solution.

To our knowledge, this is one of the first analyses of the trade-off surfaces for multi-dimensional objectives that optimize the layout of road networks at a 10 $m \times 10$ m resolution. Problem-solving in the open space is characterized by a set of partially conflicting requirements brought forward by different stakeholders. Mono-objective analysis evaluates the edges of the solution space that characterize those varying points of view.

In our example, the landowner was interested in a cost-optimal solution, whereas ornithologists would prefer our capercaillie-optimum and marshland specialists would look for the marshland-optimum. Therefore, mono-objective results are a good starting point in the negotiation process because they quantify the effects of extreme preferences on the different objectives. Systematic variations in the relative weights of the objective-function components are a prerequisite for exploring the Pareto frontier. The evaluation presented here clearly improves our understanding of problem-specific trade-offs and identifies solution clusters. Only three clusters resulted from the 10 mandatory control points analyzed in this Steiner minimum tree problem. It seems a likely supposition that the number of solution clusters would increase with the number of mandatory control points. Obtaining a Pareto solution by *a priori* "choice before search" is only

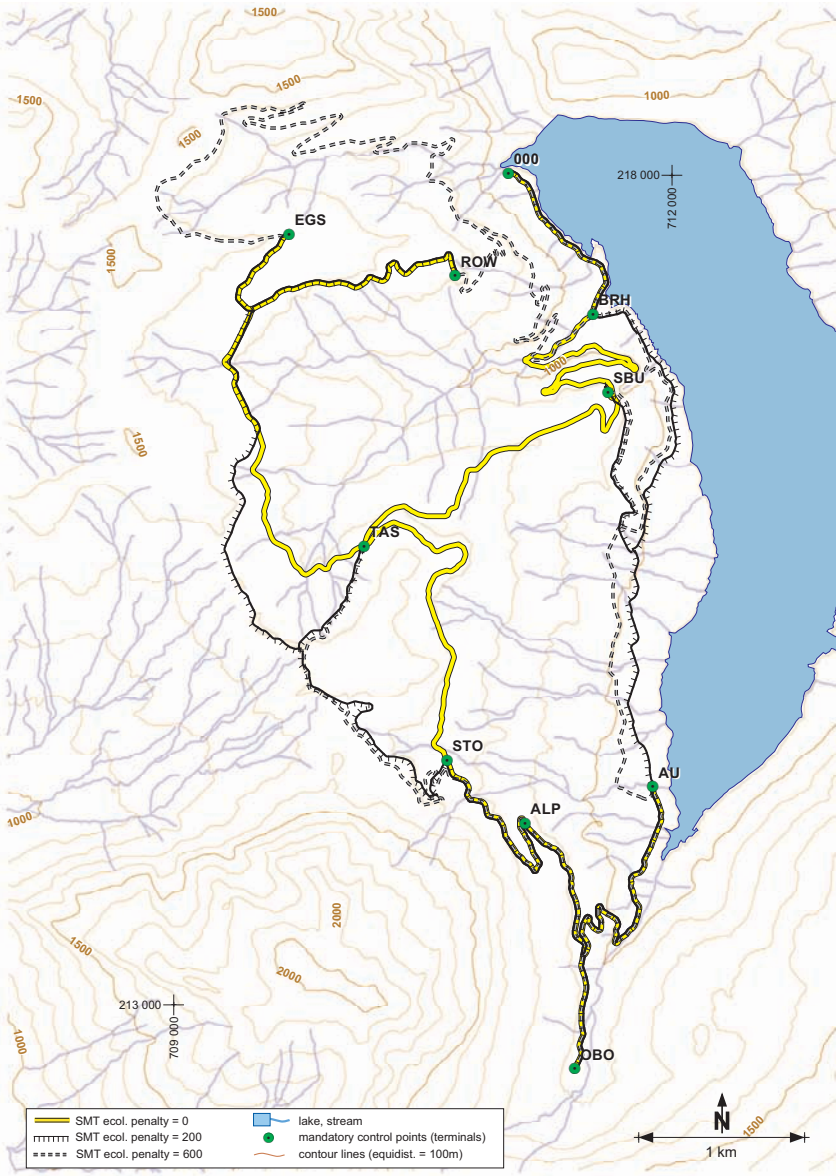

Figure 3.9: Road networks (SMT) for cost-optimal, balanced, and ecological-optimal scenarios between 10 mandatory control points. Background: contour lines, streams, and lake. Project area of Wägital (Switzerland), 5 $km \times 7$ km

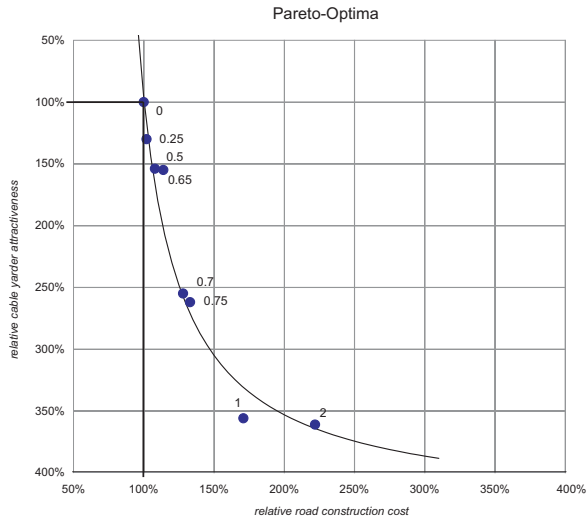

Figure 3.10: Pareto-optimal solutions and Pareto frontier of road construction costs and cable-yarder attractiveness. Area of Uetliberg (Switzerland)

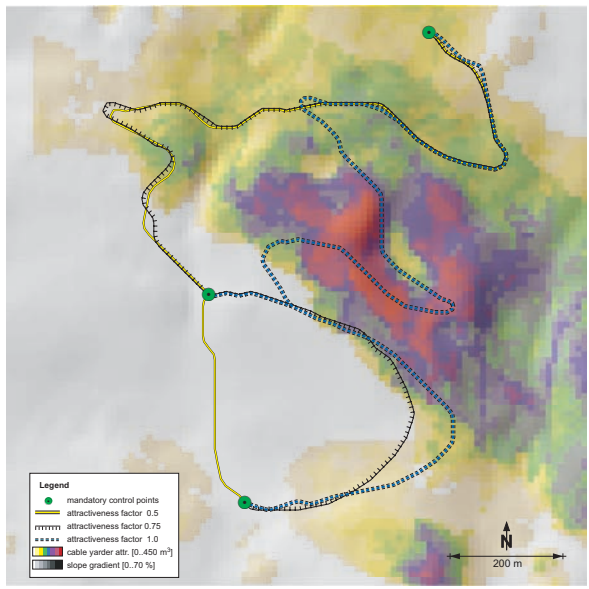

Figure 3.11: Road networks (SMT) for 3 different objective functions (weighting factors for cable-yarder attractiveness: 0.50, 0.75, or 1.00) between 3 mandatory control points (A, B, and C). Background: slope gradient and cable-yarder attractiveness. Project area Uetliberg (Switzerland), $1\ km \times 1\ km$

permissible if a problem is repeatedly solved for many different weighting factors, a task that can tremendously multiply computational efforts.

Our approach also has some shortcomings. Whereas a cost metric may adequately map a real-world situation, our ecological impact metric is based on expert knowledge that considers some weak, unclear components, which one must be aware of when interpreting these results. A basic assumption of multi-criteria-optimization is that objective values must be independent. However, our landing-attractiveness metric violates this assumption because it allocates accessible, though overlapping, areas to each grid cell. Nevertheless, this approach seems to be useful in controlling the location of routes for specific off-road transportation technologies (e.g., ground-based, cable-based, or airborne).

Chapter 4

Multi-criteria optimization procedures for designing a forest road network

Jürg Andreas Stückelberger, Hans Rudolf Heinimann, Justus Schwartz, Angelika Steger, Woodam Chung

Abstract

The sophistication of digital spatial data, such as elevation models, soil and stand information, or habituate suitability indices, has risen in the last few years. Simultaneously, enhanced computer power has enabled the solution of large combinatorial problems. These two improvements have made it possible for us to develop automatic procedures for locating road networks. However, to benefit from this increase in spatial data with better resolution, we must have suitable models for planning forest operations. Likewise, we must know and quantify the objectives to find the optimal solution. Current goals often have more than one dimension, such as monetary (e.g., road construction costs) and non-monetary (e.g., ecological impacts) components, so that the optimal solution depends on valuations from different stakeholders. This paper is intended to (1) give an overview of the framework for determining near optimal forest road network, (2) present new components of this framework, and (3) demonstrate how to implement multi-objective functions. Here, those new components were applied to a test area in the Swiss Alps, where the steep terrain provided challenging subsoil and ecological constraints. These tests led to three major findings. (1) The objective values of all model designed alternatives lay on a convex trade-off surface, (2) small changes in the objective function may lead to completely different solutions, and (3) the preferences of the stakeholders influence the solution greatly.

4.1 Introduction

Computer-aided engineering (CAE) is an emerging field that aims to support the problem-solving activities of engineering experts. The layout of road networks is a complex locational problem (Church et al., 1998), (Church, 2002) that is extremely demanding, especially in steep terrain. CAE approaches were introduced in the 1970s (Dykstra, 1976, Kirby, 1973, Mandt, 1973). Increased computing power has now resulted in software packages such as PLANS (Twito et al., 1987) and PLANEX (Epstein et al., 1994, Epstein et al., 1999, Epstein et al., 2001). The availability of spatial data has improved tremendously in the last two decades due to new remote-sensing technology (e.g., LIDAR) and enhanced high-speed data connections. However, because most existing software packages were developed in the 1990s, they do not take in account to this improved spatial data and, therefore, have the following shortcomings. (1) They assume road-building costs to be constant throughout the project area, (2) they limit the number of possible links from a specific network node to its adjacent nodes in the nearest neighborhood, and (3) they optimize the road network for one objective only. Previously, we reported on the modeling of spatial variability in road construction costs (Stückelberger et al., 2006a), on the improvement in model representation of forest roads by mathematical graphs (Stückelberger et al., 2007), and on the problem of Pareto-optimality (Stückelberger et al., 2006b).

The present paper focuses on (1) providing a framework that integrates our improved components for this road network problem and (2) reporting the effects of our new framework model and the analysis of different near optimal networks according to various objective functions.

4.2 Model framework

Road network optimization requires three major steps – accurate model representation, the defining of objectives and adequate objective functions, and intelligent optimization procedures – in order to solve an inherently complex problem.

The methods described here for automatically locating road networks comprise a framework of nine components (Fig. 4.1): for model representation (i), we need a discretization of road segments in a high resolution (1) to map road-geometry constraints (2) on a graph (3) in order to determine the topology. We define the objectives (ii) by estimating road construction and maintenance costs (4), the attractiveness for harvesting a potential road segment (5), and penalties for adverse ecological effects (6). These components and their scaling by the stakeholders (a) lead to a multi-criteria objective function (7). In order to optimize the problem (iii), we have chosen a mathematical graph representation (8), and intelligent and efficient optimization algorithms (9) to find the optimal road network between given control points (b).

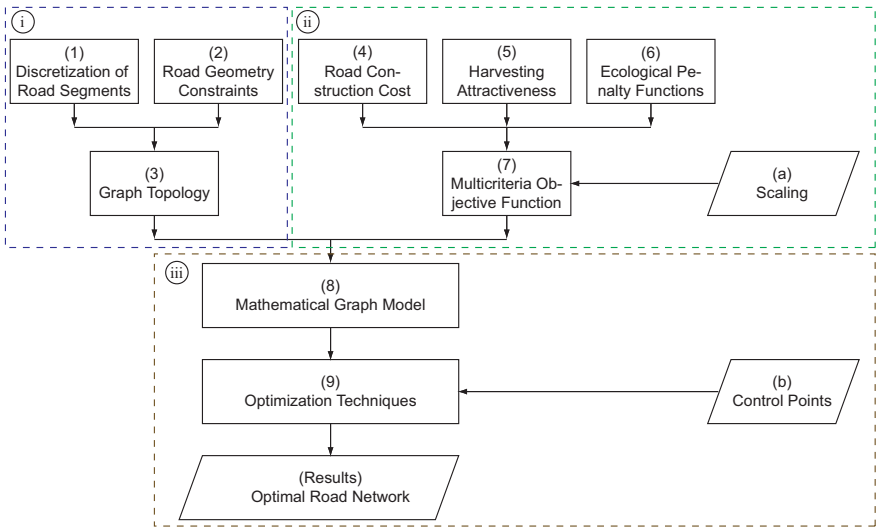

Figure 4.1: Framework of different components for automatic road network design: (i), representation of the problem; (ii), objective functions; and (iii), optimization in order to find the result

4.2.1 Discretization of road segments

Road engineers control the geometry of a road layout by following a sequence of vectors, known as a 'traverse'. The road is then designed as a series of curves inside the angles between consecutive vectors, straight segments along vectors, and curves outside the angles between successive vectors that define hairpin bends (Ervin & Gross, 1987). A geographical area is the continuous physical entity on which we can define an infinite number of points that can be used as the start- and endpoints of those vectors. However, graph optimization algorithms require a finite set of nodes and edges. Therefore, the specification of the design space follows the concept of discretization, i.e., we split up the continuous physical system into a discrete set of simple shapes. The prevailing approach utilizes a regular mesh form – a grid consisting of squares, where the node is located at the center point of the grid. As computing power has increased, grid sizes have decreased. For example, Liu & Sessions (1993) used a grid size of 91.4 $m \times 91.4$ m; Dean (1997), of 30 $m \times 30$ m; and Chung & Sessions (2001a), of 25 $m \times 25$ m. However, our research group has been using a 10 $m \times 10$ m resolution (Heinimann et al., 2003, Stückelberger et al., 2004). In mountainous and heterogeneous areas, that grid size has proved to be appropriate for low-

volume roads because it equals the lower limits of the design elements that define the centerline of a road, especially the minimum lengths for curve tangents, straight segments between curves, and the shortest radius for switchbacks (Kuonen, 1983, Walbridge et al., 1984). Nonetheless, that size can be increased if the terrain is homogenous and the minimum curve tangents and minimum road radius are $> 10\ m$. Because the finite set of all possible start-points and end-points is stipulated, we must determine the link pattern within these nodes. The predominant approach is to define links from a start-node to its adjacent nodes (Fig. 4.2a), resulting in eight links per node; this is called a Moore neighborhood of range one (Barile & Weisstein, 2002). This eight-link model is very limited and, when applied in steep terrain, it is hard to find a feasible road alignment (Stückelberger et al., 2004, 2007). Therefore we have introduced an enhanced link pattern using the connection to all nodes in a Moore neighborhood of range two (Fig. 4.2b), and a well-defined subset of nodes in a Moore neighborhood of ranges three, four, and five (Fig. 4.2c). The aim of this enhanced neighborhood is to obtain more and different road directions. We have previously presented the advantages of this improvement.

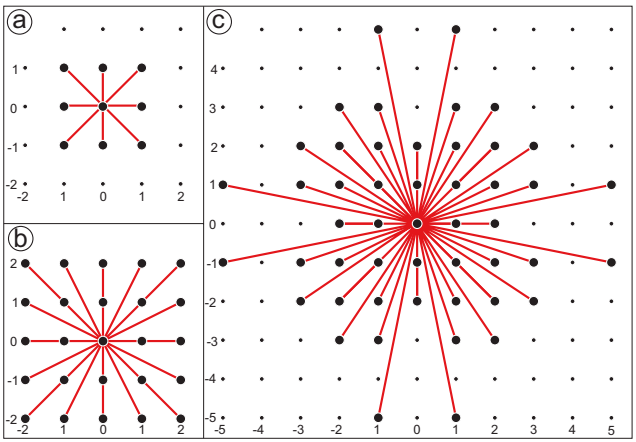

Figure 4.2: Neighborhood patterns for models with 8 (a), 24 (b), and 48 (c) links

4.2.2 Road-geometry constraints

Roads must fulfill technical requirements for safe truck traffic, especially by including a gradient that is lower than the maximum allowed and by satisfying a minimal curve radius requirement along the road centerline. Calculating the gradient for a single segment can be done easily by dividing the difference in elevation by the horizontal distance of the centerline.

The curve of a road is limited by the minimum turning clearance circle of a vehicle. For traffic comfort, the designed minimal curve radius is about two or three times the technical minimum turning clearance. We must check if the radius of each curve is above that minimum allowable in order to evaluate the feasibility of the horizontal road centerline. As explained in the previous section, our model road is controlled by a discrete number of nodes and links between nodes. To decide if a link between two consecutive nodes is feasible, we have to know the direction in which the road enters to the first node and which direction the road is going out of the second node. Three cases can be examined here: (1) for geometrical reasons, it is not possible to lay a road centerline between two given nodes with specific directions (Fig. 4.3a); (2) it is possible to

fit a theoretical centerline between two given nodes and given direction, but the radius is below the allowable minimum road radius (Fig. 4.3b); or (3) it is possible to fit a centerline between two given nodes and given directions, while keeping the curve radius above the minimum road radius (Fig. 4.3c). In the present project area, we used a minimum road radius of 20 m for the standard, but at least 10 m for switchbacks.

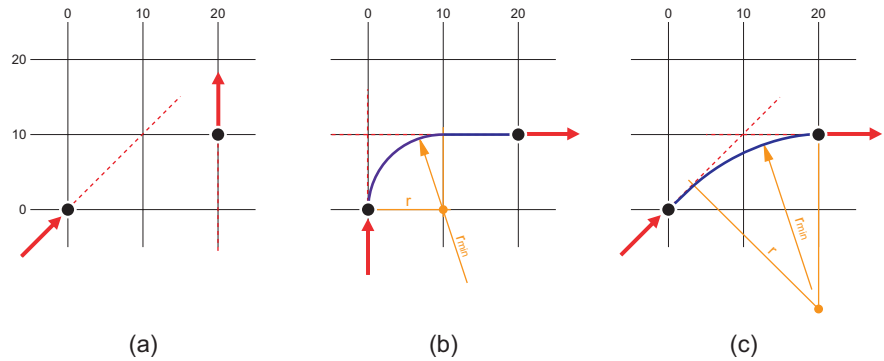

Figure 4.3: Road alignment constraints. Horizontal check from the first node at Point (0, 0) to a second node at Point (20, 10): (a) From Northeast to North: it is geometrically impossible to design a curve. (b) From North to East: the link is considered "non-feasible" because the minimum allowable road radius (r_{min}) is greater than the effective road radius (r). (c) From Northeast to East: the link is "feasible" because the effective road radius (r) is greater than the minimum allowable road radius (r_{min}).

4.2.3 Graph topology

For our purposes, a mathematical graph $G = (V, E)$ consists of a set of nodes V and a set of edges $E \subset V \times V$ (Jungnickel, 2005). To solve road network problems, a center point corresponds to a node v, and a feasible road link corresponds to an edge e in G. If we neglect turning constraints, we can map the problem on a graph where each grid cell is represented by its center point as a node in the graph. Nearly all road optimization models use such graphs. In order to contribute to the turning constraints, one has to implement special rules. For example, the PLANEX software package has a procedure that considers the feasible incoming and outgoing links related to a specific node (Epstein et al., 2001). However, such enlarged models are not part of the strict mathematical graph definition and, therefore, the wide range of graph algorithms is not applicable. Numerical graph representation of those constraints requires nodes to be split into several virtual nodes, thus increasing the problem size. Similar to the discretization of coordinates for nodes on a mesh of 10 $m \times 10$ m, we must also discretizate the directions. Here, we were considering 16 road directions per node, all identical to the 16 directions for the nodes in a Moore neighborhood of range two (Fig. 4.2b). Figure 4.4 shows an example of four feasible links from one outgoing node (O). Each set for the same outgoing direction (to the East) but with a different incoming direction (to the South, East, North, or West) is then mapped in separate directional layers. We also distinguish three types of directional change – straight line, curve, or switchback. The feasibility of directional change from an incoming to an outgoing link results from calculating the radius of the curve, which must be greater than a minimum allowable value (Fig. 4.3).

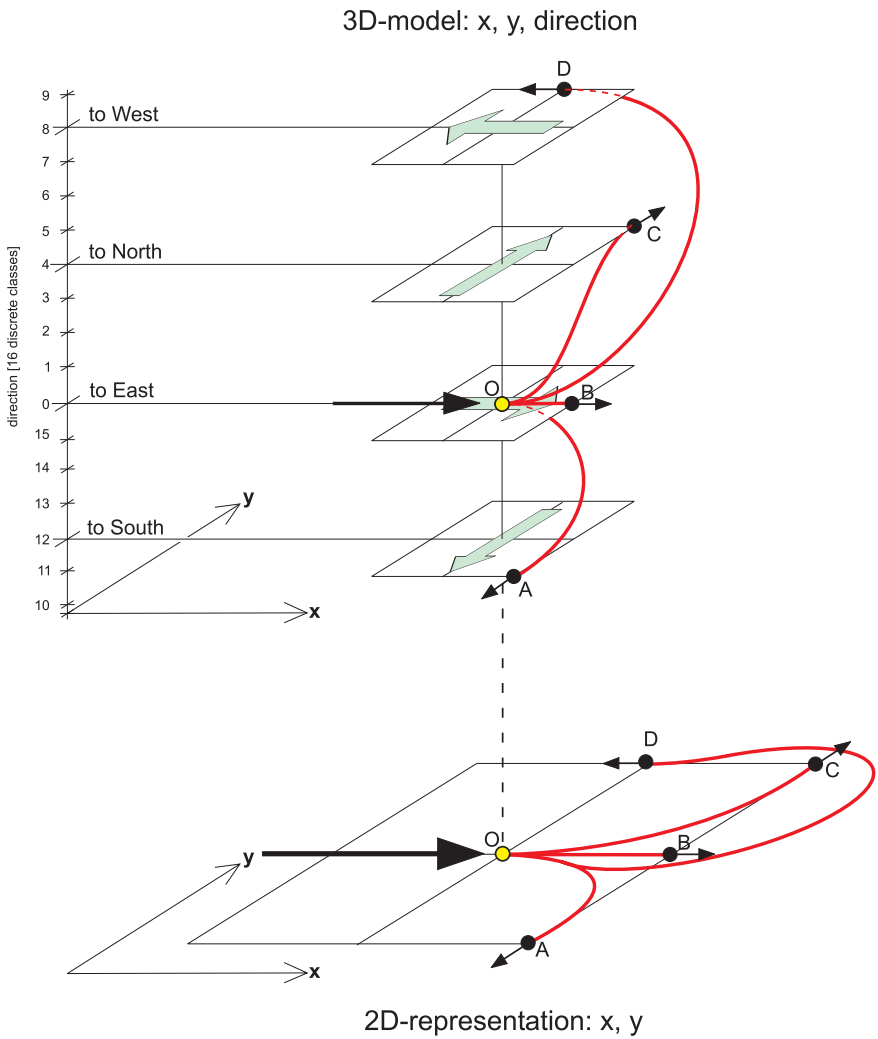

Figure 4.4: Representation of directional-change constraints. Incoming-outgoing combinations of links represent a right-hand curve (OA), straight line (OB), left-hand curve (OC), and left-hand switchback (OD). In contrast, our current implementation considers 16 possible road directions instead of the 4 shown here.

4.2.4 Road construction and maintenance costs model

Estimating the costs for construction and maintenance is the most important factor when planning the layout of forest road networks. However, the procedures now available for locating routes (Chung & Sessions, 2001a, Epstein et al., 2001) assume that construction costs are constant within a specific planning area. We previously presented a generic model that estimates the spatial variability in road construction costs as a function of five input factors: (1) a digital elevation model (DEM), (2) classification of geotechnical properties of the subsoil, (3) specification of road design parameters, (4) unit costs for structural components, and (5) a rock-excavation share model (Stückelberger et al., 2004, 2006a) (cf. Fig. 4.5). This earlier model was developed for mountainous areas, but is applicable to any project as long as topography and subsoil are the predominant factors for cost.

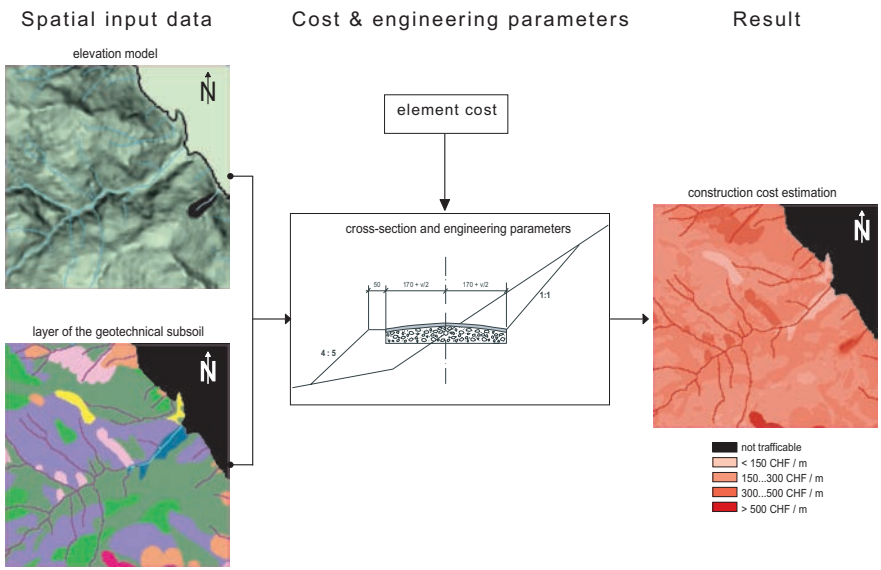

Figure 4.5: Flowchart for estimating potential road construction costs. Area (2 $km \times$ 2 km) at Wägital, Switzerland

This present approach is based on the "cost classification by elements (CCE)" framework (CCE, 1991), a hierarchical system that comprises different constructive element groups. The four element groups relevant to cost estimation of roads include structures for embankment, retaining and support, pavement, and drainage and stream-crossing (Fig. 4.6).

An analytical approach (Heinimann, 1998, Stückelberger et al., 2006a) calculates the embankment cut area (A_{cut}) and fill area (A_{fill}) as a function of both slope and the specifications for road cross-sectional geometry. Inaba et al. (2001) have developed a model to estimate rock occurrence per cross section as a function of slope, geological formation, and crown width. Combining these two models then results in Equation 4.1 for excavation and embankment cost estimations.

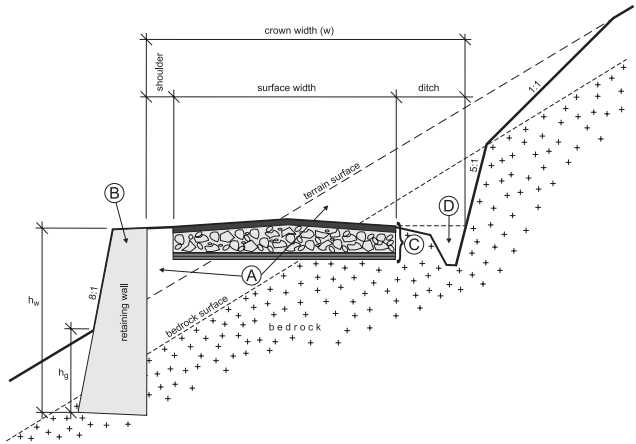

Figure 4.6: Standard design cross section with four element groups: A) embankment structure, B) retaining structure, C) pavement structure, and D) drainage and stream-crossing structures. h_w, height of retaining wall; h_g, depth of foundation for retaining wall; w, crown width (surface + shoulder + ditch). Figure is not drawn to scale, especially in the shoulder and ditch dimensions

$$C_{emb} = l \cdot \left(A_{cut} \cdot (c_{exe} + p_{rock} \cdot c_{rock}) + A_{fill} \cdot c_{comp}\right) \tag{4.1}$$

where,
C_{emb} = embankment cost per segment
A_{cut} = average cut area of the segment
c_{exe} = soil excavation cost per volume
c_{rock} = extra cost for rock excavation per volume
p_{rock} = share of rock in total cut area
A_{fill} = average fill area of the segment
c_{comp} = cost for compaction per volume
l = middle length of the arc for the road segment

Life-cycle road costs consist of initial road-building, routine and periodic maintenance, rehabilitation, and decommissioning. The model analyzed here does not consider the last two factors, and assumes the maintenance cost to be dependent only on road gradient and geology. For further analysis, we evaluate over a 50-year period. To make the maintenance cost comparable to the initial road-building costs, we calculate the net present value (NPV), and assume an interest rate of 2%.

4.2.5 Harvesting-attractiveness Model

Positioning of the landing locations for harvesting operations affects the efficiency of off-road transportation, especially for cable-based extractions. A road should not only connect mandatory access points, but also reach favorable landings. Therefore, we have introduced a landing-attractiveness factor that considers both the effectiveness and efficiency of the cable yarder (Fig. 4.7). For such an evaluation we need a grid representation of the project area. A layer for elevation (derived from the DEM) and a layer for potential harvesting volume over the next 50 years also are required. Thus, the factor for harvesting-attractiveness is calculated according to the following procedure:

1. select the first (or next) raster cell as a potential landing location L
2. for $\alpha = 0°$ to $345°$(in $15°$ increments):
3. determine the potential tailspar point T in direction α for the maximum skyline length
4. determine the terrain profile between T and L
5. for any point between T and L:
6. calculate ground clearance of the cable road
7. if ground clearance is < 0, then
8. move T one unit in the direction of L, repeat Steps 4 to 7,
9. or else fix location T, and add T to Set $\mathbb{T}$
10. increase α, repeat Steps 3 to 9
11. connect all T-points of Set $\mathbb{T}$
12. calculate the area bounded by T-points (Fig. 4.8)
13. weight the area with the timber volume to be harvested, and
14. allocate this volume as the value for harvesting-attractiveness to L
15. clear Set $\mathbb{T}$
16. repeat Steps 1 to 15 until all raster cells are evaluated

Step 13 can also be modified slightly by weighting the potential logging volume by a factor that represents installation and logging conditions (e.g., the number of intermediate supports I and logging direction). Hence, the attractiveness value is equivalent to the volume of timber. Here we use cubic meters [m^3]. A model (CableAnalysis 1.0) is available for automatically determining the landings for cable logging (Chung, 2002, Chung & Sessions, 2003). We have incorporated this model into our procedure for calculating attractiveness for a cable yarder.

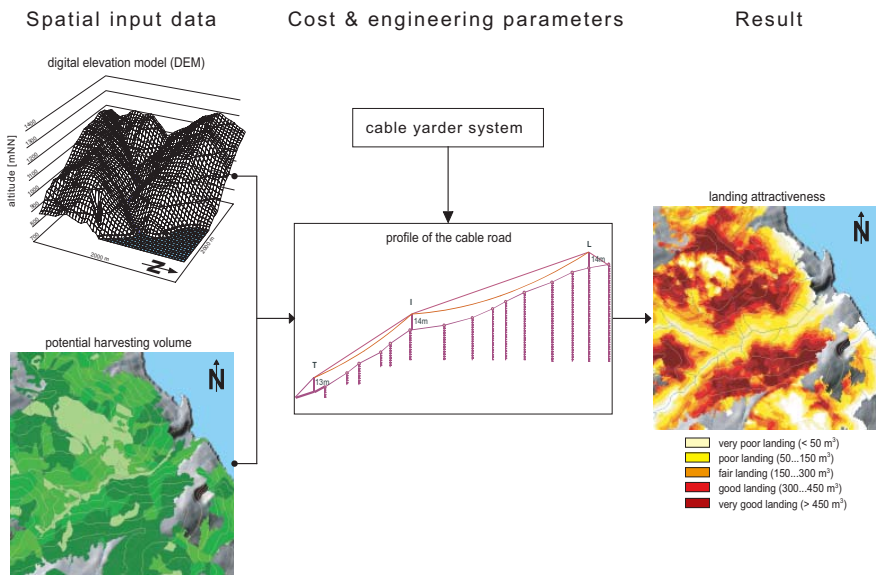

Figure 4.7: Flowchart for calculating cable-yarder attractiveness. Area ($2\ km \times 2\ km$) at Wägital, Switzerland

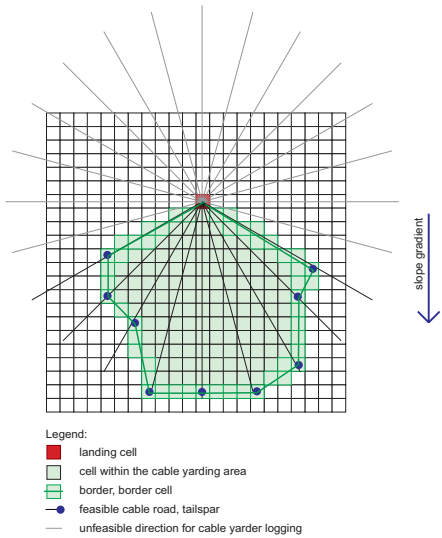

Figure 4.8: Cable-yarder landing and its over-spanning harvesting area (schematic draft)

4.2.6 Ecological penalty functions

On the one hand, a road network makes harvesting operations easier and, therefore, more efficient. On the other hand, roads may affect the environment adversely, for example, by increasing erosion and sediment content in streams or by disturbing wildlife or other members of the ecosystem. The decision as to which adverse ecological effects to examine is normative. Here, we illustrate two types of environmental impacts – habitat quality for the capercaillie (*Tetrao urogallus*) and marshland biotopes – both of which have major relevance in middle Europe, especially in the Swiss Alps. Capercaillie, the largest mountain grouse in middle Europe, is threatened with extinction (Keller et al., 2001). Its requirements for forage, cover, reproduction, and comfort are crucial variables that define habitat suitability (Bollmann, 2003). We have made our measurements of quality using Graf's (Graf et al., 2002) habitat suitability index (HSI; USDI Fish and Wildlife Service, 1981). Disturbances are assumed to be proportional to road length and HSI (Ulber, 2004). For example, a 100-m-long road segment that crosses capercaillie habitat with a suitability index of 0.2 results in an impact cost of 20, which is considered equivalent to a 20-m segment that might cross a habitat with an HSI of 1. In our further analysis, we use the unit "meter-equivalent" [m]. Marshland areas, which include upland moors, reeds, and wetlands, are important ecotypes protected by Swiss legislation. Determining their ecological value is difficult. Government agencies have established a standard evaluation procedure that considers the size of the area, the number of different vegetation types, and diversity (BUWAL, 1991). Several adverse effects on marshlands must be weighted. First, road construction directly interrupts such sites due to sealing of the surface. Second, construction activity can cause indirect disturbance by influencing the flow of groundwater (Marti et al., 1997). Third, a road can dissect a marshland biotope, leading to fragmentation (Jaeger, 2002). Therefore, we have introduced outside and inside buffer zones, each 100 m wide (Fig. 4.9). The inside buffer and center zones are assumed to have habitat values based on the considered worth of the ecotype (Ulber, 2005), whereas the habitat value of the outside buffer zone is

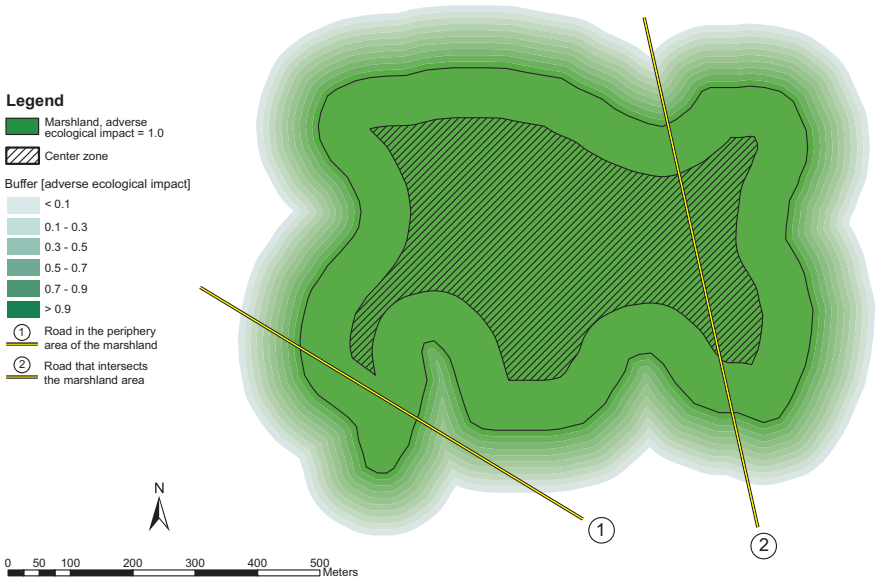

Figure 4.9: Marshland area with buffer and central zones. Road 1 affects the marshland in the buffer zone and periphery only, whereas Road 2 also influences that marshland because of the intersection effect (schematic draft).

assumed to decrease from that higher level to zero. Marshland disturbance is presumed to be proportional to road length and ecological value. If a road enters the center zone, an additional penalty is added to the disturbance factor, thereby representing the fragmentation effect. This penalty-value must be compatible with the unit "meter-equivalent". Methods, how to calculate this fragmentation penalty in a specific case is given in (Jaeger, 2002). The function we use to convert this fragmentation effect to "meter-equivalent" value in the area of Wägital is explained in (Ulber, 2005).

We can allocate a penalty for adverse outcomes along individual road segments. If we have several different ecological effects, this penalty is a function of the values for each. In our model we assume that the penalty is the sum of all single values, weighted with a user-defined factor. Moreover, we encounter ecologically very sensitive zones that are either protected by federal law or excluded by the stakeholders. These zones are considered "non-trafficable".

4.2.7 Multi-criteria objective functions

Multi-criteria decision-making can be divided into two groups: multi-criteria attribute decision-making (MADM) and multi-criteria objective decision-making (MODM) (cf., Malczewski, 1999). For example, the construction cost function produces one outcome (e.g., unit dollar, Euro, or franc), and is based on multiple attributes such as elevation or geological unit. Therefore, that functional parameter is usable for MADM.

Here, we briefly introduce the multi-criteria objective functions used for MODM. Because we have all the necessary models for generating optimization values, we can define the objectives, which will of course depend on the different interests among stakeholders. For example, an

ornithologist prefers a road network that minimizes the negative impact on capercaillie habitat whereas the landowner mainly wants to minimize road construction costs. Therefore, to reach consensus for all concerned, we have to understand the trade-offs among these various criteria.

Multi-criteria optimization is rooted in late 19th century welfare economics, as described by Edgeworth (1881) and Pareto (1896–1897). A feasible solution to a multiple-objective problem is considered Pareto-optimal if no objective component can be improved upon without worsening other components (Definition 1). Typically, there is an entire curve or surface of Pareto points, whose shape indicates the nature of the trade-off between goals (Fig. 4.10). Although various definitions of Pareto-optimal have been developed and used (Ehrgott, 2000). Here, we use one that commonly appears in most of the contemporary literature concerning operations research in multi-objective discrete and combinatorial optimization (see Hammer (2006), Collette & Siarry (2004), Ehrgott (2000), and Geoffrion (1968)). In the present case, each objective value is positive and real ($\mathbb{R}_+$), which leads to following definition of the optimization problem:

$f_i(x)$ = i$^{\text{th}}$ objective function
k = number of different objectives
X = set of feasible solutions (design space, syn. solution space)

$$\text{“}\min_{x\in X}\text{”}\big(f_1(x),...,f_k(x)\big),\ \text{subject to } x\in X \tag{4.2}$$

For all $x \in X$ we define $f(x) = \big(f_1(x),...,f_k(x)\big)$ and $f(x) \leq f(y)$ if $f_i(x) \leq f_i(y)$ for all $1 \leq i \leq k$.

In Equation 4.2, the range of f is a subset of the k-dimensional space $\mathbb{R}^k$. The “min” is defined with respect to the given order on $\mathbb{R}^k$ which for $k \geq 2$ is not a total pre-order relation.

Definition 1. *A solution $x^* \in X$ is called **Pareto-optimal**, if there is no $x \in X$ such that $f_i(x) < f_i(x^*)$, for some $i \in \{1,...,k\}$ and $f_j(x) \leq f_j(x^*)$ for all $j \in \{1,2,...,k\}$. The set of all Pareto-optimal solutions $x^* \in X$ is X_{Par}, the **Pareto set**.*

Definition 2. *A point $y^* = f(x^*) \in \mathbb{R}^k$ with $x^* \in X_{Par}$ is called **efficient**. The set of all efficient points $y^* = f(x^*) \in \mathbb{R}^k$, where $x^* \in X_{Par}$ is Y_{eff}, the **efficient set**.*

Multi-criteria objective problems are very often solved by combining all components as a subfunction into one scalar objective function (Eq. 4.3), and than minimizing the weighted sum of this aggregated function:

$$\min_{x\in X}\sum_{i=1}^{k}\lambda_i\cdot f_i(x) \tag{4.3}$$

where, λ_i = weighting factor of objective function f_i, $\lambda_i \in \mathbb{R}_+$

Let λ be the vector $\lambda = (\lambda_1,...,\lambda_k)$. The scaling for vector λ is irrelevant. This reduces the dimension of the space for weights to $k-1$. The weighting of the components $\lambda_1,...,\lambda_k$ is extremely decisive for the optimal solution. It is not possible to check every combination. Thus, we select a finite number n_i of values for each λ_i, which leads to $\prod_{i=1}^{k} n_i$ alternatives.

Even if we were able to test all combinations of weights of λ_1, ..., λ_k, we would not be able to find the entire efficient set Y_{eff}, but only the subset of Y_{eff} which matches the convex hull of Y_{eff} (Fig. 4.10)(cf., Ehrgott, 2000).

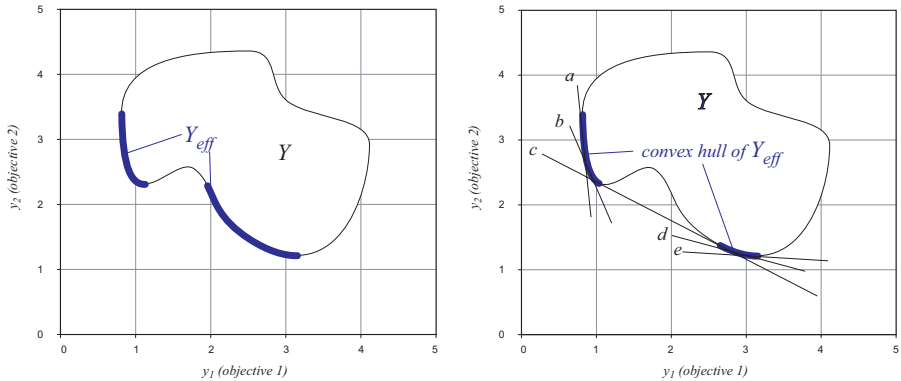

Figure 4.10: Efficient set (Y_{eff}) and convex hull around Y_{eff} in the criterion space. a, ..., e represent the tangents around Y_{eff}.

We consider a small example to demonstrate the effect of using the weighted sum as objective value in the case of a bi-objective optimization of a road layout (Fig. 4.11): (1) a shortest-path connection of a weighted sum function (Eq. 4.3), and (2) a shortest path with constraints for the objectives. Given is a model area of 20×20 grid cells, with a cell size of 10 $m \times 10$ m. Within the model area is a marshland with a constant ecological value of 1 unit per meter. The terrain is a plane, and the road construction costs are homogenous over the entire area, $= 1$ unit per m. Our aim is to find an optimal connection between two given points following the 24-link pattern (cf., Fig. 4.2b). Road A is the straight-line connection while Roads B, C, and D are the shortest path solution (cf., Subsection 4.2.9) with respect to the weighted sum of $f_1(x)$ and $f_2(x)$. The input values for λ are shown in Table 4.1. Roads e, f, g, h, i, and j represent the shortest paths under a restriction that the marshland impact (y_1) is at most 60, 50, ..., or 10, respectively. The Alternatives A, B, C, D are Pareto-optimal and they lay on the convex hull of Y_{eff} (Fig.4.12), Alternatives e, f, g, h, i, j are Pareto-optimal as well, however they lay not on the convex hull of Y_{eff}.

Alternative	Construction costs (y_2)	Ecological impact (y_1)	λ_2	λ_1	subject to
A	206.2	76.0	straight line		
B	208.9	74.7	1	0...1.886	
C	217.8	70.0	1	1.887...2.044	
e	294.9	60.0			$y_1 \leq 60$
f	303.2	50.0			$y_1 \leq 50$
g	315.5	40.0			$y_1 \leq 40$
h	327.9	30.0			$y_1 \leq 30$
i	340.2	20.0			$y_1 \leq 20$
j	352.6	10.0			$y_1 \leq 10$
D	360.9	0.0	1	≥ 2.045	

Table 4.1: Results for a model area of 20×20 grids

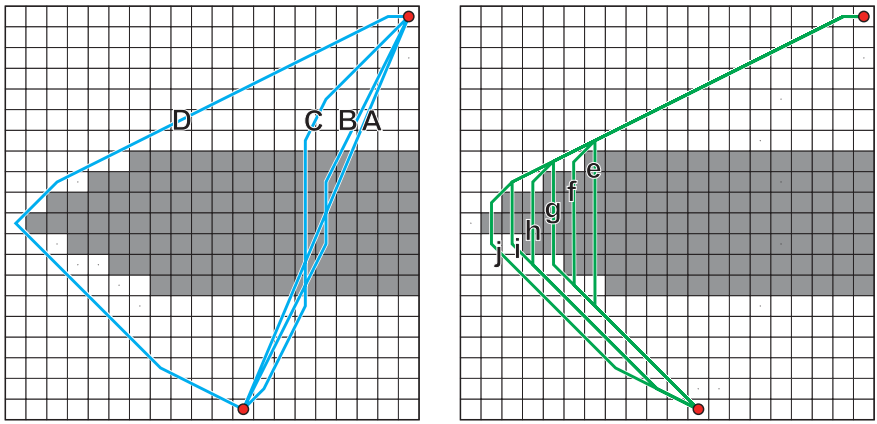

Figure 4.11: Left: Shortest Path by weighted sum function (Alternatives A, B, C, D). Right: Shortest Path under the restriction for a maximal allowable value of y_1 (Alternatives e, f, g, h, i, j). Model area of 20×20 grids. The gray grids represent marshland.

Regarding Table 4.1 and Figures 4.11 and 4.12, we see two other effects: (1) Alternatives A, B, and C build a cluster of similar solutions whereas Alternative D shows a completely different solution. (2) Only a certain and narrow range of λ_1 leads to Alternative C. By increasing the weight slightly beyond the range, the solution "jumps" very fast to Alternative D.

There are two approaches for finding the multi-criteria objective solution – "*a priori*" and "*a posteriori*". In the "a priori" approach, it is up to the stakeholders to choose appropriate weights for each component of the objective function first. The main shortcoming of this method is that the solution represents only one point in X_{Par}, and trade-offs among different objectives are not evaluated or understood.

In contrast, an "a posteriori" optimization aims at tracing the complete Pareto-solution space for each multi-objective case. The eventual computational effort is extremely high, especially for spatial problems (Duha & Brown, 2007). The stakeholders then must make their decision after knowing the Pareto-solution space. The state of the art for spatial multi-criteria optimization has been reported by Xiao et al. (2002). Xiao et al. (2007) and Malczewski (1999) also provide overviews for multi-criteria decision analysis in GIS, with both using very simplified models for the mono-objective functions, and often assuming a deterministic spatial relationship. However, the combination of different objectives and their optimization techniques is highly sophisticated.

4.2.8 Mathematical graph model

Let us first introduce some graph theoretical notions. An undirected graph $G = (V, E)$ consists of the set of nodes V and the set of edges $E \subset \{\{u, v\} \mid u, v \in V, u \neq v\}$. Graph $H = (V', E')$ is a subgraph of $G = (V, E)$ if $V' \subset V$ and $E' \subset E$. Likewise, a path P in graph G is a sequence of nodes $P = v_1, \ldots, v_k$, where $\{v_i, v_{i+1}\} \in E$ for all $1 \leq i < k$. We say P is a path from v_1 to v_k. If for each pair of nodes u, v in the graph there is a path from u to v, we say the graph is connected. A cycle in a graph is a path from a node to itself. For our purposes, a type of graph called a tree is of special interest. A tree is a connected graph without cycles, i.e., a minimally connected graph.

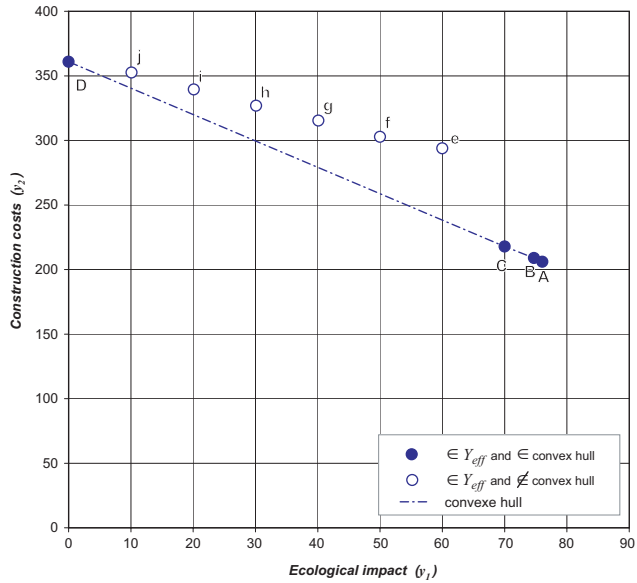

Figure 4.12: Y_{eff} of the different road alternatives for a model area of 20×20 grids

Here, we are dealing with weighted graphs; that is, we have a graph with a weight function $w : E \mapsto \mathbb{R}_+$ on the edges. In this case, the weight represents the objective function for the road links, e.g., the road construction cost. For a weighted graph G, the weight of a subgraph $w(H)$ is defined as the sum of the weights of the edges in H. An important optimization problem is to find the path of minimum weight between two nodes u, v – this is called the shortest path between u and v.

4.2.9 Optimization techniques

Closely related to our application is the problem of determining the minimum spanning tree, MST, which is the minimum-weight subgraph that is a tree and which contains all nodes. In our application, we are given a weighted graph G and a set of terminal nodes K that must then be connected by the road network. In other words, we have to find a minimum-weight connected subgraph T containing the nodes in K (terminals). This scenario is known as the *Steiner problem* in graphs, and the subgraph T is called the *Steiner minimum tree*, or SMT (see Hwang et al. (1992) and Prömel & Steger (2002)). All non-terminal nodes of degree > 2 in T are called *Steiner points*. These correspond to bifurcations or junctions in the network.

In our graph, for each 10 $m \times 10$ m square, we arrive at 16 nodes for the different directions. For a 35-km^2 project area, this leads to 5'600'000 nodes and, depending on the steepness of the area, approximately 80'000'000 edges. Therefore, we have no hope of computing the real optimum within a reasonable amount of time. In our case, the number of terminals is bounded from above by a small constant, e.g., 10, but in the running time of the Dreyfus-Wagner algorithm, the limiting factor is the $2^k n^2$ term, which, for $k = 10$, is about $32 \cdot 10^{18}$. Thus, we have to use a heuristic that gives us an approximate solution.

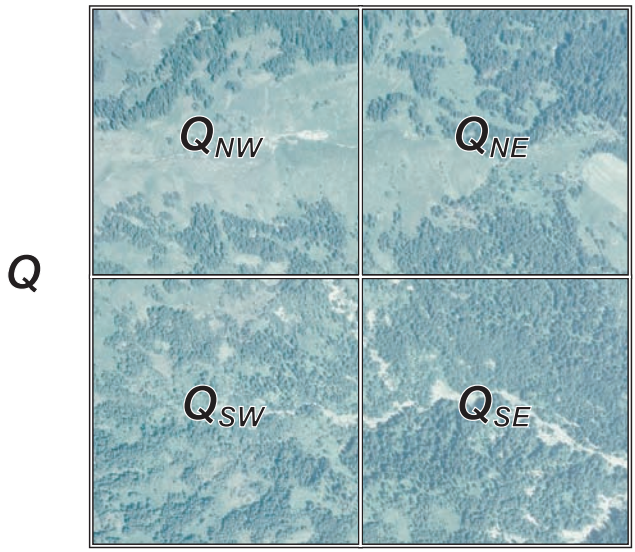

Figure 4.13: A quad Q with its subquads: Q_{NE}, Q_{NW}, Q_{SW}, and Q_{SE}

For a graph of size $n := |V|, m := |E|$ and $k := |K|$, various efficient algorithms are available for solving the above-mentioned problems. For the *shortest path problem*, Dijkstra's algorithm (Dijkstra, 1959) can compute the shortest paths from one start-node to every other node in time $\mathcal{O}(m + n \log n)$. This algorithm, widely used to locate the shortest route (e.g., Anderson & Nelson, 2004), is only applicable for positive edge weights. For the MST problem, Prim's algorithm (Prim, 1957) is for computing an MST in time $\mathcal{O}(m + n \log n)$. However, for the SMT problem, the situation is different, being termed $\mathcal{NP}$-hard because it is quite unlikely that an efficient algorithm exists. Currently, only algorithms with exponential running times are known. In contrast, an algorithm described by Dreyfus & Wagner (1971/72) based on dynamic programming, has a running time of $\mathcal{O}\left(3^k n + 2^k n^2 + n^2 \log n + nm\right)$. For constant k, this is a polynomial algorithm. Here, we use a variant of the so-called MST heuristic, which can only guarantee an approximation ratio of $2 - \frac{2}{k}$ but works well in practice Hwang et al. (1992). This MST heuristic works in the following way:

1. For all k terminals, compute the shortest paths to all other nodes.
2. Build a weighted graph on k nodes with all nodes connected. The weight on the edge (i, j) is the weight of the shortest path from the i^{th} to the j^{th} terminal. This graph is called the *distance network*.
3. Compute an MST on the distance network. This MST corresponds, by taking the union of the individual shortest paths, to a connected subgraph of the original graph.
4. Because the graph that results at this point may not yet be a tree, we obtain the final tree after a post-processing step.

The MST heuristic described above is often not good enough. To obtain better results, therefore, we calculate a set of candidate Steiner points by determining the optimal Steiner point for

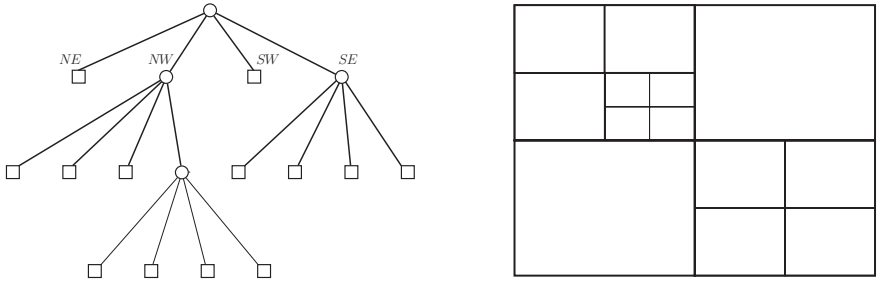

Figure 4.14: A quadtree and the corresponding subdivision. The labels show to which quadrant the children correspond.

each 3-tuple of nodes. If the shortest paths from the terminals to all nodes are pre-computed (in time $\mathcal{O}(k(m + n \log n))$), then for each 3-tuple the optimal Steiner point can be found in time $\mathcal{O}(n)$ leading to $\mathcal{O}(k^3 n)$ time for this step. Then, either the best subset of these candidate points is found by complete enumeration or a nearly best subset is found by a heuristical approach, e.g., Simulated Annealing (Kirkpatrick et al., 1983).

The main difficulty when evaluating the quality of the approximate solutions is to provide good lower bounds on the optimum value. Unfortunately, different known techniques, such as those using reduction tests to gain a smaller graph, do not work in our circumstances.

Here, we used a *quadtree*-based approach to get a good lower bound on the optimal solution. A quadtree is a rooted tree, where every internal node has four children. A node in the quadtree corresponds to a rectangle and, if the node has children, they correspond to the four quadrants of the rectangle (Fig. 4.13). A quadtree corresponds to a subdivision of the rectangle of the root node. See Figure 4.14 for an example of a quadtree and the corresponding subdivision. The rectangles of the leaf nodes (in Figure 4.14 being the rectangular nodes) form the subdivision. Hereafter we will call the rectangles of the quadtree *quads*.

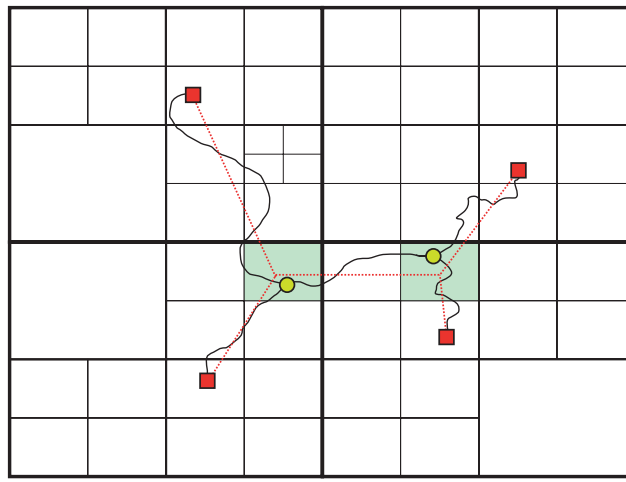

Figure 4.15: Partition into quads, and a Steiner Tree with two Steiner Points and four terminals

We define the distance between two quads as the minimum of the distances between points in the two quads. A lower bound on the optimum SMT can then be computed using a suitable partitioning of the area into quads and running an exact algorithm on the smaller graph given by the quads. For an illustration, see Figure 4.15.

We cannot split the area in a regular fashion because the number of quads becomes too large. Using a branch-and-bound technique, however, a good partition of the project area is found, an example of which is given in Figure 4.16.

By taking this approach in the current study, we were able to show that, for our input instances, the solutions returned by the heuristic were usually less than 2% and never more than 4% worse than the optimum. For further explanation we refer to Schwartz & Stückelberger (2008).

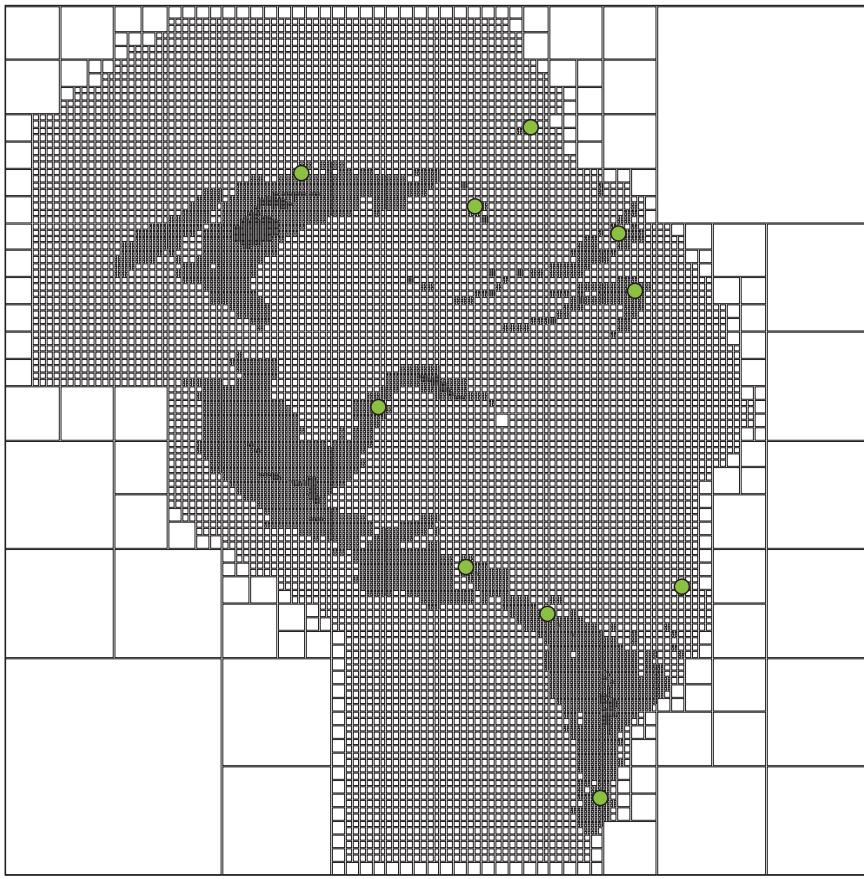

Figure 4.16: Partition obtained by applying a branch-and-bound process in the area of Wägital. [circle-symbol] mandatory access points.

4.3 Model evaluation and results

4.3.1 Project area

The project area for our evaluation was located at "Wägital", a 35-km^2 site on the northern slopes of the Swiss Alps. This region is characterized by steep terrain (average slope gradient of approximately 35%), difficult geotechnical conditions, a dense water channel network, and high-value ecotypes and habitats. It, therefore, is an ideal study site for investigating scenarios with multiple, conflicting objectives. The digital elevation model and the geotechnical layer had a grid resolution of 10 $m \times 10$ m, which resulted in 350'000 grid cells. Up to now the area was either roadless or its few existing roads were not suited to contemporary harvesting and transport systems. Our goal was to find the optimal road network that encompassed 10 given access points. Various student project results and expert opinions were analyzed and compared with model outputs.

4.3.2 Evaluation layout

For the optimization procedures, we had four objectives: (1) minimizing road construction costs, (2) maximizing harvesting-attractiveness, (3) minimizing disturbances for the capercaillie, and (4) minimizing adverse ecological effects in marshland areas. In order to find Pareto-optimal solutions, we use the weighted sum approach (Eq. 4.1).

We assumed the following factors to be constant in order to make this evaluation comparable.

1. Terminals: Mandatory access points, such as mountainous farms, important lumber yards, and indispensable landings were given. In fact, it was the responsibility of the stakeholders to determine whether access to individual locations should be mandatory or optional.

2. Road construction costs: Our focus was the life-cycle cost, which entailed initial, first-year construction costs plus maintenance costs. The latter was assumed to be a function of the geotechnical subsoil as well as the gradients for the road and the hill-slope. We calculated the net present value (NPV) over a period of 50 years and at an interest rate of 2%.

3. Harvesting-attractiveness: We considered only one harvesting system, cable-yarding. However, most of this project area is logged with a combination of ground-, cable-, and airship-based systems.

4. The aggregate weighting function was a linear combination of four sub-functions after Equation 4.4. We incorporated attractiveness as a negative weight. To apply Dijkstra's algorithm, however, no aggregate weight can be negative. For that reason, we introduced Equation 4.5 to guarantee that every link had a non-negative weight.

$$f(x) = \lambda_c \times f_c(x) + \lambda_h \times f_h(x) + \lambda_t \times f_t(x) + \lambda_m \times f_m(x) \tag{4.4}$$

$$w(x) = \begin{cases} 0, & f(x) \leq 0 \\ f(x), & \text{otherwise} \end{cases} \tag{4.5}$$

where, x = road link x
$w(x)$ = aggregate weight of the link x (aggregated function)
λ_i = weighting factor of the i^{th} objective
$f_i(x)$ = i^{th} objective function
i = index indicating the objective:
c, construction costs;
h, harvesting attractiveness;
t, ecological impact on capercaillie (*T. urogallus*);
m, ecological impact on marshland

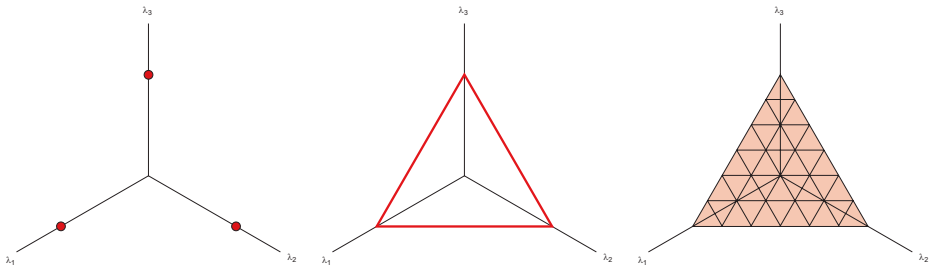

Figure 4.17: Space for weighting vector $\lambda = (\lambda_1, \lambda_2, \lambda_3)$ and the plane area for $\lambda_1 + \lambda_2 + \lambda_3 = 1$ in $\mathbb{R}^3_+$. (a) corner points for mono-objective solutions, (b) border line for bi-objective solutions, and (c) entire area for tri-objective solutions.

We first tested three mono-objective alternatives, then bi-objectives, followed by multi-criteria objective alternatives. The solutions were controlled by the direction of the weighting vector λ only. Most studies let $\lambda_1 + \lambda_2 + \ldots + \lambda_i = 1$. In the tri-objective case, λ described a triangular area in $\mathbb{R}^3_+$ (Fig. 4.17c). Mono-objective alternatives corresponded to the corner points within this area (Fig. 4.17a). Here, we evaluated the cost-optimal alternative (C!), where $\lambda_c = 1$ and all $\lambda_i = 0\{\forall i \neq c\}$. Likewise, the capercaillie-optimal alternative (T!) used $\lambda_t = 1$, and the marshland-optimal alternative (M!) put $\lambda_m = 1$.

The bi-objective alternatives corresponded to the border line of the weighting area (Fig. 4.17b).

In our case, alternatives that did not consider construction costs were not of practical relevance. Therefore, we primarily analyzed combinations where $\lambda_c \neq 0$. Without loss of generality, and in order to make the different objectives comparable to costs, we let $\lambda_c = 1$ and varied λ_h, λ_m, λ_t. We recall from Section 4.2.7 that the scaling of the vector λ is irrelevant and we therefore may drop the condition $\sum_{i=1}^{k} \lambda_i = 1$.

Capercaillie-friendly alternatives showed $\lambda_c = 1$, $\lambda_t \in \{5, ..., 100'000\}$, $\lambda_h = \lambda_m = 0$. Labels for these alternatives were "T5", ..., "T100k". Likewise, the marshland-friendly alternatives stipulated $\lambda_m \in \{5, ..., 50'000\}$, with labels of "M5", ..., "M50k". To maximize harvesting-attractiveness, λ_h had to be negative. To obtain reasonable results, the attractiveness could not exceed the construction costs (Eq. 4.5). Therefore $-\lambda_h$ had to be small. We tested alternatives from $-\lambda_h \in \{0.002, ..., 0.3\}$, with labels of "H.002", ..., "H.3".

The tri-objective alternatives were gained by analyzing the entire weighting area regularly (Fig. 4.17c). Here, we assessed only construction costs and the adverse ecological impacts on capercaillie and marshland. The weight for harvesting-attractiveness was fixed as $-\lambda_h = 0.05$ (*a priori* choice, cf., Subsection 4.2.7). Similar to the bi-objective alterna-

tives, we let $\lambda_c = 1$. For the weighting factors for capercaillie, we tested a discrete set for $\lambda_t : \mathbb{T} \in \{200, 339, 574, 972, 1'646, 2'788, 4'723, 8'000\}$; for marshland, we used a discrete set for $\lambda_m : \mathbb{M} \in \{20, 44, 97, 213, 469, 1'032, 2'272, 5'000\}$. Spacing was evenly distributed geometrically (multiplier = 7^{th} root of the range). The labels for these alternatives were "[t,m]", where t was the element number of Set $\mathbb{T}$ and m was the element number of Set $\mathbb{M}$ (e.g., Alternative [2,4] had $\lambda_t = 339$, $\lambda_m = 213$; and constants were $\lambda_c = 1$, $-\lambda_h = 0.05$). Additionally, we considered Alternative [0,0], with $\lambda_c = 1$, $-\lambda_h = 0.05$, $\lambda_t = \lambda_m = 0$; as well as Alternative "eco!", with $\lambda_c = -\lambda_h = 0$, $\lambda_t = \lambda_m = 1$.

4.3.3 Mono-objective optimizations

In the remainder of this section we will refer to the solution found by our approach as the optimal solution. As our lower bounds show that the solutions we obtain are usually indeed within 2% of the optimal solution (cf., Subsection 4.2.9) and such a small error is insignificant comparing to the fuzziness of the objective functions of about 5% to 10% (cf., Stückelberger et al., 2006a).

The layouts for different road networks are shown in Figures 4.18, 4.19, and 4.20, with key values presented in Table 4.2. The cost-optimal alternative served as our reference. The capercaillie-optimal alternative involved costs that were more than three times higher than the reference, but habitat disturbance was reduced by about two-thirds. However, theoretical adoption of this alternative also increased marshland disturbances by one-third. In contrast, the marshland-optimal alternative led to almost no disturbance for its ecotypes. Nonetheless, the accompanying costs rose by nearly three times, and disturbance to the capercaillie also increased by about one-third.

Alternative label	Description	Distance [m]	Cost [1000 CHF]	T-imp. [m]	M-imp. [m]
C!	Cost-optimal	20'916 (100%)	5'161 (100%)	6'263 (100%)	2'598 (100%)
T!	Capercaillie-optimal	29'546 (141%)	16'046 (311%)	2'222 (35%)	3'359 (129%)
M!	Marshland-optimal	23'173 (111%)	14'198 (275%)	7'526 (120%)	24 (1%)

Table 4.2: Key data for results from mono-objective optimizations. T-imp., adverse ecological impact for capercaillie (*T. urogallus*) [m-equivalent]; M-imp., adverse ecological impact for marshland [m-equivalent]

4.3.4 Harvesting volume versus construction costs

Harvesting-attractiveness is a metric value for the potential yield volume that can be extracted to a specific location within the project area. If we are able to harvest the entire accessible area using only one landing, the attractiveness will be decreased for all neighboring landings with an overlapping catchment area (Fig. 4.21). Correct implementation of such problems leads to dynamic optimizations. However, Dijkstra's shortest path algorithm, which was part of our optimization, is applicable for static weights only. To verify whether the attractiveness considered here was correlated with yield volume, i.e., the actual target value, we calculated a linear regression (Fig. 4.22). Even though we did not use a dynamic optimization, we found good correspondence with potential volume. Regarding our tests, two solutions turned out to be slightly

Figure 4.18: Cost-optimal road network (Alternative C!) indicated in yellow (length = 20.9 km). Area (5 $km \times 7$ km) at Wägital, Switzerland

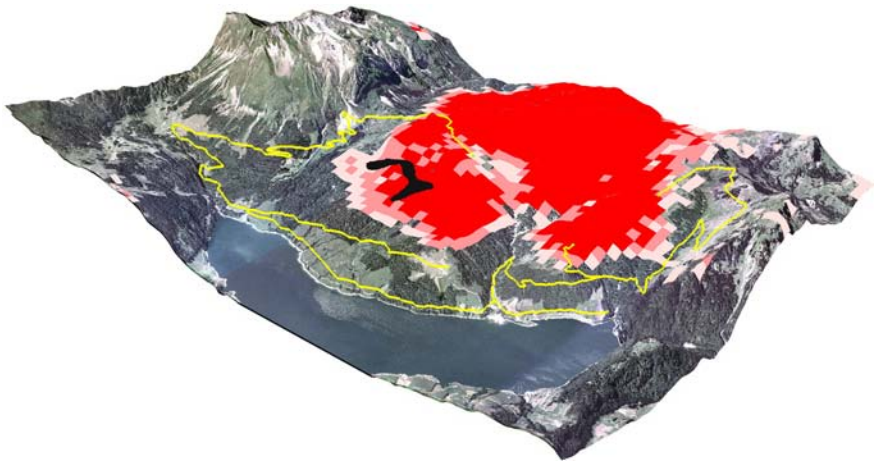

Figure 4.19: Capercaillie-optimal road network (Alternative T!), indicated in yellow (length = 29.5 km). Red region, habitat suitability index for capercaillie; black region, exclusion area (known courtship sites). Area (5 $km \times 7$ km) at Wägital, Switzerland

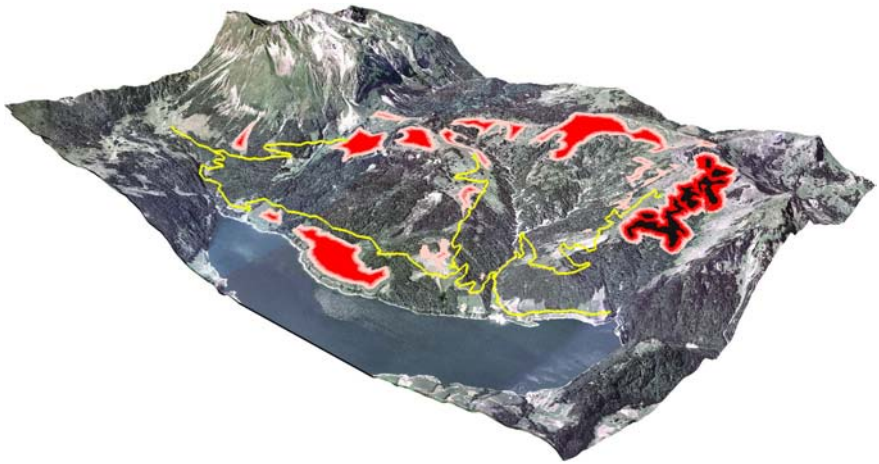

Figure 4.20: Marshland-optimal road network (Alternative M!), indicated in yellow (length = 23.2 km). Red region, marshland and buffer zone; black region, exclusion area (rare ecotypes). Area (5 $km \times$ 7 km) at Wägital, Switzerland

not Pareto-optimal. Compared with C! (the cost-optimal reference), Alternative H.002 resulted in 0.6% less volume while Alternative H.04 was associated with 0.6% less volume and 0.08% higher costs. Nevertheless, these discrepancies were very small, and within the range of model accuracy.

Figure 4.23 shows the relationship between road construction costs (at NPV) and harvesting volume. The curve for the data points was nearly hyperbolic, even though there were a few inconsistencies. Knowing that our approach to include the harvesting attractiveness as a reference for harvesting volume is limited, we fixed $-\lambda_h = 0.05$ for the tri-objective analysis, a low weighting factor comparing to λ_c, λ_t and λ_m. Such an alternative led to a road network that was about 5% more expensive but approximately 5% more attractive for harvesting.

4.3.5 Adverse ecological impacts versus construction costs

The data for costs and adverse ecological impacts are shown in Figure 4.24. An increase of 10% for costs caused the adverse impact to decline by 5% for capercaillie and by 55% for the marshland. When costs rose by 25%, the adverse impact dropped by 21% for capercaillie and 97% for marshland. This demonstrated that, in the Wägital project area, it is much harder to improve the solution for capercaillie than to optimize for marshland.

The distribution of solution points mapped on the criterion space (Y_T, Y_M, see Fig. 4.24) was monotonic, decreasing for both values and describe the convex hull of Y_{eff}. Y_T and Y_M are not even distributed but build numerous clusters. For example, from T5 to T450, we had a dense cluster within an improvement of 7%. By increasing the weight only slightly, we were able to see a big leap in that improvement, from 7% to 36%. The next cluster occurred from T500 to T1.2k; the last, T1.5k to T100k. Distribution of the marshland solutions area clustered as well, though not as strongly as noted with the capercaillie alternatives. Such knowledge of this effect helps the stakeholder make a final decision. Furthermore, these different solutions can be reduced to a few alternatives that are all Pareto-optimal.

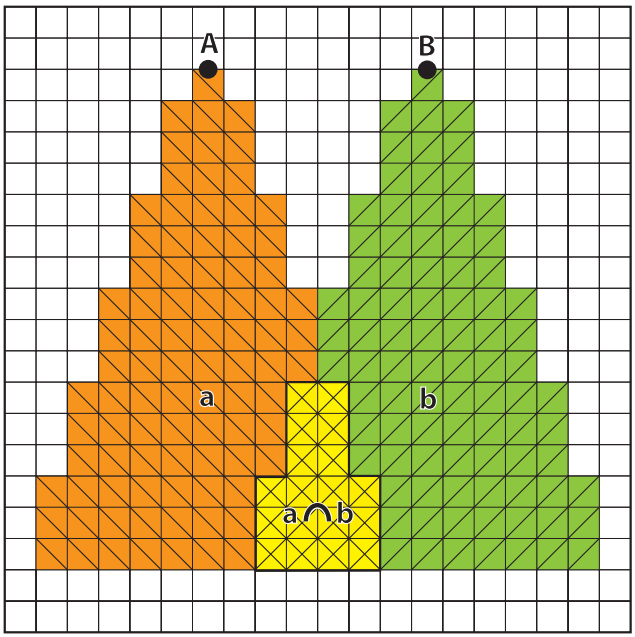

Figure 4.21: Two overlapping catchment areas (a, b) for two cable yarder landings (A, B). The harvesting attractiveness for A as well for B is 106, i.e., 212 in total. The total accessible volume in A and B – without multiple counting of overlaps a∩b – is 194.

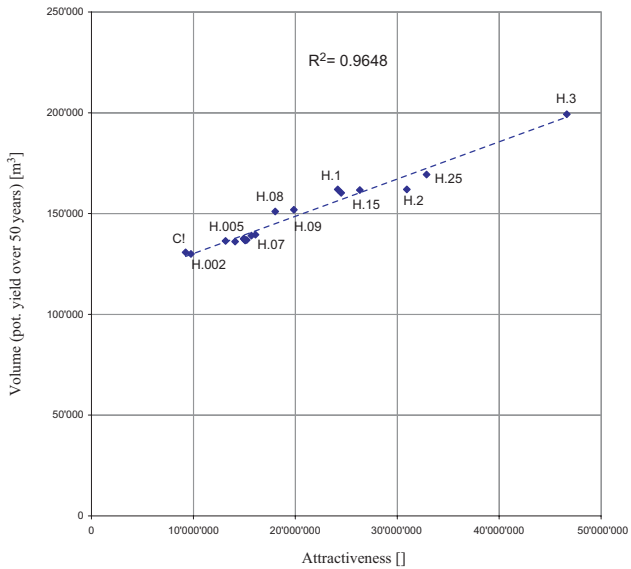

Figure 4.22: Correlation between harvesting-attractiveness (with multiple counting of overlaps) and potential yield volume (without multiple counting of overlaps)

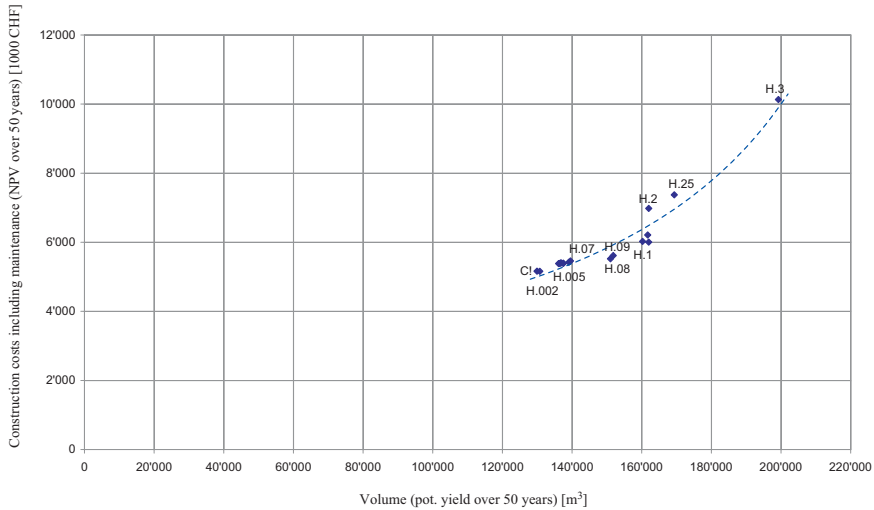

Figure 4.23: Potential yield volume (without multiple counting of overlaps) versus construction costs, over 50 years

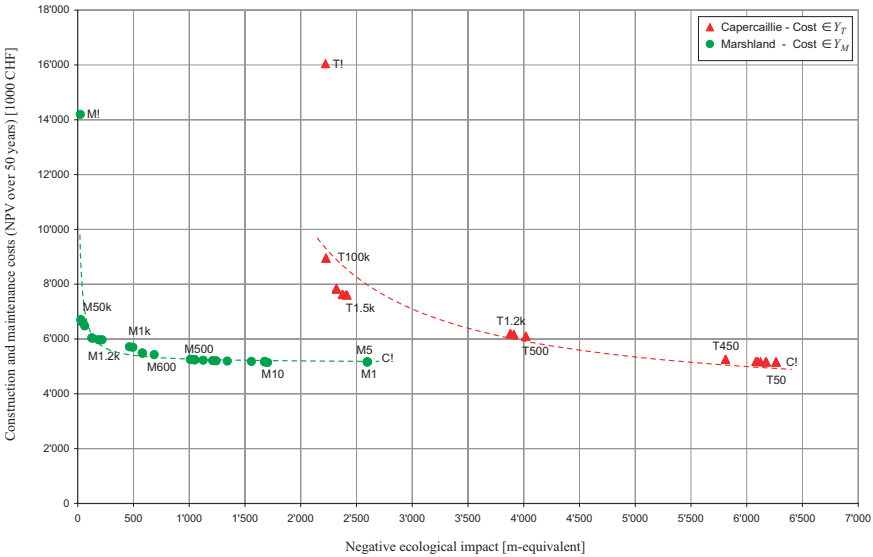

Figure 4.24: $Y_T \subset Y_{eff}$ for the capercaillie-friendly and $Y_M \subset Y_{eff}$ for the marshland-friendly alternatives. Dashed line, hyperbolic trend

4.3.6 Tri-objective optimization

The 66 tri-objective alternatives resulted in the building of three clusters (A, B, and C) on Y_{eff} (Fig. 4.25). These corresponded to the three clusters found with the bi-objective alternatives for capercaillie and costs. Tables 4.3, 4.4, and 4.5 present these data numerically.

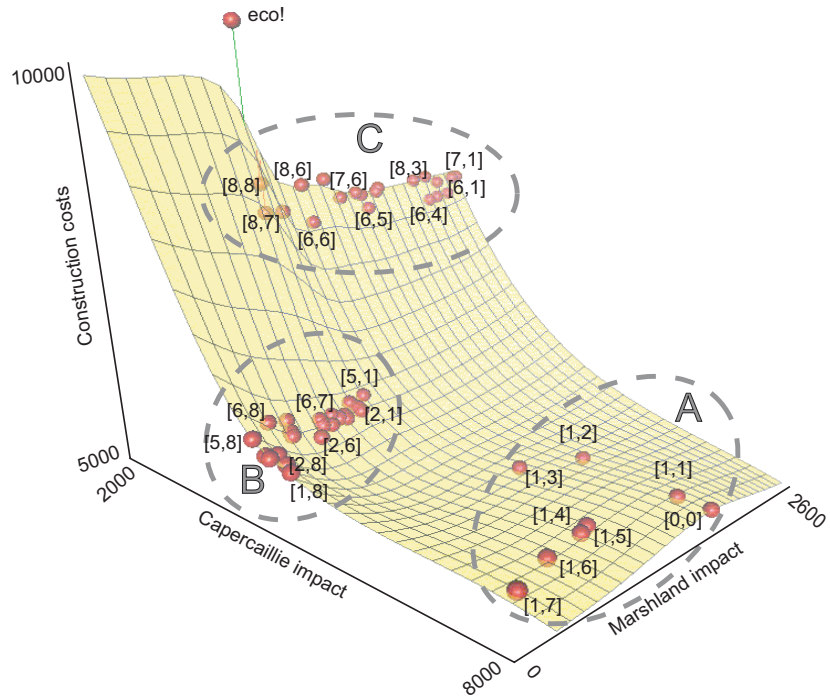

Figure 4.25: Pareto-optimal solutions within the criterion space for construction costs, and adverse impacts on capercaillie and marshland. These criterion points are efficient, and group into 3 clusters – A, B, and C. The yellow area is a fitted shape through the efficient points in order to visualize the 3-dimensional effect.

Figures 4.26, 4.27, and 4.28 show three examples of road alignment for Clusters A, B, and C.

Cluster A takes a wide span on Y_{eff}. Therefore, the road alignments from the three alternatives are much different. Alternative [1,1], which is close to the cost-optimal alternative, connects Locations C3 over A1, A2, A3, and B3, and the Steiner point near C3. This alternative has the shortest total road length, 19.9 km. Alternatives [1,5] and [1,7] connect C3 directly over A1, and B1 and C2.

Clusters B and C connect locations – without regard to Steiner points – in the same order: 00, A1, B2, A2, A3, B3, C3, C2; and 00, A1, B1, C1, respectively. However, small differences exist. For example Alternative [1,8] does not cross any marshland between Locations C3 and C2, but takes a route through the capercaillie area that is longer than the one specified with the other alternatives. Vice versa, although the alternatives in Cluster C do cross marshland near Location C1, less of that ecotype is traversed than when the alternatives in Cluster B are utilized.

	[,1]	[,2]	[,3]	[,4]	[,5]	[,6]	[,7]	[,8]
[0,0]	5'198							
[1,]	5'199	5'200	5'245	5'638	5'655	5'793	6'158	6'566
[2,]	5'971	5'971	5'977	5'977	6'012	6'015	6'288	6'631
[3,]	5'995	5'995	6'002	6'002	6'016	6'068	6'332	6'631
[4,]	6'009	6'010	6'017	6'017	6'031	6'085	6'333	6'638
[5,]	6'088	6'088	6'095	6'095	6'110	6'244	6'360	6'900
[6,]	8'545	8'545	8'547	8'551	8'805	8'947	6'406	6'937
[7,]	8'825	8'827	8'835	9'055	9'096	9'171	9'317	9'440
[8,]	9'018	9'018	9'024	9'114	9'167	9'649	9'683	9'983
eco!								12'855

Table 4.3: Road construction and maintenance costs (at NPV) associated with Alternatives [0,0], [1,1], ..., [8,8], and eco! (in 1000 CHF). The small borders delineate Clusters A (top left), B (middle), and C (bottom).

	[,1]	[,2]	[,3]	[,4]	[,5]	[,6]	[,7]	[,8]
[0,0]	8'077							
[1,]	7'867	7'639	5'810	7'277	7'302	7'303	7'509	4'694
[2,]	3'853	3'853	3'853	3'853	3'853	3'961	4'397	4'364
[3,]	3'817	3'817	3'817	3'817	3'817	3'817	4'254	4'364
[4,]	3'796	3'796	3'796	3'796	3'796	3'796	3'856	4'242
[5,]	3'691	3'691	3'691	3'691	3'748	3'748	3'790	4'142
[6,]	2'311	2'311	2'311	2'321	2'272	2'338	3'682	3'758
[7,]	2'230	2'230	2'230	2'185	2'191	2'186	2'292	2'354
[8,]	2'178	2'178	2'178	2'175	2'179	2'181	2'212	2'306
eco!								2'283

Table 4.4: Adverse ecological impacts on capercaillie that result from the implementation of Alternatives [0,0], [1,1], ..., [8,8], and eco! (in m-equivalent). The small borders delineate Clusters A (top left), B (middle), and C (bottom).

	[,1]	[,2]	[,3]	[,4]	[,5]	[,6]	[,7]	[,8]
[0,0]	1'399							
[1,]	1'399	1'399	1'130	793	725	458	123	48
[2,]	823	823	719	719	614	499	124	48
[3,]	825	825	721	721	684	569	130	48
[4,]	825	825	721	721	684	568	357	65
[5,]	910	910	806	806	653	574	369	38
[6,]	2'327	2'327	2'224	2'147	1'624	1'166	388	252
[7,]	2'459	2'412	2'266	1'727	1'601	1'438	978	843
[8,]	2'177	2'177	2'065	1'751	1'563	1'326	1'151	846
eco!								798

Table 4.5: Adverse ecological impacts on marshland that result from the implementation of Alternatives [0,0], [1,1], ..., [8,8], and eco! (in m-equivalent). The small borders delineate Clusters A (top left), B (middle), and C (bottom).

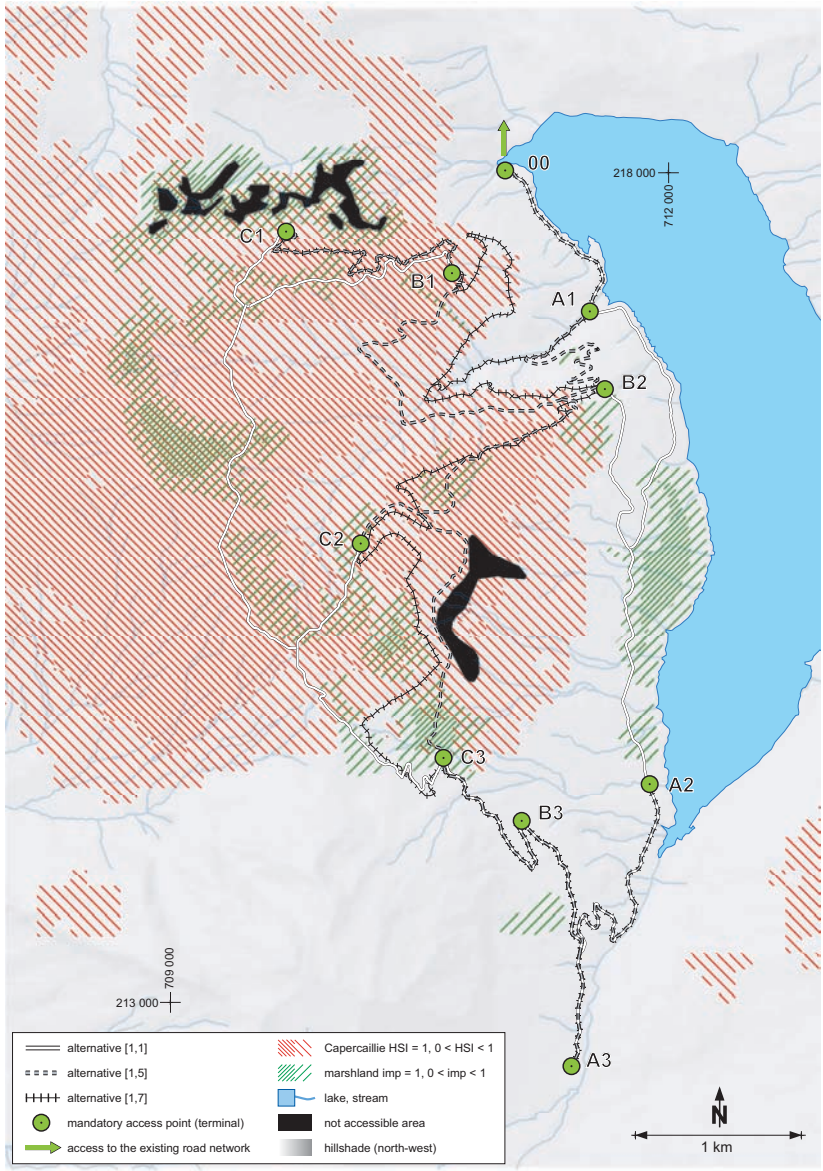

Figure 4.26: Road alignments from Alternatives [1,1], [1,5], and [1,7] for Cluster A. Area (5 $km \times 7\ km$) at Wägital, Switzerland

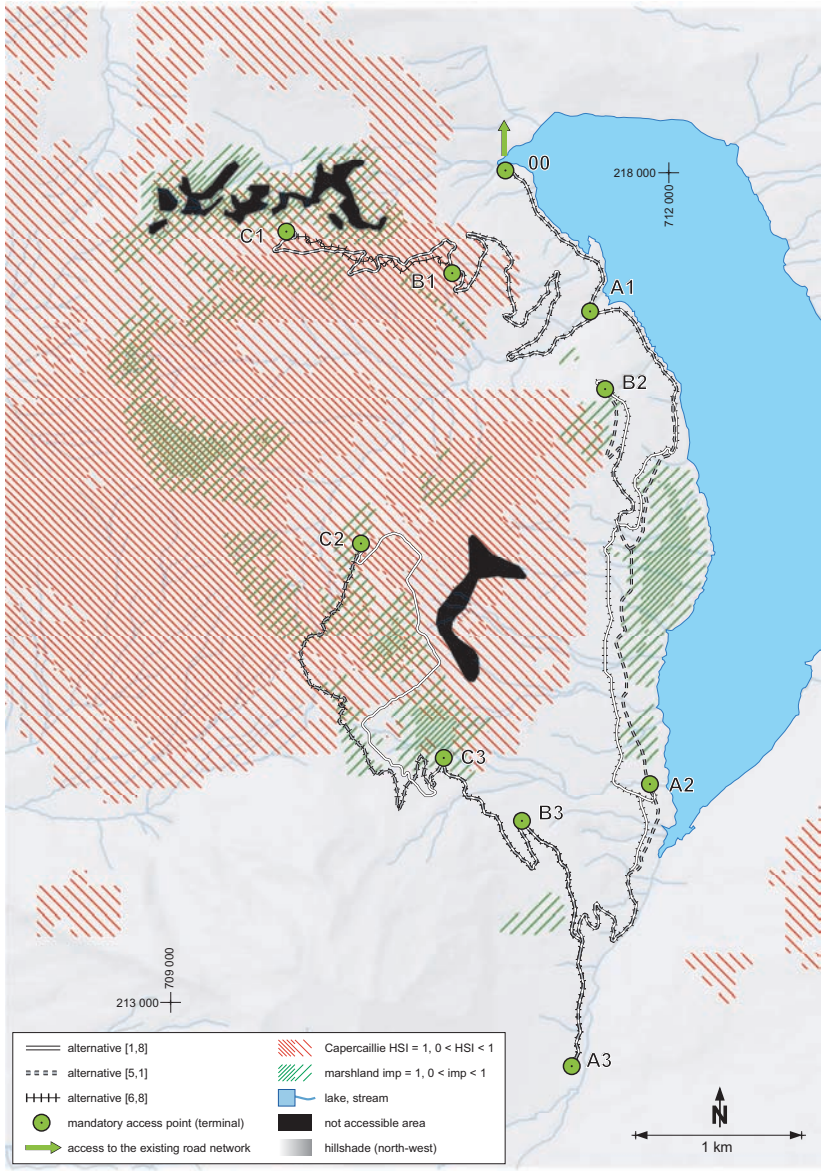

Figure 4.27: Road alignments from Alternatives [1,8], [5,1], and [6,8] for Cluster B. Area (5 $km \times 7\ km$) at Wägital, Switzerland

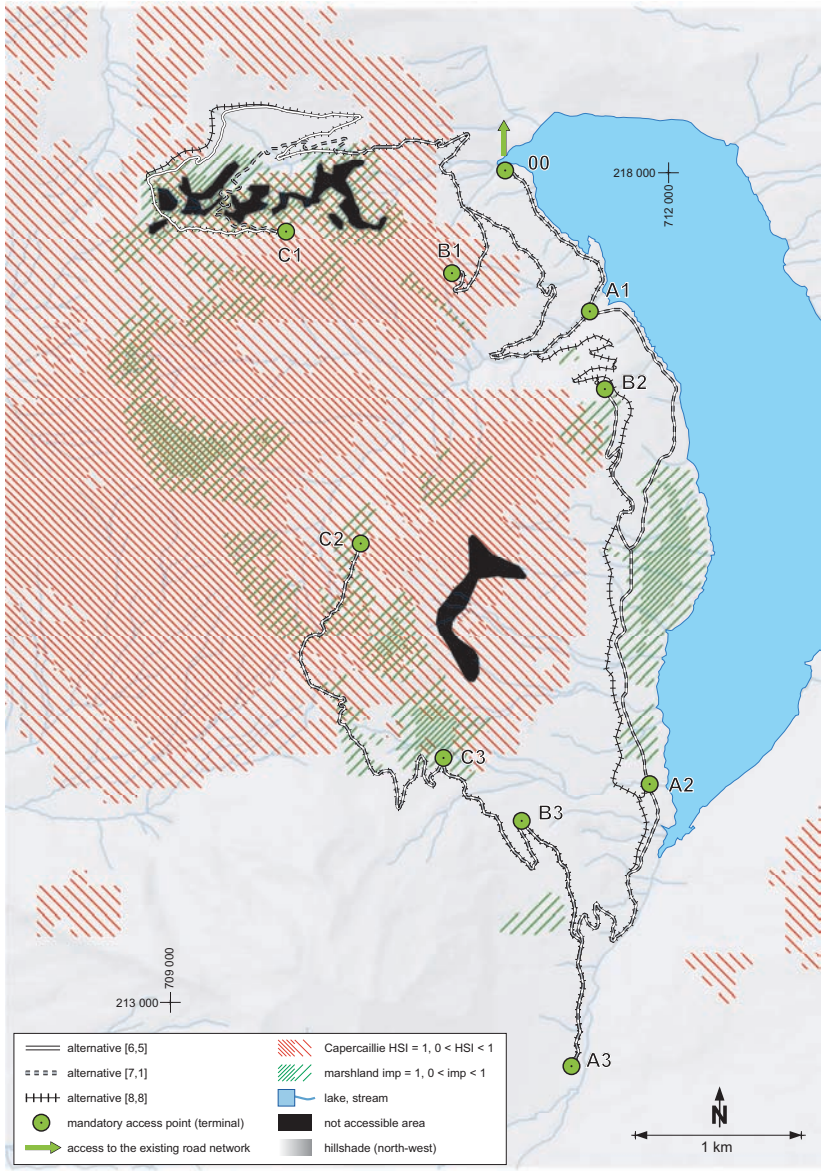

Figure 4.28: Road alignments from Alternatives [6,5], [7,1], and [8,8] for Cluster C. Area (5 $km \times 7\ km$) at Wägital, Switzerland

4.4 Discussion

4.4.1 Evaluation and rating of the different components

With the framework described here, it is possible to find a near-optimal road network layout automatically by considering different objectives. This layout seems reasonable even if not all components have the same quality. In its present form, the entire framework is applicable only to the Wägital project area. However, we should be able to customize or exclude certain components or incorporate new models for specific uses. Table 4.6 provides ratings for the different components.

4.4.2 Evaluation of the results

As demonstrated with the tests described here, a step-wise change in the weights for different objectives can lead to a set of feasible and Pareto-optimal solutions. Even though we had checked various combinations of different weights, the results could be grouped into only a few clusters. Small changes in scaling for the objective function may result in a completely different road network (e.g., T450 to T500). There, the solutions are "jump" from one cluster to another. In contrast, big changes in scaling may produce nearly identical alternatives (e.g., T500 to T1.2k), when such changes do not affect the solution.

The weighted sum approach, which we used in our evaluation, can only find a subset of the entire Pareto-set. We have to consider that there are most probably more Pareto-optimal solutions between the "jumps". Pareto-optimal solutions which are not laying on the convex hull are most probably not preferred by the stakeholders (cf., Fig. 4.11). A Pareto-optimal solution, that is not located on the convex hull of Y_{eff} leads often to an unfavorable ratio between the increase in one objective to decrease in another one.

Few general patterns exist for connecting the different mandatory control points only. Knowing the behavior of these effects is useful for the various stakeholders, who then can concentrate on just a small number of solutions and can find the most desirable alternative within a few road network alignments that are Pareto-optimal.

Within our project area, the two ecological objectives are inverse. The most capercaillie-friendly alternative (T!) is 29% less favorable to marshland than the cost-optimal alternative (C!), whereas the most marshland friendly-alternative (M!) is 20% less suitable for capercaillie habitat than C!. However, the penalty for capercaillie affects the adverse marshland impact more than the penalty for marshland influences the adverse impact on capercaillie. For example, Alternative [8,8] is about 18 times worse for marshland than Alternative [1,8]. Vice versa, Alternative [8,8] is only about 6% worse for capercaillie than Alternative [8,1]. The reason for this effect is as follows: The capercaillie area is large and coherent, while the marshland areas are small and not contiguous. Consequently, it is possible to find a road that can curve around the sides of the different marshland sites. However, because Locations B1, C1, and C2 are within the capercaillie impact area, the SMT must cross it.

One of the crucial optimization problems in forestry is to minimize both off- and on-road transportation costs and road construction costs (Chung et al., 2007). Our framework excludes those transportation costs and, instead, considers an auxiliary value of potential landing volume, which should lead the SMT to a more harvesting-friendly alternative. Off-road costs will decrease indirectly. Still, our approach is useful only with small weights for harvesting-attractiveness because Dijkstra's algorithm does not allow for adverse weights. In central Europe, road standards are high and must often fulfill different criteria for forestry and agriculture simultaneously. As a con-

Nr.	Component	Quality / estimated error [a]	Transferability	Comment
1	Discretization of the road	$< 1\%$	yes	We used a 10 $m \times 10$ m grid resolution and 16 road directions (cf., Stückelberger et al., 2007). The highest possible resolution for the grid is constrained by the accuracy of the spatial data.
2	Road geometry constraints	$< 1\%$	yes	Same standards as used for manual road design (cf., Kuonen, 1983 or US Forest Service, 2006)
3	Graph topology	exact	yes	Each potential and feasible road segment in the project area is mapped to a link in the graph G (cf., Section 4.2.3).
4	Road construction cost model	5% - 10%	good	In order the construction cost model is generic, the model is applicable for nearly every project, as long as the input data are known (cf., Stückelberger et al., 2006a).
5	Harvesting attractiveness model	10% - 30%	good	It is common for planners to consider the potential landing volume when locating optimal landings (Chung & Sessions, 2002). However, the degree of difficulty for installing and operating is not considered in our model.
6	Ecological penalty functions	10% - 30%, assuming the presumptions are correct	The presented capercaillie model and marshland model are applicable in Central Europe only. However, similar models for other species should be developable in most case.	The applied penalty functions are common in the science of ecology (cf., USDI Fish and Wildlife Service, 1981, Jaeger, 2002). However, the influence of forest roads on different species is based on numerous presumptions. Furthermore, the set of species and ecotypes considered relevant is subjective.
7	Multiple-objective function	is considered a good approach but has limited utility	good	The linear combination of all single objectives may be faulty. It seems reasonable to combine construction costs and ecological penalties linearly. In contrast, the linear combination of harvesting-attractiveness and construction costs is applicable within only a small range (Stückelberger et al., 2006b).
8	Mathematical graph model	exact	yes	Any path P in graph G leads to a feasible road (cf., Section 4.2.8)
9	Optimization techniques	0% - 4%	yes	The method used to find the SMT on a graph most probably leads to a near mathematical optimum (Schwartz & Stückelberger, 2008).

Table 4.6: Quality and transferability of the different components of the model framework. [a] compared to the theoretical optimal objective value

sequence, construction costs there are more critical factors compared with harvesting costs. This is why our approach leads to reasonable results even though transportation costs are included only indirectly.

4.5 Conclusion

This paper presents models for mapping the spatial variability of different objective functions in forest road design (life-cycle costs, adverse ecological effects, and landing-attractiveness). Three major findings have emerged from this investigation. (1) The Steiner minimum tree solutions are located on convex trade-off surfaces, as predicted by the multi-objective optimization theory. (2) Single-point solutions are clustered on the Efficient set for Pareto-optimal solutions; even small changes in the relative weights of objective-function components can trigger jumping from one cluster to the next. (3) The allocation of relative weights to those components greatly influences the solution.

Problem-solving in road network design is characterized by a set of partially conflicting requirements brought forward by different stakeholders. Mono-objective analysis evaluates the edges of the solution space that characterize those varying points of view.

In our example, the landowner was interested in a cost-optimal solution, whereas ornithologists would prefer the capercaillie-optimum and marshland specialists would look for the marshland-optimum. Therefore, mono-objective results are a good starting point in the negotiation process because they quantify the effects of extreme preferences on the different objectives. Systematic variations in the relative weights of the objective-function components are a prerequisite for exploring the Pareto solution space. The evaluation presented here clearly demonstrates our improved understanding of problem-specific trade-offs among different objective functions, and identifies solution clusters. Only three clusters resulted from the 10 mandatory control points analyzed in this Steiner minimum tree problem. It seems a likely supposition that the number of solution clusters would increase with the number of mandatory control points.

Our approach also has some shortcomings. Whereas a cost metric may adequately map a real-world situation, our ecological impact metric is based on expert knowledge that considers some weak, unclear components, which one must be aware of when interpreting these results. A basic assumption of multi-criteria optimization is that objective values must be independent. However, our landing-attractiveness metric violates this assumption because it allocates accessible, though overlapping, areas to each grid cell. Nevertheless, this approach seems to be useful in controlling the location of routes for specific off-road transportation.

Synthesis

Goals

This thesis presents a model framework that automatically designs the spatial layout of an optimal forest road network. Project areas of up to 50 km^2 can be accommodated, assuming a resolution of 10 m for the underlying digital elevation model. Goals here included (1) estimating the spatial variability of road construction costs, (2) improving road link patterns in order to map turning constraints on a mathematical graph and extend the set of different road directions, and (3) balancing one's consideration of construction costs, attractiveness for harvesting systems, and disturbances to various ecological factors.

Main results

(1) In a first step, we set up a model for predicting road construction and maintenance costs based on a digital elevation model (DEM), the geotechnical subsoil, and design parameters for a specific road. This model was tested in two mountainous areas, and was compared with state-of-the-art approaches that assume construction costs to be homogenous over the entire project area. When the spatial variability of those costs was considered, expenses were about 25% lower but the road length increased by about 10% compared with previous approaches. A model that incorporated the DEM but neglected the geotechnical subsoil resulted in 17% higher costs than with the current model. Here, the correlation between road network length and cost was low, although previous approaches had assumed this relationship to be very strong. This can be explained as follows. About 15% of the project area was located in terrain units where construction costs ordinarily are three times the average. However, our optimization approach avoided road assignments in those high-cost sites, resulting in longer routes but at a lower price. Our new model distinguished among straight segments, curves, and switchbacks. In steep terrain, a switchback would have entailed extremely high costs due to earth and rock excavation, as well as the installation of retaining structures. Those details accounted for up to 60% of the total cost. Therefore, the siting of switchbacks was a crucial task. Furthermore, previous models had assumed the road centerline to be a series of straight lines, with cost proportional to line length. However, that would have been inappropriate for sharp changes in road direction between two following segments. Introducing a constant penalty for any directional changes of more than 120 degrees, which is especially true for switchbacks, slightly improved the layout by suppressing the occurrence of "zigzagging". Nevertheless, none of the existing models estimated the costs for switchbacks based on an actual centerline and cost figures for those construction elements. Our new model led to an approximately 20% improvement in network layout effectiveness compared with models that called for a constant switchback penalty.

(2) The geometry of the road centerline is controlled by a maximum road gradient and a minimum curve radius. Steeper terrain means fewer feasible alternatives for the centerline. State-of-the-art representations of the road network assume a finite set of regularly spaced nodes, and road segments linking adjacent nodes. A widely used approach defines eight possible links between a node and its directly adjacent nodes (8-link pattern). The maximum road gradient is limited due to the gradeability constraints of vehicles. Within the 8-link pattern in steep terrain, this limitation for the maximum road gradient results in a low number of feasible links or even entirely non-feasible links. Our investigation demonstrated that the 8-link pattern did not present feasible solutions for conditions with an average slope gradient of $\geq 35\%$. We therefore considered links to the second-order neighborhood, consisting of 16 additional nodes, thereby

producing a 24-link pattern. This enhanced pattern proved favorable in steep terrain because it gave better layout alternatives. However, this approach still did not lead to smooth centerline layouts for rolling terrain with a complex morphology. Therefore, we developed a 48-link pattern that provided smooth road centerlines that were well adapted to the terrain morphology.

Turning constraints are decisive controls for ensuring a feasible horizontal alignment of two consecutive road links. Here, we introduced 16 different road directions for each physical node and mapped each direction on a separate layer. This was equivalent to 16 virtual nodes per physical node, and it enlarged the solution space by a factor of 16^2. Such an approach made it possible for us to map the turning constraints directly on a mathematical graph. In general, the solution of graph problems, e.g., determining a minimum path between two nodes, occurs in an enlarged solution space with virtual nodes. A solution may easily be mapped back to the "real world" by re-merging the 16 virtual nodes to the physical node. The location of the mandatory control points is assumed to be known. The optimal road network that connects all the control points by a spanning tree is known as the Steiner Minimum Tree (SMT) problem. Applying our approach to a real-world road network layout resulted in a cost improvement of about 35% compared with previous approaches that had neglected turning constraints. Our results clearly indicated that representation of the road network solution space – including link patterns and turning constraints – is absolutely essential for finding solutions that fit well to a complex terrain morphology. This might be more important than algorithmic power for real-world applications.

(3) Real-world road network layout problems must always take several objectives into account, e.g., reducing costs while minimizing adverse ecological impacts. We introduced multiple-objective configurations here. First, we simultaneously analyzed the trade-offs between two objectives – e.g., construction costs versus detrimental effects on the environment, or costs vs. harvesting-attractiveness. Second, we analyzed the trade-offs among three objectives simultaneously – construction costs and the ecological impacts on both marshland and the capercaillie. To do so, we used a main objective function that consisted of a linear combination of cost, impact, and attractiveness objective components. Trade-offs were investigated by applying a set of scaling vectors to the objective components (i.e., evaluating different weighting factors for the objectives), which resulted in the set of Pareto-optimal solutions that are located on the convex hull of Y_{eff}.

Our evaluation demonstrated that economical and ecological objectives were in conflict. That is, the solutions that could improve ecological performance also increased costs by 2- to 3-fold compared with a cost-optimal solution. Moreover, within our particular project area, the "Wägital" (which is representative of Switzerland), even our two ecological objectives clashed. The capercaillie-optimal alternative caused 30% more disturbance to the marshland compared with the cost-optimal alternative. Likewise, the marshland-optimal alternative was associated with 20% greater interruption of capercaillie habitat over the cost-optimal solution. In fact, the bi-objective optimization for construction cost and harvesting-attractiveness was valid only for the low weighting factors assigned to attractiveness. Nonetheless, in the "Wägital" area, the increments for road construction costs and accessible harvesting volume were balanced, with 5% higher costs resulting in about 5% more available volume.

Preferences for different objectives (i.e., weighting factors of the objective function) by the stakeholders are extremely decisive for the solution. At certain areas in the criterion space, small changes in preferences (weights) may cause the solution to jump dramatically from one efficient point to another. In other areas of the criterion space, solutions are less sensitive to changes in preference weights. In the "Wägital" area, we found three major clusters for the tri-objective optimization. Therefore, our approach will help both experts and laymen understand the trade-offs between different objectives, thereby enabling them to make a final decision that is Pareto-optimal.

Limitations

Mathematical formulation of a problem leads to an SMT problem, where the terminals are defined by the mandatory access points within a specific project area. However, this approach has two major difficulties. First, the situation is complex and belongs to the 21 recognized $\mathcal{NP}$-complete problems in graph theory (Karp, 1972). There is no known algorithm for finding the mathematically optimal solution within polynomial time. In the case of "Wägital", a full enumeration of all possible Steiner trees would have resulted in a problem size of 10^{55} alternatives, which is far too large to be enumerated within a reasonable period of time[1]. We instead took a heuristic approach that introduced one Steiner point for any triple of adjacent terminals. The best Steiner Minimum Tree solution found was then improved upon by looking for additional second-order Steiner points for triples of one first-order Steiner point and two adjacent terminals. We proved, via quad tree analyses, that our solution for the quasi-SMT was $< 2\%$ lower in performance than the theoretically optimal SMT. This demonstrated that our approach most likely produces a solution very close to the real optimum.

Problem size is a second difficulty. A project area of 50 km^2 – with a node spacing of 10 $m \times$ 10 m, 16 different road directions, and a 48-link pattern – results in $8 \cdot 10^6$ vertices and about $2 \cdot 10^8$ feasible edges. This reaches the memory limit for modern computers with about 2 GB RAM. Therefore, clever memory management is necessary in order to provide model stability. Here, we had to develop and compile a stand-alone application because such problems cannot possibly be run within a spread sheet or standard GIS program. In fact, our software required about 6 hours (Pentium 4, 2.66 GHz) to solve this problem.

An SMT approach is favorable if the graph is static, if the weight of each edge can be assigned by a weighted sum of the different objectives, and if the main objective value is the sum of the weights for all edges chosen for the solution. These assumptions are correct if we map cost figures directly on the graph. Conventional wisdom says that two road segments with individual costs of 1'000 and 2'000 units will be equal to one road segment with a cost of 3'000 units. It is more difficult to compare ecological impacts, e.g., two road segments with capercaillie disturbance values of 200 and 300 versus one road segment with an impact value of 500. Even though the models that calculate these impacts may need some improvement, the assumption that one must add those different weights is usually appropriate. However, those assumptions are no longer valid if we are also mapping harvesting-attractiveness on the graph. For example, if a particular road link is chosen, the attractiveness for neighboring road links may decrease. This is the case when a road follows a slope so that timber can be transported to an area that is easily accessed from the road, thus improving its harvesting-attractiveness. If, however, that road turns in a switchback, then a stand can be reached from either the upper or lower section, drastically reducing the attractiveness of the road below the switchback. This is why "zigzag" roads are not efficient when opening the forest for harvesting. Correct implementation of this problem requires a graph that must be updated after each step during the optimization process. With our approach we were unable to handle such dynamic weights for a graph, making this one of the biggest shortcomings of the present model. However, when harvesting-attractiveness had low-weighting factors, this model produced reasonable and nearly optimal solutions.

Outlook

Because the standard graph model reaches the memory limit of currently available computers, one must reduce the problem size. Some parts of a project area will never be accessible, perhaps

[1] the supposed age of the universe is $< 10^{18}$ *sec.*

because of lakes, slopes that are too steep, or a lack of interest in resources. These non-accessible areas then lead to isolated nodes within the graph model. Such nodes can be eliminated, which reduces the graph but not the solution space. However, a graph may still remain large due to the introduction of 16 vertices for the different directions within each physical node, as well as the inclusion of up to 48 edges per vertex. This is very desirable for steep terrain but is not required on flat sites. The link pattern in our presented model was always consistent, having a pattern of 8, 24, or 48 links. Moreover, fewer road links were feasible in the steeper terrain. Thus, a possible solution would have been to raise the number of links with increasing slope.

Our new model called for a regular road spacing within a $10\ m \times 10\ m$ grid. However, Anderson & Nelson (2004) have introduced irregular node spacing, with the big advantage being that one can find road centerlines that are at the feasible limit of the maximum road gradient. However, complexity is dramatically increased by this irregular spacing. Therefore, a combination of regular node spacing on flat ground plus irregular spacing along contour lines in steep terrain may be a promising approach.

Up to now, no one has been able to provide an algorithm that can exactly solve the problem of minimizing road construction costs and harvesting transportation costs simultaneously within a real-world application[2]. Our models are mostly deterministic. The way they work is much different from the manner in which a human being might search for a good road network. A computer model is based on many iterative calculations whereas a person will try to find a solution graphically and intuitively. To implement intuition is very difficult. However, many non-deterministic algorithms used in the field of operations research are based on biological strategies, e.g., ant colony system optimization (ACO) (Dorigo, 1992, 1996) or genetic algorithms (GA) (Holland, 1975). GA in particular has some potential for problem-solving here. For example, we could add additional random points to the set of mandatory access points and resolve the Minimum Spanning Tree (MST) problem. This MST-problem is a $\mathcal{P}$-problem, thereby making it solvable within polynomial time. By choosing different sets of additional random access points we then obtain a population of solutions. We can use a fitness function (e.g., one that corresponds to overall costs) to select favorable candidates that will be the parents of the next generation of solutions. Our approach may be combined with such artificial-intelligence algorithms in order to find faster and/or better solutions.

Two aspects of this model framework that might benefit from improvements include variable graph representation and the use of artificial intelligence. However, we must never lose sight of the practicality of any potential solution. For example, if a construction company is unable to build a road to a satisfying standard and in an economical way, they will have no use for highly sophisticated optimization techniques. Moreover, if the spatial data are out-dated and the resolution is lower than the mesh of the nodes, then it is futile to introduce a complex graph model. Therefore, before this proposed model framework can be adapted to more general applications, we ought to test it, step-by-step, under various project conditions and in a wide range of geographical areas in order to receive more feedback from design engineers in the field.

[2]Although there are authors who claim to have a solution, many of them do not realize, how complicated the problem actually is.

Bibliography

AASHTO (1993): *AASHTO guide for design of pavement structures.* American Association of State Highway and Transportation Officials, Washington DC, U.S.A.

Anderson, A.E. and Nelson, J. (2004): Projecting vector-based road networks with a shortest path algorithm. In: *Canadian Journal of Forest Research*, Vol. 34, pp. 1444–1457.

Aruga, K., Sessions, J., Akay, A. and Chung, W. (2004): Optimizing horizontal and vertical alignments of forest roads using a high resolution DEM. In: Clark, M. (Ed.): *A Joint Conference of IUFRO 3.06 Forest Operations under Mountainous Conditions and the 12th International Mountain Logging Conference.* June 13–16, 2004. FERIC, University of British Columbia, Vancouver, BC, Canada. CD-ROM.

Barile, M. and Weisstein, E.W. (2002): *Neighborhood.* [online] MathWorld–A Wolfram Web Resource. http://mathworld.wolfram.com/Neighborhood.html (retrived June 10, 2005).

Bollmann, K. (2003): Selten, seltener, am seltensten: Drei Waldhühner mit unterschiedlichen Ansprüchen [Rare, rarer, the rarest. Three grouse and their different ecological needs]. In: *Ornis*, (4), pp. 4–10.

Brassel, P. and Brändli, U.B. (1999): *Schweizerisches Landesforstinventar: Ergebnisse der Zweitaufnahme 1993–1995 [Swiss national forest inventory: Results of the second inventory 1993–1995].* Eidgenössische Forschungsanstalt für Wald, Schnee und Landschaft, WSL, Birmensdorf, Switzerland, p. 442. ISBN 3-258-05897-0.

Burlet, E. (1980): *Dimensionierung und Verstärkung von Strassen mit geringem Verkehr und flexiblem Oberbau [Dimensioning and reinforcement of low volume road with flexible pavement structure].* Ph.D. thesis, ETH Zurich, Switzerland.

BUWAL (1991): *Flachmoorinventar der Schweiz 1986–1989. Grundlage zum Inventar der Flachmoore von nationaler Bedeutung. Technischer Bericht zu Vorbereitung, Feldarbeit, Begriffe, Bewertung [Marshland Inventory of Switzerland 1986–1989. Principles for inventorying marshland of national importance].* Bundesamt für Umwelt Wald und Landschaft [Swiss Agency for the Environment, Forests and Landscape], p. 19.

CCE (1991): *Elementarkostengliederung EKG – Kostengliederung nach Elementen für Hoch- und Tiefbau mit Projektkostengliederung [Cost classification by elements CCE – cost classification by elements for building and civil engineering].* No. 506 502 in SN. Swiss Research Center for Rationalization and Civil Engineering, Zurich.

Chew, E.P., Goh, C.J. and Fwa, T.F. (1989): Simultaneous optimization of horizontal and vertical alignments for highways. In: *Journal of Transportation Research*, Vol. 23B (5), pp. 315–329.

Chung, W. (2002): *Optimization of cable logging layout using a heuristic algorithm for network programming.* Ph.D. thesis, Department of Forest Engineering, Oregon State University, Corvallis OR, U.S.A.

Chung, W. and Sessions, J. (2001a): Designing a Forest Road Network using Heuristic Optimization Techniques. In: Wang, J., Wolford, M. and McNeel, J. (Eds.): 24^{th} *Meeting of the Council on Forest Engineering*. July 15–19, 2001. Snowshoe WV, U.S.A.

Chung, W. and Sessions, J. (2001b): NETWORK 2001 – Transportation Planning Under Multiple Objectives. In: Schiess, P. and Krogstad, F. (Eds.): *The International Mountain Logging and* 11^{th} *Pacific Northwest Skyline Symposium 2001*, pp. 194–200. December 10–12, 2001, College of Forest Resources, University of Washington, Seattle WA, U.S.A.

Chung, W. and Sessions, J. (2002): *CPLAN 1.0. A program to optimize cable harvesting layout and road locations using digital terrain model.* Department of Forest Engineering, Oregon State University. Corvallis OR, U.S.A.

Chung, W. and Sessions, J. (2003): *CableAnalysis 1.0. A program to determine cable logging feasibility using GIS produced data.* Department of Forest Engineering, Oregon State University. Corvallis OR, U.S.A.

Chung, W., Sessions, J. and Heinimann, H.R. (2004): An Aplication of a Heuristic Network Algorithm to Cable Logging Layout Design. In: *International Journal of Forest Engineering*, Vol. 15 (1), pp. 11–24.

Chung, W., Stückelberger, J.A., Aruga, K. and Cundy, T.W. (2007): Forest Road Network Design Using a Trade-off Analysis between Skidding and Road Construction Costs. In: *Canadian Journal of Forest Research.* (Accepted, in press).

Church, R.L. (2002): Geographical information systems and location science. In: *Computers & Operations Research*, Vol. 29 (6), pp. 541–562. Doi:10.1016/S0305-0548(99)00104-5.

Church, R.L., Murray, A.T. and Weintraub, A. (1998): Location issues in forest management. In: *Location Science*, Vol. 6 (4), pp. 137–153.

Coello, C.A.C. (2000): An updated survey of GA-based multiobjective optimization techniques. In: *ACM Computing Surveys*, Vol. 32 (2), pp. 109–143. Doi 10.1145/358923.358929.

Coello, C.A.C. (2001): A short tutorial on evolutionary multiobjective optimization. In: Zitzler, E., Deb, K., Thiele, L., Coello, C.A.C. and Corne, D. (Eds.): *First International Conference on Evolutionary Multi-Criterion Optimization*, pp. 21–40. Springer-Verlag. Lecture Notes in Computer Science No. 1993, March 7–9, 2001, Zurich, Switzerland. ISBN 978-3-540-41745-3.

Collette, Y. and Siarry, P. (2004): *Multiobjective Optimization – Principles and Case Studies.* Decision Engineering. Springer-Verlag, Berlin, 2^{nd} Edn., p. 293. ISBN 978-3-540-40182-7.

Coulomb, C.A. (1776): ESSAI Sur une application des règles de Maximis & Minims à quelques Problèmes de Statique, relatifs à l'Architecture [An essay on an application of rules of maximum and minimum to some statical problems, relevant to architecture]. In: *Mémoires de Mathématique & de Physique, présentés à l'Académie Royale de Sciences par divers Savants*, Vol. 7 (1773), pp. 343–382. Reprinted in 1972.

Dean, D.J. (1997): Finding optimal routes for network of harvesting site access roads using GIS-based techniques. In: *Canadian Journal of Forest Research*, (27), pp. 11–22.

Dijkstra, E.W. (1959): A note on two problems in connexion with graphs. In: *Numerische Mathematik*, Vol. 1, pp. 269–271.

Dorigo, M. (1992): *Ottimizzazione, apprendimento automatico, ed algoritmi basati su metafora naturale [Optimization, Learning, and Natural Algorithms].* Ph.D. thesis, Politecnico di Milano, Italy. (unverified).

Dorigo, M. (1996): The Ant System: Optimization by a colony of cooperating agents. In: *IEEE Transactions on Systems, Man, and Cybernetics Part B: Cybernetics*, Vol. 26 (1), pp. 1–13.

Dreyfus, S.E. and Wagner, R.A. (1971/72): The Steiner problem in graphs. In: *Networks*, Vol. 1, pp. 195–207.

Duha, J.D. and Brown, D.G. (2007): Knowledge-informed Pareto simulated annealing for multi-objective spatial allocation. In: *Computers, Environment and Urban Systems*, Vol. 31 (3), pp. 253–281.

Durston, T.A. and Ou, F.L. (1983): Simplified Cost-Estimation Method for Low-Volume Roads. In: *Transportation Research Record: Journal of the Transportation Research Board*, (898), pp. 47–51.

Dykstra, D.A. (1976): *Timber harvest layout by mathematical and heuristic programming.* Ph.D. thesis, Department of Forest Engineering, Oregon State University, Corvallis OR, U.S.A.

Edgeworth, F.Y. (1881): *An Essay on the Application of Mathematics to the Moral Sciences.* Mathematical Psychics. C. Kegan Paul and Co., London, p. 150. (unverified).

Edgeworth, F.Y. (1889): The Mathematical Theory of Political Economy. In: *Nature*, Vol. 40, pp. 496–509.

Ehrgott, M. (2000): *Multicriteria Optimization.* No. 491 in Lecture Notes in Economics and Mathematical Systems. Springer, Berlin, p. 243. ISBN 3-540-67869-7.

Epstein, R., Morales, R., Seron, J. and Weintraub, A. (1999): Use of OR systems in the Chilean forest industries. In: *Interface*, Vol. 29 (1), pp. 7–29.

Epstein, R., Weintraub, A., Sapurnar, P., Sessions, J. and Sessions, B. (1994): PLANEX – Software for operational planning international seminar on forest operations under mountainous conditions. In: Sessions, J. (Ed.): *International seminar on forest operations under mountainous conditions*, pp. 52–57. July 24–27, 1994. Harbin, P.R. of China.

Epstein, R., Weintraub, A., Sessions, J., Sessions, B., Sapunar, P., Nieto, E., Bustamante, F. and Musante, H. (2001): PLANEX: A System to Identify Landing Locations and Access. In: Schiess, P. and Krogstad, F. (Eds.): *The International Mountain Logging and 11th Pacific Northwest Skyline Symposium 2001*, pp. 190–193. December 10–12, 2001, College of Forest Resources, University of Washington, Seattle WA, U.S.A.

Ervin, S.M. and Gross, M.D. (1987): RoadLab – A constraint based laboratory for road design. In: *Artificial Intelligence in Engineering*, Vol. 2 (4), pp. 224–234.

Euler, L. (1741): Solutio problematis ad geometriam situs pertinentis [The solution of a problem relating to the geometry of position]. In: *Commentarii academiae scientiarum Petropolitanae*, Vol. 8, pp. 128–140. (unverified).

FAO (2007): *State of the World's Forests 2007*. Tech. Rep., Food and Agriculture Organization of the United Nations, Rome, Italy.

Garey, M.R., Graham, R.L. and Johnson, D.S. (1977): The Complexity of Computing Steiner Minimal Trees. In: *SIAM Journal on Applied Mathematics*, Vol. 32 (4), pp. 835–859.

Garey, M.R. and Johnson, D.S. (1977): The rectilinear Steiner problem is NP complete. In: *SIAM Journal on Applied Mathematics*, Vol. 32 (4), pp. 826–834.

Geoffrion, A.M. (1968): Proper Efficiency and the Theory of Vector Maximization. In: *Journal of Mathematical Analysis and Applications*, Vol. 22 (3), pp. 618–630.

Ghanwani, A. (1998): Neural and delay based heuristics for the Steiner problem in networks. In: *European Journal of Operational Research*, Vol. 108 (2), pp. 241–265. Doi:10.1016/S0377-2217(97)00369-X.

Graf, R.F., Bollmann, K. and Mollet, P. (2002): Das Auerhuhn [The capercaillie]. In: *Wildbiologie [Information service for wildlife and ecology]*, Vol. 1/26a, p. 16.

Hammer, P.L. (2006): *Multiobjective discrete and combinatorial optimization*, Vol. 147 of *Annals of operations research*. Springer, Berlin, p. 360. ISSN 0254 5330.

Heinimann, H.R. (1998): A computer model to differentiate skidder and cable-yarder based road network concepts on steep slopes. In: *Journal of Forest Research (Japan)*, Vol. 3, pp. 1–9.

Heinimann, H.R., Stückelberger, J. and Chung, W. (2003): Improving automatic grid cell based road route location procedures. In: Stampfer, K. (Ed.): *Proceedings Austro 2003*. October 5–9, 2003. Schlaegl, Austria. CD-ROM.

Holland, J.H. (1975): *Adaptation in natural and artificial systems: an introductory analysis with applications to biology, control, and artificial intelligence*. University of Michigan Press, p. 183. ISBN 0-472-08460-7.

Hwang, F.K., Richards, D.S. and Winter, P. (1992): *The Steiner Tree Problem*. Elsevier Science Publishers B.V. ISBN 0-444-89098-x.

Inaba, S., Heinimann, H.R. and Shiba, M. (2001): A Model to estimate rock excavation volume of forest roads in steep terrain conditions. In: Anonymous (Ed.): *Proceedings of the 112th Meeting of the Japanese Forestry Society*. April 2–4, 2001, Japan.

Jaeger, J.A.G. (2002): *Landschaftszerschneidung. Eine transdisziplinäre Studie gemäss dem Konzept der Umweltgefährdung [Fragmentation of the landscape. A transdisziplinary study of the concept according to the environmental hazard]*. Eugen Ulmer, Stuttgart, p. 447. ISBN 3-8001-3670-8.

Jungnickel, D. (2005): *Graphs, Networks and Algorithms*, Vol. 5 of *Algorithms and computation in mathematics*. Springer, Berlin, 2nd Edn., p. 611. ISBN 3-540-21905-6.

Karp, R.M. (1972): Reducibility Among Combinatorial Problems. In: Miller, R.E. and Thatcher, J.W. (Eds.): *Complexity of Computer Computations*, pp. 85–103. Plenum Press, March 20–22, 1972. IBM Thomas J. Watson Res. Center, New York. ISBN 0-306-30707-3.

KELLER, V., ZBINDEN, N., SCHMID, H. and VOLET, B. (2001): *Rote Liste der gefährdeten Arten der Schweiz: Brutvögel [Red list of endangerad species of Switzerland: breeding birds].* Vollzug Umwelt. Bundesamt für Umwelt Wald und Landschaft [Swiss Agency for the Environment, Forests and Landscape], Bern, Switzerland.

KIRBY, M. (1973): An example of optimal planning of forest roads and projects. In: O'LEARY, J.E. (Ed.): *Planning and decisionmaking as applied to forest harvesting*, pp. 75–83. Forest Research Laboratory, School of Forestry, Oregon State University, Corvallis OR, U.S.A.

KIRKPATRICK, S., GELATT, C.D. and VECCHI, M.P. (1983): Optimization by Simulated Annealing. In: *Science*, Vol. 220 (4598), pp. 671–680.

KRUSKAL, J.B. (1956): On the shortest spanning subtree of a graph and the travelling salesman problem. In: *Proceedings of the American Mathematical Society*, Vol. 7, pp. 48–50.

KUONEN, V. (1983): *Wald- und Güterstrassen [Low volume forest roads].* Eigenverlag, Pfaffhausen, Switzerland, p. 743.

LAUNHARDT, W. (1869): *Ueber Rentabilität und Richtungsfeststellung der Strassen [About efficiency and defining directions of roads].* Schmorl von Seefeld, Hannover, p. 54.

LAUNHARDT, W. (1872): *Kommercielle Tracirung der Verkehrswege [Economical route planning of lines of communication].* Schmorl von Seefeld, Hannover, p. 32.

LIU, K. and SESSIONS, J. (1993): Preliminary Planning of Road Systems Using Digital Terrain Models. In: *International Journal of Forest Engineering*, Vol. 4 (2), pp. 27–32.

MALCZEWSKI, J. (1999): *GIS and multicriteria decision analysis.* John Wiley & Sons, New York, p. 392. ISBN 0-471-32944-4.

MANDT, C.I. (1973): Network analyses in transportation planning. In: O'LEARY, J.E. (Ed.): *Planning and decisionmaking as applied to forest harvesting*, pp. 95–101. Forest Research Laboratory, School of Forestry, Oregon State University, Corvallis OR, U.S.A.

MARKOW, M.J. and AW, W.B. (1983): Estimating Road Construction Cost for Sector Planning in Developing Countries. In: *Transportation Research Record: Journal of the Transportation Research Board*, (898), pp. 52–61.

MARTI, K., KRÜSI, B., HEEB, J. and THEIS, E. (1997): *Pufferzonen-Schlüssel. Leitfaden zur Ermittlung von ökologisch ausreichenden Pufferzonen für Moorbiotope [Principles for buffer zone layout. Guidelines for the determination of sufficient marshland buffer zones].* Bundesamt für Umwelt Wald und Landschaft [Swiss Agency for the Environment, Forests and Landscape], Berne, Switzerland, 2^{nd} Edn., p. 52.

O'NEAL, B.S., LAKEL III, W.A., AUST, W.M. and VISSER, R.M. (2006): AVLO: A Simplified Cost Analysis Approach for Estimating Construction Costs for Forest Roads. In: CHUNG, W. and HAN, H.S. (Eds.): *The 29^{th} Council on Forest Engineering*, pp. 165–169. July 30 – August 2, 2006, Coeur d'Alene, ID, U.S.A.

PARETO, V. (1896–1897): *Cours d'économie politique [Instructions for political economics].* Université de Lausanne, Suisse [University of Lausanne, Switzerland].

Park, C.S. and Sharp-Bette, G.P. (1990): *Advanced Engineering Economics*. John Wiley & Sons, Inc., New York, p. 740. ISBN 0-47179989-0.

Polzin, T. (2003): *Algorithms for the Steiner Problem in Networks*. Ph.D. thesis, Universität des Saarlandes, Germany. Urn:nbn:de:bsz:291-scidok-2182.

Prim, R.C. (1957): Shortest connection networks and some generalizations. In: *The Bell System Technical Journal*, Vol. 36, pp. 1389–1401.

Prömel, H.J. and Steger, A. (2002): *The Steiner tree problem: a tour through graphs, algorithms and complexity*. Advanced lectures in mathematics. Vieweg, Braunschweig/Wiesbaden, 2^{nd} Edn., p. 241. ISBN 3-528-06762-4.

Rosenwein, M.B. and Wong, R.T. (1995): A constrained Steiner tree problem. In: *European Journal of Operational Research*, Vol. 81 (2), pp. 430–439. Doi:10.1016/0377-2217(93)E0245-S.

Sakurai, R., Nitami, T. and Kobayashi, H. (2002): The Construction of Forest Road Planning System with Graph Theorem. In: Yoshimura, T. (Ed.): *Proceedings of the international seminar on new roles of plantation forestry requiring appropriate tending and harvesting operations*, pp. 129–134. IUFRO 3.04/3.06/3.07, September 29 – October 5, 2002. The Japan Forest Engineering Society, Tokyo, Japan.

Scaparra, M.P. and Church, R.L. (2005a): *Corridor location: The multi-gateway model*. Working paper, 40 p., University of California at Santa Barbara, U.S.A.

Scaparra, M.P. and Church, R.L. (2005b): A GRASP and Path Relinking Heuristic for Rural Road Network Development. In: *Journal of Heuristics*, Vol. 11 (1), pp. 89–108. Doi:10.1007/s10732-005-7000-4.

Schwartz, J. and Stückelberger, J. (2008): Computing Lower Bounds for Steiner Trees in Road Network Design. In: *Proceedings of the* 7^{th} *international workshop on experimental algorithms*, p. to appear. May 30 – June 2, 2008. Provincetown, Cape Cod, Massachusetts, USA.

Stadler, W. (1988): *Multicriteria Optimization in Engineering and in the Sciences*, Vol. 37 of *Mathematical Concepts and Methods in Science and Engineering*. Plenum Press, cop, New York, pp. XIV, 405. ISBN 0-306-42743-5.

Stückelberger, J.A. (2006): GIS-gestützte Erschliessungsplanung [GIS-based road network planning]. In: *Bündnerwald [Journal of Forest Service, Canton of Grisons, Switzerland]*, (3), pp. 19–24.

Stückelberger, J.A., Heinimann, H.R. and Burlet, E.C. (2006a): Modelling spatial variability in the life-cycle costs of low-volume forest roads. In: *European Journal of Forest Research*, Vol. 125 (5), pp. 377–390. Doi:10.1007/s10342-006-0123-9.

Stückelberger, J.A., Heinimann, H.R. and Chung, W. (2004): Improving the effectiveness of automatic grid cell based road route location procedures. In: Clark, M. (Ed.): *A Joint Conference of IUFRO 3.06 Forest Operations under Mountainous Conditions and the* 12^{th} *International Mountain Logging Conference*. June 13–16, 2004, FERIC, University of British Columbia, Vancouver, BC, Canada. CD-ROM.

Stückelberger, J.A., Heinimann, H.R. and Chung, W. (2007): Improved road network design models with the consideration of various link patterns and road design elements. In: *Canadian Journal of Forest Research*, Vol. 37 (11), pp. 2281–2298. Doi:10.1139/X07-036.

Stückelberger, J.A., Heinimann, H.R., Chung, W. and Ulber, M. (2006b): Automatic road-network planning for multiple objectives. In: Chung, W. and Han, H.S. (Eds.): *The 29th Council on Forest Engineering*, pp. 233–248. July 30 – August 2, 2006, Coeur d'Alene, ID, U.S.A.

Sylvester, J.J. (1878): Chemestry Algebra. In: *Nature*, Vol. 18, p. 284.

Tan, J. (1999): Location Forest Roads by a Spatial and Heuristc Procedure Using Microcomputers. In: *Journal of Forest Engineering*, Vol. 10 (2), pp. 91–100.

Terzaghi, K. (1944): *Theoretical Soil Mechanics*. Wiley, New York, 2nd Edn., p. 510.

Twito, R.H., Reutebuch, E. and Stephen, E. (1987): *Preliminary logging analysis system (PLANS): overview*. Technical Report, PNW-BTR-199. USDA, Forest Service, Pacific Northwest Research Station, Portland OR, U.S.A., p. 24.

Ulber, M. (2004): *Berücksichtigung von Auswirkungen auf das Auerhuhn bei der Planung von Forststrassen [Influence and impact of forest roads on capercaillie habitat. Guidelines for the preliminary forest road planning]*. Internal Report, Forest Engineering Group, ETH Zurich, CH-8092 Zurich, Switzerland.

Ulber, M. (2005): *Einfluss von Forststrassen auf Moore und Feuchtgebiete [Impact of forest roads on marshland and reeds]*. Internal Report, Forest Engineering Group, ETH Zurich, CH-8092 Zurich, Switzerland.

US Forest Service (2006): *Cost Estimating Guide for Road Construction. Northern Region Engineering, US Department of Agriculture*. [online] http://www.fs.fed.us/r1/projects/costguide/ (retrived July 7, 2006).

USDI Fish and Wildlife Service (1981): *Standards for the Development of Habitat Suitability Index Models*. No. 103 in ESM. USDI Fish and Wildife Service. Division of Ecological Services, Department of the Interior, Washington DC, U.S.A.

Walbridge, T.A., Franklin, B.D., Griffiths, R.C. and Jarck, W. (1984): *Forestry handbook*, chap. Forest road engineering. John Wiley & Sons, New York, 5th Edn., pp. 1041–1087.

Westney, R.E. (1997): *The Engineer's Cost Handbook*. Marcel Dekker eBooks. ISBN 0-8247-4687-2 (electronic).

www.cprogramming.com (2005a): *Dijkstra's Algorithm for Shortest Paths*. [online] http://www.cprogramming.com/tutorial/computersciencetheory/dijkstra.html (retrived June 10, 2005).

www.cprogramming.com (2005b): *Minimum Spanning Trees*. [online] http://www.cprogramming.com/tutorial/computersciencetheory/mst.html (retrived June 10, 2005).

Xiao, N., Bennett, D.A. and Armstrong, M.P. (2002): Using evolutionary algorithms to generate alternatives for multiobjective site-search problems. In: *Environment and Planning A*, Vol. 34 (4), pp. 639–656. Doi:10.1068/a34109.

Xiao, N., Bennett, D.A. and Armstrong, M.P. (2007): Interactive evolutionary approaches to multiobjective spatial decision making: A synthetic review. In: *Computers, Environment and Urban Systems*, Vol. 31 (3), pp. 232–252. Doi:10.1016/j.compenvurbsys.2006.08.001.

Acknowledgments

First of all, I would like to express my gratitude to all my co-authors of the four papers that are leading to my thesis. Through all publications I was guided by Prof. Dr. Hans Rudolf Heinimann, to whom I express my deepest thanks. Even more, I am grateful to him for giving me the opportunity to write this thesis in his research group, and above all for the confidence and support, both personal and scientific, he gave me throughout these years. Dr. Edouard Burlet was my teacher in forest road construction during my graduate studies in forest engineering, and I was lucky to profit from his well-founded practical knowledge. Prof. Dr. Woodam Chung, one of the leading scientists in forest operational research, gave me the opportunity for two study visits at his institute at The University of Montana in Missoula, which was for me a very inspiring time. Marcus Ulber, an expert in ornithology and conservation, preprocessed all the ecological functions so that it was easy for me to incorporate these in the model presented here. During the implementation of the model, I relied on the help in mathematics and computer science that I found from Justus Schwartz and Prof. Dr. Angelika Steger, Institute of Theoretical Computer Science, ETH-Zurich.

Besides these co-authors, there are a lot of other persons whom I must thank. Prof. Dr. Hans Jakob Lüthi and Dr. Thomas Herrmann, Institute for Operation Research, ETH-Zurich, gave me very important hints on how to formulate the problem mathematically and how to optimize for multi-criteria objectives. Andreas Weissl, Institute of Theoretical Computer Science, was helpful in implementing the source code, together with Justus Schwartz. In our Institute I was able to count on others for assistance. The GIS team, especially Dr. Adrian Eichrodt, Dr. Tobias Meyer, Norbert Knechtle, Monika Niederhuber, Dr. Bernd Hebel, and Riccardo de Filippi, provided and supported my geo data. Dr. Lorenz Fahse gave me some input for ecological modeling and its implementation for C++ and Object Pascal, and Dr. Jochen Jaeger gave me important hints for intersection effects for ecological biotopes by roads. Dr. PD. Daniel Mandallaz helped me in mathematical affairs, while Dr. Mario Gellrich assisted me with the statistical analysis in R, and with formatting my thesis in LaTeX. Pauline Bart set up the literature database for my thesis and corrected the French summary. Other useful hints I got from Dr. Kurt Hollenstein, Prof. Dr. Richard Hirt, Regina Wollenmann, Jochen Breschan, and Leo Bont. A big thank I give to the administrative staff at our Institute, Ottilia Benz and Esther Jampen, who took care of my administrative affairs.

During the evaluation of my tools, I was dependent on field information, practical advice, and recent spatial data. I thank Urs Thali, forest engineer in the Canton of Uri, who is conducting an on-going forest road project in the mountainous area in which I was able to apply a prototype of my model; as well as Josef Hess and Dr. Andreas Bacher, forest service of the Canton of Obwalden, who provided my recent projects and spatial data for model calibration.

Last but not least I thank Priscilla Licht, who corrected my English into proper English and edited all my papers.

Curriculum vitae

Jürg Andreas Stückelberger
born September 24, 1972, at Berne (BE), Switzerland
citizen of Basel (BS) and Winterthur (ZH), Switzerland

1979–1985	Basic education at Berne
1985–1991	High school education at Berne, Matura in Economics
1991/92, 93–95	Undergraduate studies in Forest Sciences, ETH-Zurich
1993	Mandatory military service (artillery)
1995/96	Practical trainee: 7 months at District Forestry Agency, Canton of Fribourg; 5 months at Swiss Federal Institute for Forest, Snow and Landscape Research
1996–1998	Graduate studies in Forest Sciences. Diploma of Forest Engineer, ETH-Zurich
1998–2000	Junior assistant at ETH, Forest Engineering group
2001	Project master for reconstruction in Kosovo (KFOR)
2002–2007	Research assistant at ETH, Forest Engineering group (part time)
2002–2004	Staff at consulting geologists Geo7 (Berne), with projects in erosion control, natural hazards, geoinformatics (part time)
since 2004	Lecturer at the University for Applied Science, Berne, Forest Engineering (part time)
since 2005	Several freelance projects in forestry, civil engineering and geoinformatics (part time)
2003–2007	Ph.D. thesis, ETH-Zurich; with study visits in 2004 and 2006 at the College of Forestry and Conservation, University of Montana, Missoula, USA

ISBN 978-3-7281-3217-8
DOI 10.3218/3217-8